AD-A074 737 PENNSYLVANIA STATE UNIV UNIVERSITY PARK APPLIED RESE--ETC F/G 20/11
VIBRATION ISOLATION ON RIGID AND NONRIGID FOUNDATIONS.(U)
JUL 79 J C SNOWDON N00024-79-C-6043
UNCLASSIFIED ARL/PSUTM-79-137 NL

1 OF 2
AD A074737

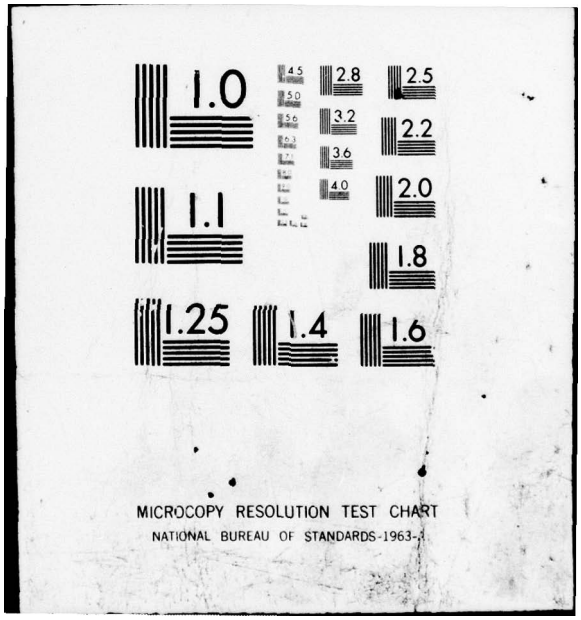
1.0
1.1
1.25
1.4
1.6
1.8
2.0
2.2
2.5
2.8
3.2
3.6
4.0
4.5
5.0
5.6
6.3
MICROCOPY RESOLUTION TEST CHART
NATIONAL BUREAU OF STANDARDS-1963-A

(12) B.S.

LEVEL II

(6) VIBRATION ISOLATION ON RIGID AND NONRIGID FOUNDATIONS

by

(10) J. C. Snowdon

(14) ARL/PSU/TM-79-137

(9) Final rept.

Technical Memorandum
File No. 79-137
(11) 23 July 1979

(12) 118

Copy No. 56

Contract No. N00024-79-6043

(15)

C-

The Pennsylvania State University
Institute for Science and Engineering
APPLIED RESEARCH LABORATORY
Post Office Box 30
State College, PA 16801

Approved for public release: distribution unlimited

NAVY DEPARTMENT

NAVAL SEA SYSTEMS COMMAND

391 007

UNCLASSIFIED

SECURITY CLASSIFICATION OF THIS PAGE (When Data Entered)

REPORT DOCUMENTATION PAGE		READ INSTRUCTIONS BEFORE COMPLETING FORM
1. REPORT NUMBER TM 79-137	2. GOVT ACCESSION NO.	3. RECIPIENT'S CATALOG NUMBER
4. TITLE (and Subtitle) Vibration Isolation on Rigid and Nonrigid Foundations (U)		5. TYPE OF REPORT & PERIOD COVERED Final 6. PERFORMING ORG. REPORT NUMBER
7. AUTHOR(s) J. C. Snowdon		8. CONTRACT OR GRANT NUMBER(s) N00024-79-6043
9. PERFORMING ORGANIZATION NAME AND ADDRESS Applied Research Laboratory, P. O. Box 30 State College, PA 16801		10. PROGRAM ELEMENT, PROJECT, TASK AREA & WORK UNIT NUMBERS
11. CONTROLLING OFFICE NAME AND ADDRESS U.S. Naval Sea Systems Commande, Code 05H U.S. Office of Naval Research, Code 222		12. REPORT DATE July 23, 1979 13. NUMBER OF PAGES 119
14. MONITORING AGENCY NAME & ADDRESS(if different from Controlling Office)		15. SECURITY CLASS. (of this report) UNCLASSIFIED 15a. DECLASSIFICATION/DOWNGRADING SCHEDULE

16. DISTRIBUTION STATEMENT (of this Report)

Approval for public release; distribution unlimited.
As per letter dated August 27, 1979.

17. DISTRIBUTION STATEMENT (of the abstract entered in Block 20, if different from Report)

18. SUPPLEMENTARY NOTES

19. KEY WORDS (Continue on reverse side if necessary and identify by block number)

Vibration isolation.
Rigid and nonrigid substructures.
Clamped-clamped beams.
Simply supported plates.
Damping of the solid type.
Simple mounting system.
Compound mounting system.
Nonrigid supporting feet.
Dynamic vibration absorbers.
Lumped masses.
Multiple antivibration mounts.

20. ABSTRACT (Continue on reverse side if necessary and identify by block number)

The problem of isolating machinery vibration from rigid and nonrigid substructures is analyzed in detail. The nonrigid substructures are modeled by clamped-clamped beams and by simply supported plates with small internal damping of the solid type. Both simple and compound mounting systems are analyzed. The advantages that result from the use of the compound mounting system are clearly apparent. The loss in isolation is described that results when nonrigid flanges or feet support the simply mounted item or the inter-

DD FORM 1 JAN 73 1473 EDITION OF 1 NOV 65 IS OBSOLETE

UNCLASSIFIED

SECURITY CLASSIFICATION OF THIS PAGE (When Data Entered)

mediate mass of the compound mounting system. The use is also analyzed of dynamic vibration absorbers or lumped masses to load the beamlike and plate-like substructures at each mount location. The item of machinery is supported either by eight or by four antivibration mounts that have small damping of the solid type. It is shown how the number of beam and plate resonances that are excited can be reduced by judicious placement of the antivibration mountings.

This investigation was sponsored by the U. S. Naval Sea Systems Command, Code 05H, and by the U. S. Office of Naval Research, Code 222.

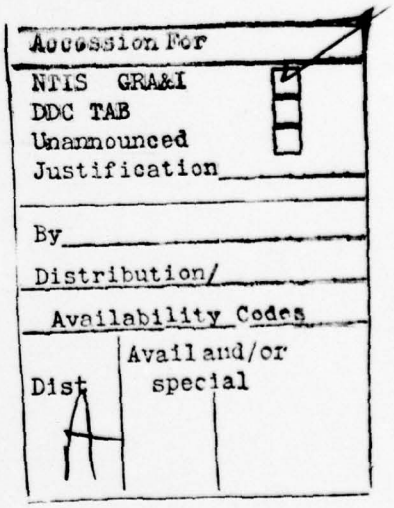

ABSTRACT

The problem of isolating machinery vibration from rigid and nonrigid substructures is analyzed in detail. The nonrigid substructures are modeled by clamped-clamped beams and by simply supported plates with small internal damping of the solid type. Both simple and compound mounting systems are analyzed. The advantages that result from the use of the compound mounting system are clearly apparent. The loss in isolation is described that results when nonrigid flanges or feet support the simply mounted item or the intermediate mass of the compound mounting system. The use is also analyzed of dynamic vibration absorbers or lumped masses to load the beamlike and platelike substructures at each mount location. The item of machinery is supported either by eight or by four antivibration mounts that have small damping of the solid type. It is shown how the number of beam and plate resonances that are excited can be reduced by judicious placement of the antivibration mountings.

1. INTRODUCTION

The basic principles of vibration isolation are reviewed initially. Reasons why theoretical predictions of isolation are not always realized in practice are then outlined, and some of these reasons are examined in detail. A two-stage or compound mounting system is shown to be effective when especially low levels of transmitted vibration are required at high frequencies. Several aspects of the problem of isolating machinery vibration from nonrigid foundations are also examined. The foundations are represented by two parallel clamped-clamped beams or by simply supported rectangular plates. Sometimes the beams and plates are loaded by concentrated masses or by dynamic vibration absorbers placed directly beneath the antivibration mountings. Even though the levels of the transmitted vibration may sometimes appear to be low, it must be recognized that this vibration can excite the natural modes of vibration of neighboring (and sometimes of distant) platelike structures. Many of the plate modes will be relatively efficient radiators of unwanted sound. Motion is assumed to occur only in the vertical direction. The internal damping of the substructures and of the antivibration mounts is considered to be of the solid type for which the appropriate damping factors are independent of frequency. Because these damping factors are assigned relatively small values here, they remain directly equivalent to such measures of damping as (quality factor Q)$^{-1}$, $(1/2\pi)$ (specific damping capacity), and $(1/\pi)$ (logarithmic decrement). Symbols with superior tildes represent quantities that vary sinusoidally with time; symbols with a star superscript represent complex quantities.

2. SIMPLE MOUNTING SYSTEM: PRINCIPLES OF VIBRATION ISOLATION

Figure 1(a) shows a machine of mass M supported by antivibration mountings on a foundation, such as a concrete factory floor, which is assumed to be ideally rigid. To the foundation is transmitted a force $2\tilde{F}_2$ that is produced by a sinusoidally varying force $\tilde{F}_1$ applied to or generated within M. The mounts are visualized as rubber springs with a stiffness K and with internal damping represented by a damping factor δ_K. The performance of the mounts is best described by assigning to them a complex stiffness K^* such that

$$K^* = K(1 + j\delta_K) \quad , \tag{1}$$

where $j = \sqrt{(-1)}$, K is stiffness, and δ_K is the damping factor (the ratio of the imaginary to the real part of the complex stiffness). This concise equation states that the relative displacement across the mounts lags in phase behind the vibratory force that they experience by an angle the tangent of which is δ_K. The internal damping of the mounts will be represented here by a value of $\delta_K = 0.05$, which typifies, for example, the damping of natural, neoprene, and SBR rubbers, for which the very small dependence of K and δ_K on frequency can realistically be disregarded.[1]

A quantity of basic interest is the so-called transmissibility T across the simple mounting system of Fig. 1(a). An equation for T, which is defined as the magnitude of the force ratio $|2\tilde{F}_2/\tilde{F}_1|$ can be stated as follows[1]:

$$T = \left|\frac{2\tilde{F}_2}{\tilde{F}_1}\right| = \left[\frac{1 + \delta_K^2}{(1 - \Omega^2)^2 + \delta_K^2}\right]^{1/2} \quad . \tag{2}$$

In this equation,

$$\Omega = \omega/\omega_o \quad , \tag{3}$$

where ω is the frequency of the impressed vibratory force, hereafter known simply as frequency, and

$$\omega_o = (2K/M)^{\frac{1}{2}} \quad , \tag{4}$$

is the natural frequency of the system for which, in the absence of mount damping, T would become infinitely large. Calculations of transmissibility made from Eq. (2) are plotted on a decibel scale [$20 \log_{10} T(dB)$] in Fig. 2 as a function of the frequency ratio Ω. Negative values of T(dB) mean that the input force $\tilde{F}_1$ has been attenuated; positive values of T(dB) mean that undesired magnification has occurred. The magnification is high at resonance ($\Omega = 1$) because for the small values of damping considered here, transmissibility becomes equal to $(1/\delta_K)$. It is evident from Fig. 2 that only for values of $\Omega > \sqrt{2}$ -- that is, for values of $\omega > \sqrt{2}\,\omega_o$ -- do the antivibration mountings provide the desired attenuation of force (refer to the hatched area). Consequently, to assign to ω_o the smallest value possible without endangering the lateral stability of the mounting system should always be an advantage.

It is appropriate now to mention some reasons why larger values of transmissibility (reduced isolation) may occur at frequencies above resonance than the curve of Fig. 2 indicates. These reasons (1) may simply be mechanical or (2) they may be basic. Thus,

(1) Vibration isolation may be impaired by mechanical links that have significant stiffness and hence that bypass, to some extent, the antivibration mounts. For example, vibration from a resiliently mounted diesel engine may reach its foundation via an exhaust pipe that is still rigidly connected to a surrounding enclosure, or it may reach the

foundation via a bearing pedestal that supports a rotating shaft that extends from the engine.

(2) Vibration isolation may not be predicted adequately at higher frequencies for the basic reason that the simple system pictured in Fig. 1(a) is then too simplified a model of the practical situation; for example, the antivibration mounts may cease to behave as ideally resilient members at high frequencies. In this event, so-called wave effects will be apparent[1-3] at frequencies for which the mount dimensions become comparable with multiples of the half wavelengths of the elastic waves traveling through the mountings. Alternatively, wave effects may be thought of as occurring when the elasticity and distributed mass of the rubber mountings interact at high frequencies. At these frequencies, resonant peaks appear in the transmissibility curve. However, these peaks will not always be of primary concern because (a) the peaks will be suppressed to some extent by the internal damping of the rubber mounts, and (b) even the first of the peaks invariably occurs at frequencies higher than 20 ω_o, where significant isolation has already been achieved. As an example, wave-effect calculations based on the long-rod theory[1] are plotted in Fig. 3 for values of the mass ratio $\gamma = M/M_R = 50$, 100, and 250, where M is the machine mass and M_R is the mass of the mount. It has been assumed that both the dynamic Young's modulus and the associated damping factor are frequency independent, that $\delta_E = 0.1$, and that the first natural frequency of the system is $f_o = \omega_o/2\pi = 5$ Hz. The curves of Fig. 3, which may be thought of as describing the transmissibility of natural-rubber mounts that are heavily reinforced (filled) with carbon black, show how the level to which T is increased by the wave resonances depends upon the value of γ. Note that the wave resonances are shifted

to higher frequencies (where greater isolation exists) as the ratio γ of the mass of the machine to the mass of the mounts is increased, and that the occurrence of wave effects becomes of less concern as γ becomes larger; from this point of view, therefore, it is desirable to utilize mounts as near their maximum rated load as possible, thereby making γ a relatively large quantity.

One other reason why the high-frequency isolation predicted by Fig. 2 may be impaired is of sufficient interest to be discussed in some detail. Thus, the flanges or feet on which the machine is mounted may not be ideally rigid but may be multiresonant, so giving rise to other peaks in the transmissibility curve at high frequencies. These peaks may well be troublesome because the internal damping of the metal feet will be at least 5 or 10 times smaller than the damping of the rubber mounts in which the previously discussed wave effects occurred. The feet may protrude from the bottom of the machine, or from its sides, as in Fig. 1(b). This will be the case if the usually beneficial step is taken to locate the mounts in a plane that passes through the center of gravity of the machine (so minimizing the rocking motion it experiences when subjected to horizontally directed forces). This is not a contrived problem; in fact, one does not have to look far to find examples of such situations. For instance, a marine engine attached to a subframe having significant unsupported length is shown in Fig. 4; here, the subframe is fashioned so that the mounting points lie on the same horizontal as the center of gravity of the engine.[4]

A guide to the force transmissibility across the simple system of Fig. 1(b) has been obtained by visualizing the machine feet as short shear beams; that is, as beams with length-to-depth ratios of approximately 3 or less for which it can realistically be assumed that the beam deflection due to bending is negligible as compared to the deflection due to shear.[5] The force transmissibility can then be expressed as follows[6]:

$$T = |2\tilde{F}_2/\tilde{F}_1| = [\psi^* - (n^*\ell)\,\Gamma^*\eta^*]^{-1} \quad , \tag{5}$$

where

$$\psi^* = [\cos n^*\ell - \gamma_F(n^*\ell)\,\sin n^*\ell] \quad , \tag{6}$$

$$\eta^* = [\sin n^*\ell + \gamma_F(n^*\ell)\,\cos n^*\ell] \quad , \tag{7}$$

$$(n^*\ell) = (p + jq) \quad , \tag{8}$$

and

$$\Gamma^* = \Gamma(1 + j\delta_F)/(1 + j\delta_K) \quad . \tag{9}$$

In these equations, n^* is the complex wavenumber of the shear-beam feet, ℓ is their length,

$$\gamma_F = M/2M_F \quad , \tag{10}$$

and

$$\Gamma = K_F/K \quad , \tag{11}$$

where M_F and K_F are the mass and static stiffness of each machine foot, and δ_F and δ_K are the damping factors of the feet and of the antivibration mounts, respectively. In addition,

$$p = \frac{n\ell}{D_F}\left(\frac{D_F + 1}{2}\right)^{\frac{1}{2}} \tag{12}$$

and

$$q = -\frac{n\ell}{D_F}\left(\frac{D_F - 1}{2}\right)^{\frac{1}{2}} \quad , \tag{13}$$

where

$$D_F = (1 + \delta_F^2)^{\frac{1}{2}} \tag{14}$$

and

$$n\ell = N_R(\omega/\omega_o) = N_R\Omega \quad . \tag{15}$$

Here, the natural frequency ω_o of the mounting system is given by the equation

$$\omega_o^2 = \frac{2KK_F}{M(K + K_F)} = \frac{2K}{M}\left(\frac{\Gamma}{1 + \Gamma}\right) \quad , \tag{16}$$

and N_R is the value of n for which the first peak value of T would be observed (when $\omega = \omega_o$) if $\delta_F = \delta_K = 0$. A close guide to this value of N_R can be obtained from the relation

$$N_R \approx [(\gamma_F + 1)\ \Gamma + \gamma_F]^{-\frac{1}{2}} \tag{17}$$

or, if both γ_F and Γ are large, from

$$N_R \approx (\gamma_F\Gamma)^{-\frac{1}{2}} \quad . \tag{18}$$

Therefore, as the angular frequency ω of the impressed force is varied, corresponding values of $n\ell$ are specified by Eq. (15), and the expressions for p and q, and hence T, may be evaluated.

The results of representative calculations of T are plotted as a function of the frequency ratio $\Omega = \omega/\omega_o$ in Fig. 5, where $\gamma_F = M/2M_F = 40$, $\Gamma = K_F/K = 5$, 25, and 100, $\delta_K = 0.05$, and $\delta_F = 0.01$. As might be anticipated, for the given

value of γ_F, the resonances of the machine feet, which give rise to the pronounced peak values of T at higher frequencies, are of the least consequence when Γ is large. Actually, the first resonance of the feet occurs at a frequency ω_1 given by the approximate equation

$$\omega_1 \approx \frac{\pi\omega_o}{2}\sqrt{(\gamma_F\Gamma)} = \frac{\pi}{2}\sqrt{(K_F/M_F)} \quad , \tag{19}$$

provided that γ_F and Γ are relatively large ($\Gamma > 5$). Therefore, since ω_1 is advantageously kept at the highest possible frequency, it is desirable to design the feet to have a maximum ratio of static stiffness to mass; namely, to keep the feet as short as possible.

3. COMPOUND MOUNTING SYSTEM

If added mass can be tolerated, a two-stage or compound mounting system[1] can provide especially low values of transmissibility at high frequencies. This situation is described by Fig. 6(a), where two antivibration mounts of complex stiffness K_1^* and K_2^* in the upper and lower stages of the compound system are separated by a secondary or intermediate mass M_2. The compound system possesses a secondary as well as a primary resonance, which is a disadvantage, but above the secondary resonant frequency ω_2, transmissibility falls off in proportion to $1/\omega^4$ (24 dB/octave), provided that the mount stiffness and damping remain constant, as assumed here. This is twice the rate of 12 dB/octave at which the transmissibility curve of Fig. 2 for the simple mounting system decreases at high frequencies.

Examples of small- and large-scale applications of the compound system are given in Refs. 7 and 8, which describe the compound mounting of a motor-driven compressor of a household refrigerator, and the compound mounting of

two 80,000 lb and two 17,000 lb diesel generators on one extensive intermediate mass. An adaption of the latter arrangement is redrawn here as Fig. 7. Two, much smaller, applications are described in Refs. 3 and 9, in both of which the compound system has been effectively compacted into an "off-the-shelf" antivibration mount. The design of one mount[9] is shown in Fig. 8, where the secondary mass comprises two cylindrical lumped masses 10 and a spacer yoke 12, and the resilient elements comprise 16. A small-scale torsional equivalent of the compound system that has been used in quieting textile machinery is described in Ref. 10.

For the compound system to have the greatest effectiveness as an antivibration mounting at high frequencies, it is desirable that the secondary resonance ω_2 occur, for any given value of the primary resonance ω_1, at the lowest possible frequency. This situation can be realized[1] when the mount stiffness ratio is assigned the optimum value

$$(K_2/K_1) = [1 + (M_2/M_1)] = (1 + \beta) \quad , \tag{20}$$

where M_1 is the mass of the vibrating machine and M_2 is the intermediate mass. This is otherwise an appropriate result because the lower mounts support a static load that is greater, by the same factor $(1 + \beta)$, than the load supported by the upper mounts. For this optimum stiffness ratio, the transmissibility T across the compound system can be expressed as follows:

$$T = \left| \frac{2\tilde{F}_2}{\tilde{F}_1} \right| = \frac{(1 + \delta_K^2)}{\{[\beta\lambda(1 - \lambda)\,\Omega^4 - 2\lambda\Omega^2 + 1 - \delta_K^2]^2 + (2\delta_K)^2(1 - \lambda\Omega^2)^2\}^{\frac{1}{2}}} \quad , \tag{21}$$

where

$$\lambda = (1 + \beta)/(2 + \beta) \tag{22}$$

and $\Omega = \omega/\omega_o$ is again a frequency ratio against which T is conveniently plotted. The reference frequency $\omega_o \approx \omega_1$ is actually the natural frequency of the simple system obtained when $M_2 = 0$; thus,

$$\omega_o^2 = \frac{2K_1K_2}{(K_1 + K_2)M_1} \quad . \tag{23}$$

It is instructive to note that, at high frequencies, Eq. (21) can be written as

$$T_{HF} = \frac{(1 + \delta_K^2)(2 + \beta)^2}{\beta\Omega^4(1 + \beta)} \approx \frac{4(1 + \delta_K^2)}{\beta\Omega^4} \quad , \qquad (\beta \leq 0.5) \tag{24}$$

so that it will normally be advantageous to employ the largest acceptable value of β; that is, the largest possible intermediate mass M_2.

The transmissibility of a compound system that utilizes mounts with a damping factor $\delta_K = 0.05$ is shown in Fig. 9, where the transmissibility of three compound mounting systems with $\beta = 0.1$, 0.2, and 1.0 is compared with the transmissibility of the simple mounting system ($\beta = 0$). The potential advantages of the compound system as an especially effective antivibration mounting at high frequencies are immediately apparent. It will be recognized that the system can be of particular value in mitigating the increase in transmissibility that occurs when it is necessary to mount an item of machinery upon a nonrigid foundation such as a system of steel girders, which will have many resonances and very small internal damping. The effectiveness of the compound system in this situation has been well illustrated in Ref. 1. The use of a dynamic vibration absorber attached to the intermediate mass of the compound system to suppress effectively its secondary resonance is described elsewhere (Ref. 11).

If the compound mounting system is to provide the small values of transmissibility as predicted, it is vital that the intermediate mass M_2 remains masslike. If it does not, the performance of the system will be seriously impaired at high frequencies. This situation is described in Fig. 6(b), where the flanges from which M_2 is supported behave as springs at some high frequencies because of their poor design. To provide a quantitative illustration of the increase in transmissibility that can be expected in this case, the compound system of Fig. 6(b) has been analyzed by modeling the nonrigid (multiresonant) flanges as short shear beams. In fact, the expression for the transmissibility across the system becomes

$$T = \left|\frac{2\tilde{F}_2}{\tilde{F}_1}\right| = \left\{\frac{(1 + \delta_K^2)}{[\Omega^2(\lambda\zeta_R - 1) + (1 - \zeta_R + \delta_K\zeta_I)]^2 + [\lambda\zeta_I\Omega^2 - \delta_K\zeta_R - \zeta_I + \delta_K]^2}\right\}^{\frac{1}{2}}, \tag{25}$$

where λ Eq. [(22)] and δ_K have the same significance as before, and ζ_R and ζ_I are the real and imaginary parts of a quantity ζ^* that is defined as follows:

$$\zeta^* = (\eta^*/\psi^*)(n^*\ell)\Gamma^* \quad . \tag{26}$$

In this equation, ψ^*, η^*, $n^*\ell$, and Γ^* are given by Eqs. (6) - (9) in which γ_F and M_F are given by Eqs. (10) and (11) where M_F, K_F, and ℓ are the mass, static stiffness, and length of each shear-beam flange projecting from the intermediate mass M_2. Finally, the frequency ratio $\Omega = \omega/\omega_o$ and the shear-beam variable $n\ell$ are related by the equation

$$n\ell = N_R\Omega\left[\frac{\lambda\beta}{(1 + \beta) - (1 + \beta)^{\frac{1}{2}}}\right]^{\frac{1}{2}}, \tag{27}$$

where N_R is now the value of $n\ell$ for which the first peak value of T would be observed (when $\omega = \omega_1 \approx \omega_o$) if $\delta_F = \delta_K = 0$.

The results of one calculation of transmissibility made from Eq. (25) are plotted in Fig. 10 as the chain-line curve for which $\gamma_F = 40$, $\Gamma = 5$, $\delta_F = 0.01$, and $\beta = 0.2$, $\delta_K = 0.05$. Pronounced peaks now occur in the transmissibility curve at high frequencies where the shear-beam flanges resonate, their ends having large motion and their roots, which are attached to M_2, having relatively small motion. In addition, pronounced minima occur in the transmissibility curve at the antiresonant frequencies of the flanges for which the flange ends have little motion and their roots, together with M_2, have relatively large motion; in fact, at these frequencies, M_2 and the flanges are analogous in their behavior to the mass and stiffness of a dynamic vibration absorber.[1] The solid-line curve shows the transmissibility when the intermediate mass (for which $\beta = 0.2$) is ideally rigid.

4. NONRIGID FOUNDATIONS

Attention is now turned to the problem of isolating machinery vibration from nonrigid foundations; that is, foundations that have many self resonances. This problem is of permanent concern in marine and aeronautical applications (see, for example, Refs. 8 and 12), it is becoming of greater concern in land-based applications where, for example, increased mention is being made of steel-frame rather than concrete foundations for large modern turbines and auxiliary equipment.[13]

Two nonrigid foundations are considered here: (1) two identical clamped-clamped beams that have small internal damping and that lie beneath and parallel to the length of the machine. Discussions are directed to one of these beams and to the half of the machine mass that it supports on antivibration mountings (the other half of the machine mass is supported by the same number of

antivibration mountings located at identical positions on the second foundation beam). The mounts lie equidistant from the beam center but their positions are otherwise arbitrary. (2) A simply supported rectangular plate that has small internal damping and that supports the mounted item with at least four antivibration mounts that are arbitrarily but symmetrically located about the plate center.

4.1 Beamlike Foundations

Figure 11(a) shows, for example, how one-half of the machine mass has been isolated by eight mounts of complex stiffness K^* [Eq. (1)] from a foundation beam. The other half of the machine mass is isolated by eight identical mounts located at identical positions to these on a second foundation beam, which is separated from the beam shown by one machine width. The mounts are symmetrically located in pairs that lie equidistant from the beam centers, but their location is otherwise arbitrary. Transmissibility T is again defined as the magnitude of the total output force divided by the impressed force. To design for the lowest possible values of T is always desirable, and it is shown that small values of T can be obtained through broad ranges of frequency when multispan beams are employed, the use of which is desirable, in any case, when long, heavy machinery is to be supported. This situation is pictured in Fig. 11(b).

In addition to the foundation beams of Fig. 11, consideration is also given to the change in transmissibility that occurs (1) when multiple dynamic vibration absorbers are attached to the foundation beams, (2) when the beams are mass loaded, and (3) when beams of single span are supported at each end by an additional antivibration mount to form a so-called floating foundation.

4.1.1 Machine with Eight Mounts per Side Supported by Single- or by Four-Span Foundation Beams

Expressions for the transmissibility across the mounting systems of Figs. 11(a) and 11(b), derived in terms of the normal modes of vibration of the foundation beams, are as follows[14]:

Single-Span Foundation Beams

$$T = \left|\frac{4\tilde{F}_2}{\tilde{F}_1}\right| = \left|\sum_{m=1,3,5,\ldots}^{\infty} \frac{4\theta_m}{(n_m a)} \left[\frac{(\beta^*)^4}{(\beta^*)^4 - 1}\right] \frac{\eta^*}{\theta^*}\right| \quad . \tag{28}$$

In this equation,

$$\eta^* = [-(AA)^* \varphi_m(h_1) + (BB)^* \varphi_m(h_2) - (CC)^* \varphi_m(h_3) + (DD)^* \varphi_m(h_4)] \tag{29}$$

and

$$\theta^* = [-(AA)^*(2 - C^*) + (BB)^*(2 - G^*) - (CC)^*(2 - J^* + \Gamma^*) + (DD)^*(2 - L^*)] \quad , \tag{30}$$

where

$$(AA)^* = \{(GG)^*[(LL)^*(QQ)^* - (RR)^*(MM)^*] - (HH)^*[(KK)^*(QQ)^* - (PP)^*(MM)^*] + (II)^*[(KK)^*(RR)^* - (PP)^*(LL)^*]\} \quad , \tag{31}$$

$$(BB)^* = \{(FF)^*[(LL)^*(QQ)^* - (RR)^*(MM)^*] - (HH)^*[(JJ)^*(QQ)^* - (NN)^*(MM)^*] + (II)^*[(JJ)^*(RR)^* - (NN)^*(LL)^*]\} \quad , \tag{32}$$

$$(CC)^* = \{(II)^*[(JJ)^*(PP)^* - (KK)^*(NN)^*] + (FF)^*[(KK)^*(QQ)^* - (PP)^*(MM)^*] - (GG)^*[(JJ)^*(QQ)^* - (NN)^*(MM)^*]\} \quad , \tag{33}$$

and

$$(DD)^* = \{(HH)^*[(JJ)^*(PP)^* - (KK)^*(NN)^*] + (FF)^*[(KK)^*(RR)^* - (PP)^*(LL)^*]$$

$$- (GG)^*[(JJ)^*(RR)^* - (NN)^*(LL)^*]\} \quad . \tag{34}$$

In turn, in these equations,

$$(FF)^* = (B^* - A^* + \Gamma^*) \quad , \tag{35}$$

$$(GG)^* = (E^* - B^* - \Gamma^*) \quad , \tag{36}$$

$$(HH)^* = (G^* - C^*) \quad , \tag{37}$$

$$(II)^* = (H^* - D^*) \quad , \tag{38}$$

$$(JJ)^* = (D^* - C^*) \quad , \tag{39}$$

$$(KK)^* = (H^* - G^*) \quad , \tag{40}$$

$$(LL)^* = (L^* - J^* + \Gamma^*) \quad , \tag{41}$$

$$(MM)^* = (N^* - L^* - \Gamma^*) \quad , \tag{42}$$

$$(NN)^* = (C^* - A^* + \Gamma^*) \quad , \tag{43}$$

$$(PP)^* = (G^* - B^*) \quad , \tag{44}$$

$$(QQ)^* = (L^* - D^*) \quad , \tag{45}$$

and

$$(RR)^* = (J^* - C^* - \Gamma^*) \quad , \tag{46}$$

where

$$A^* = 2\gamma \sum_{m=1,3,5,\ldots}^{\infty} \frac{\varphi_m^2(h_1)}{[(\beta^*)^4 - 1]} \quad , \tag{47}$$

$$B^* = 2\gamma \sum_{m=1,3,5,\ldots}^{\infty} \frac{\varphi_m(h_1)\varphi_m(h_2)}{[(\beta^*)^4 - 1]} \quad , \tag{48}$$

$$C^* = 2\gamma \sum_{m=1,3,5,\ldots}^{\infty} \frac{\varphi_m(h_1)\varphi_m(h_3)}{[(\beta^*)^4 - 1]} \quad , \tag{49}$$

$$D^* = 2\gamma \sum_{m=1,3,5,\ldots}^{\infty} \frac{\varphi_m(h_1)\varphi_m(h_4)}{[(\beta^*)^4 - 1]} \quad , \tag{50}$$

$$E^* = 2\gamma \sum_{m=1,3,5,\ldots}^{\infty} \frac{\varphi_m^2(h_2)}{[(\beta^*)^4 - 1]} \quad , \tag{51}$$

$$G^* = 2\gamma \sum_{m=1,3,5,\ldots}^{\infty} \frac{\varphi_m(h_2)\varphi_m(h_3)}{[(\beta^*)^4 - 1]} \quad , \tag{52}$$

$$H^* = 2\gamma \sum_{m=1,3,5,\ldots}^{\infty} \frac{\varphi_m(h_2)\varphi_m(h_4)}{[(\beta^*)^4 - 1]} \quad , \tag{53}$$

$$J^* = 2\gamma \sum_{m=1,3,5,\ldots}^{\infty} \frac{\varphi_m^2(h_3)}{[(\beta^*)^4 - 1]} \quad , \tag{54}$$

$$L^* = 2\gamma \sum_{m=1,3,5,\ldots}^{\infty} \frac{\varphi_m(h_3)\,\varphi_m(h_4)}{[(\beta^*)^4 - 1]} \quad , \tag{55}$$

and

$$N^* = 2\gamma \sum_{m=1,3,5,\ldots}^{\infty} \frac{\varphi_m^2(h_4)}{[(\beta^*)^4 - 1]} \quad , \tag{56}$$

The normal functions are given by the equation

$$\varphi_m(h_i) = [(\cosh n_m h_i - \cos n_m h_i) - \theta_m(\sinh n_m h_i - \sin n_m h_i)] \quad , \qquad (i = 1,2,3,4) \tag{57}$$

where h_i is the distance of the ith mount from the nearest beam termination (some arbitrary fraction of the beam half-length a), and

$$\theta_m = (\cosh 2n_m a - \cos 2n_m a)/(\sinh 2n_m a - \sin 2n_m a) \quad , \tag{58}$$

where

$$2n_1 a = 4.73004 \quad , \tag{59}$$

$$2n_3 a = 10.99561 \quad , \tag{60}$$

and

$$2n_m a = (2m + 1)\pi/2 \quad , \qquad m \geq 5 \quad . \tag{61}$$

Note that, when m is large, the normal functions can be expressed more simply as

$$\varphi_m(h_i) = (\sin n_m h_i - \cos n_m h_i) \qquad (i = 1,2,3,4) \quad . \tag{62}$$

In addition

$$\Gamma^* = -8(\Omega^*)^2 = -8\Omega^2/(1 + j\delta_K) \tag{63}$$

and

$$\beta^* = n_m a/(p + jq) \quad , \tag{64}$$

where

$$p = \alpha\left[\frac{1}{2\sqrt{D_E}} + \frac{\sqrt{(1 + D_E)}}{2\sqrt{2}\,D_E}\right]^{\frac{1}{2}} \tag{65}$$

and

$$q = -\alpha\left[\frac{1}{2\sqrt{D_E}} - \frac{\sqrt{(1 + D_E)}}{2\sqrt{2}\,D_E}\right]^{\frac{1}{2}} \quad . \tag{66}$$

Finally,

$$\alpha = 2.36502\ (\Omega/\Xi)^{\frac{1}{2}} \quad , \tag{67}$$

$$D_E = (1 + \delta_E^2)^{\frac{1}{2}} \quad , \tag{68}$$

$$\gamma = M/2M_b \quad , \tag{69}$$

$$\Omega = \omega/\omega_o \quad , \tag{70}$$

and

$$\Xi = \omega_1/\omega_o \quad , \tag{71}$$

where ω_1 is the fundamental resonant frequency of each unloaded foundation beam of mass M_b, and

$$\omega_o = (16K/M)^{\frac{1}{2}} \tag{72}$$

is the natural frequency of the machine of mass M when it is supported by the sixteen antivibration mounts considered here on an ideally rigid foundation. The quantity δ_E is the damping factor of the foundation beams.

Four-Span Foundation Beams

The transmissibility across this system follows directly from Eq. (28) in which $h_1 = h_2 = h_3 = h_4$ but the parameter α is given by the modified equation

$$\alpha = 0.591255\ (\Omega/\Xi)^{\frac{1}{2}} \quad . \tag{73}$$

In the frequency ratios $\Omega = \omega/\omega_o$ and $\Xi = \omega_1/\omega_o$, ω_1 is the fundamental resonant frequency of the unloaded foundation beams without intermediate support and ω_o is again given by Eq. (72). Odd values of m through a range of at least 1-99 have always been considered in the summations of Eq. (28). Even values of m do not contribute to transmissibility.

Calculations of transmissibility are plotted in Fig. 12. Here, and throughout, reference is made to a machine that is ten times more massive than the two foundation beams of mass M_b that support it from below ($\gamma = 2M/M_b = 10$), to a beam damping factor $\delta_E = 0.01$, and to a mount damping factor $\delta_K = 0.05$.

Transmissibility is plotted in terms of a frequency ratio $\Omega = \omega/\omega_o$ and is phrased in terms of a second frequency ratio $\Xi = \omega_1/\omega_o$, where ω_1 is the first natural frequency of each complete foundation beam when it is free to vibrate without constraint. A value of $\Xi = 10$ has been employed in the calculations to be described so that, if the natural frequency of the mounting

system is $\omega_o/2\pi$ = 5 Hz, for example, the first foundation resonance occurs at $\omega_1/2\pi$ = 50 Hz. In Fig. 12, the first two peaks occur very near the frequencies ω_o and ω_1, and so are separated by essentially the same factor of 10 in frequency.

The solid-line curve of Fig. 12 shows the transmissibility across the mounting system of Fig. 11(a) when the mounts are equally spaced to represent closely the performance of a rail-type antivibration mount of continuous run. Actually, the distances $h_1 = 0.125a$, $h_2 = 0.375a$, $h_3 = 0.625a$, and $h_4 = 0.875a$, where a is the beam half-length. The peak values of transmissibility at higher frequencies ($\Omega \geq 10$) correspond to the first, second, third, and fourth symmetrical resonances of the foundation beams. At intervening frequencies, the forces transmitted to the beams by the multiple antivibration mountings produce forces of different phase at the beam terminations that conflict with one another to produce minima in the net transmitted force and, hence, in the transmissibility curve.

The dashed-line curve of Fig. 12 shows, for example, how judicious placement of the antivibration mounts, which are now located where $h_1 = 0.063a$, $h_2 = 0.438a$, $h_3 = 0.688a$, and $h_4 = 0.938a$, can effectively reduce the heights of the transmissibility peaks at the second and third symmetric resonances of the foundation beams where $\Omega \approx 54$ and 133. Note, however, that at the fundamental resonance of the foundation beams, where $\Omega \approx 10$, transmissibility takes the much greater value shown in Fig. 12 regardless of the mount locations selected; note also that the choice of some other mount locations can increase rather than reduce the peak values of transmissibility at higher frequencies.

The severe loss in isolation associated with the fundamental resonance of the foundation beams can be mitigated in several ways, one of which is to divide the beams into separate spans. This approach, which is particularly

feasible for long, heavy machinery installations that require multiple antivibration mountings, results in a configuration such as that already referred to in Fig. 11(b), where rigid supports divide the foundation beams into four spans of equal length. The forces exerted on the spans by the antivibration mountings produce equal forces $\tilde{F}_2$ at the original beam terminations and an in-phase force $2\tilde{F}_2$ at each intermediate support. At the supports the beam deflection and slope are constrained to zero.

The transmissibility across the mounting system of Fig. 11(b) is plotted in Fig. 12 as the chain-line curve. Now, because the fundamental resonant frequency of the foundation spans of length a/2 is sixteen times greater than that of the original foundation beams of length 2a, the level of the corresponding transmissibility peak (where $\Omega \approx 160$) is significantly reduced because of the much greater effectiveness of the antivibration mountings at this higher frequency--even though the "abruptness" of the peak remains essentially unchanged. Within the range of frequencies considered, the chain-line transmissibility curve is relatively insensitive to mount location, which in this example actually duplicates the regular mount spacing assumed when the solid-line curve of Fig. 12 was calculated [in Fig. 11(b), the distance $h_1 = 0.125a$]. The second resonance of the foundation spans occurs at frequencies above the range considered here, so that no further transmissibility peaks appear in the chain-line curve of Fig. 12.

Note that the mutual interference observed between forces applied to the foundation beams of single span by judiciously positioned antivibration mountings can be exploited further if fewer mounts are used to support the machine. If the mount stiffness is halved, for example, the transmissibility of either system of Fig. 13 can readily be determined from the foregoing equations; thus, if $h_3 = h_1$ and $h_4 = h_2$ in Fig. 11(a), and if $h_1 = a/4$ in Fig. 11(b), these equations will relate equally well to the mounting systems shown in Figs. 13(a)

and 13(b) where the machine is supported by only four mounts per side.

Representative calculations of the transmissibility across the mounting system of Fig. 13(a) are plotted in Fig. 14 as the solid- and dashed-line curves. The dashed-line curve refers to what will be considered as an average mount spacing with $h_1 = 0.25a$ and $h_2 = 0.75a$. As in Fig. 12, pronounced transmissibility peaks are introduced at higher frequencies ($\Omega \geq 10$) at the first four symmetric resonances of the foundation beams. The solid-line curve shows how, through appropriate choice of mount spacing, it is possible to eliminate almost entirely the transmissibility peak at the second beam resonance where $\Omega \approx 54$. In this example, two of the four mounts shown in Fig. 13(a) are positioned at essentially one-quarter of the beam length from the left- and the right-hand beam terminations ($h_1 = 0.49a$) and the other two mounts are placed close together at the beam center ($h_2 = 0.98a$).

The magnitude of the transmissibility peak at the fundamental beam resonance, where $\Omega \approx 10$, is again uninfluenced by the choice of mount location. However, through division of the foundation beams into four spans--each span supporting a central antivibration mount, as in Fig. 13(b)--the first foundation resonance is again shifted to sixteen times greater frequency ($\Omega \approx 160$) and, as illustrated by the chain-line curve of Fig. 14, the associated transmissibility peak occurs at a greatly reduced level.

4.1.2 Machine with Four Mounts per Side Supported by Single- and by Four-Span Beams to Which a Damping Coating is Applied, or to which Dynamic Vibration Absorbers or Lumped Masses Are Attached

Because transmissibility exhibits a high peak level at the fundamental resonance of the foundation beams considered here, and because it is also likely to do so when nonrigid foundations of other design are utilized, it is appropriate to discuss alternative ways in which such resonances can be suppressed.

One relatively straightforward approach is to damp the foundation beams by applying tiles or a constrained coating of highly dissipative viscoelastic

material.[15-17] For example, if the foundation beams of Fig. 13(a) are treated in this way to increase their damping factor to the value $\delta_E = 0.05$, then the transmissibility shown by the dashed-line curve in Fig. 14, which was calculated for an average mount spacing, becomes that shown by the dashed-line curve in Fig. 15. It is apparent that the peak values of transmissibility have been reduced by essentially 14 dB at the second and higher resonances of the foundation beams, and by 11.5 dB at the fundamental resonance.

Peak values of transmissibility can also be reduced effectively by attaching one or more dynamic vibration absorbers to the foundation beams. A dynamic absorber[1] comprises a lumped mass M_a that is connected via a damped resilient element to a vibrating item or structure, the motion of which is excessive at some resonant frequency. The absorber is tuned to resonate at a closely similar frequency at which its motion becomes relatively large, whereas that of the vibrating item or structure is minimized. Many practical applications of the dynamic vibration absorber have been described recently as, for example, in Refs. 18-23.

Figure 16 shows one foundation beam of single span to which four identical, viscously damped, dynamic absorbers are attached immediately beneath the anti-vibration mounts that support one-half of the mass of the mounted item. The dynamic absorbers, of natural frequency ω_a, are advantageously tuned in this situation to resonate near the frequency ω_1 of the fundamental mode of beam vibration, which is potentially the most troublesome mode. Four dynamic absorbers are likewise positioned on the second foundation beam.

An expression for the transmissibility across this mounting system is as follows:

$$T = \left|\frac{4\tilde{F}_2}{\tilde{F}_1}\right| = \left|\sum_{m=1,3,5,\ldots}^{\infty} \frac{4\theta_m}{(n_m a)} \left[\frac{(\beta^*)^4}{(\beta^*)^4 - 1}\right] U^* [\varphi_m(h_1) + V^* \varphi_m(h_2)]\right| \quad . \qquad (74)$$

Here, as before, the quantities $\varphi_m(h_i)$--(i = 1,2), θ_m, and β^*, are defined by Eqs. (57), (58), and (64), and the values of $(n_m a)$ are specified by Eqs. (59) - (61). In addition,

$$U^* = \lambda^*(\lambda^*\upsilon^* - 1)\,[\lambda^*(B^* - E^*) - 4(\Omega^*)^2]/T^*(\Omega^*)^2 \tag{75}$$

and

$$V^* = [\lambda^*(B^* - A^*) - 4(\Omega^*)^2]/[\lambda^*(B^* - E^*) - 4(\Omega^*)^2] \quad , \tag{76}$$

where

$$\lambda^* = [1 - \Phi^*(\Omega^*)^2] \quad , \tag{77}$$

$$\upsilon^* = [1 - (\Omega^*)^2] \quad , \tag{78}$$

and

$$T^* = \{-[2(\Omega^*)^2(2\lambda^*\upsilon^* - 1) + \lambda^*A^*(\lambda^*\upsilon^* - 1)][2(\Omega^*)^2(2\lambda^*\upsilon^* - 1) + \lambda^*E^*(\lambda^*\upsilon^* - 1)]$$
$$+ [2(\Omega^*)^2 + \lambda^*B^*(\lambda^*\upsilon^* - 1)]^2\}/(\Omega^*)^4 \quad . \tag{79}$$

The quantities A^*, B^*, and E^* are again defined by Eqs. (47), (48), and (51), and Ω^* is given by Eq. (63) in terms of the frequency ratio $\Omega = \omega/\omega_o$, where ω_o is now defined as

$$\omega_o = (8K/M)^{\frac{1}{2}} \quad . \tag{80}$$

Finally,

$$\Phi^* = \gamma_a\Gamma^*/\gamma \quad , \tag{81}$$

an equation in which

$$\gamma_a = 4M_a/M_b \tag{82}$$

and

$$\Gamma^* = \left[\frac{1 + 2j(\omega/\omega_a)\delta_R}{1 - (\omega/\omega_a)^2 + 2j(\omega/\omega_a)\delta_R}\right] , \tag{83}$$

where

$$\frac{\omega}{\omega_a} = \left(\frac{\alpha}{2.36502}\right)^2 \frac{1}{(\omega_a/\omega_1)} = \frac{(\Omega/\Xi)}{(\omega_a/\omega_1)} . \tag{84}$$

In these equations, M_a and ω_a are the mass and the natural frequency of each dynamic absorber; and α, γ, and Ξ are defined by Eqs. (67), (69), and (71). Values of the frequency ratio (ω_a/ω_1) and of the absorber damping ratio δ_R that are advantageously utilized when the mass ratio M_a/M_b takes various values are listed in Table I.

Table I. Values of the frequency ratios ω_a/ω_1 and ω_a/ω_m, and of the damping ratio δ_R, for dynamic absorbers tuned to the fundamental resonance of clamped-clamped beams that have a damping factor $\delta_E = 0.01$ (Ref. 14).

$\gamma_a = 4M_a/M_b$			
Single-Span Beam	Four-Span Beam	ω_a/ω_1 and ω_a/ω_m	δ_R
1.0	0.25	0.644	0.392
0.4	0.10	0.820	0.278
0.25	0.0625	0.880	0.226
0.2	0.05	0.901	0.204
0.1	0.025	0.948	0.147

The results of one calculation of transmissibility across the system are plotted in Fig. 15 as the solid-line curve for which $\gamma_a = 4M_a/M_b = 0.25$ and for which the mounts and dynamic absorbers have the same average spacing as employed when the dashed-line curves of Figs. 14 and 15 were calculated. Despite the fact that each dynamic absorber is only 6.25 percent of the beam mass M_b, the absorbers are together remarkably effective in suppressing the fundamental mode of foundation vibration. In fact, reference to the analogous dashed-line curve of Fig. 14 shows that the absorbers have suppressed the transmissibility peak where $\Omega \approx 10$ by more than a factor of 10 in magnitude. Moreover, as observed previously for cantilever beams[1] and circular plates,[24] not only are the absorbers effective in suppressing the resonance to which they are tuned, but their relatively large damping is also effective in suppressing resonances at higher frequencies. This is because the displacement of the absorber masses decreases rapidly at frequencies above ω_a, so that the masses effectively become "fixed" points from which the absorber dashpots can restrain the vibratory motion of the foundation beams at their higher resonances.

Dynamic vibration absorbers can also be used to suppress the fundamental resonance of the four-span foundation beams considered previously. If the absorbers are attached to the beams at midspan, immediately beneath the antivibration mounts that support the mounted item in the manner of Fig. 13(b), then the relevant expression for the transmissibility across the mounting system becomes

$$T = \left|\frac{16\tilde{F}_2}{\tilde{F}_1}\right| = \left|\left\{\frac{(1 + j\delta_K)\Lambda_1^*}{(1 - \Omega^2 + j\delta_K)[\Lambda_2^* + \zeta^*(\alpha^*/4)\Lambda_3^*] + \gamma(\alpha^*/4)(1 + j\delta_K)\Lambda_3^*}\right\}\right| , \quad (85)$$

where

$$\Lambda_1^* = [\sinh(\alpha^*/4) + \sin(\alpha^*/4)] \quad , \tag{86}$$

$$\Lambda_2^* = [\sinh(\alpha^*/4)\cos(\alpha^*/4) + \cosh(\alpha^*/4)\sin(\alpha^*/4)] \quad , \tag{87}$$

$$\Lambda_3^* = [\cosh(\alpha^*/4)\cos(\alpha^*/4) - 1] \quad , \tag{88}$$

and

$$\alpha^* = (p + jq) \quad . \tag{89}$$

The quantities p and q are again given by Eqs. (65) and (66) in which, as before, the parameter α is given by Eq. (67) in which the frequency ratios $\Omega = \omega/\omega_o$ and $\Xi = \omega_1/\omega_o$, where ω_1 is again the fundamental resonant frequency of the foundation beams prior to their subdivision, and ω_o is defined by Eq. (80). In Eq. (85), γ is the mass ratio defined by Eq. (69), and δ_K is the damping factor of each antivibration mount. Finally,

$$\zeta^* = 4Z_a/j\omega M_b = \gamma_a \Gamma^* \quad , \tag{90}$$

where Γ^* is defined by Eq. (83). The frequency ratio that appears in Eq. (83), however, is given here by the modified equation

$$\frac{\omega}{\omega_a} = \left(\frac{\alpha}{9.46008}\right)^2 \frac{1}{(\omega_a/\omega_m)} \quad , \tag{91}$$

where ω_a is the natural frequency of the absorbers and ω_m is the fundamental resonant frequency of each span of the subdivided foundation beams.

One calculation of transmissibility is plotted in Fig. 15 as the chain-line curve for which, as before, $\gamma_a = 0.25$. The dynamic absorbers, which are

individually as massive as the foundation spans of mass $M_b/4$ to which they are attached, are again extremely effective in suppressing the fundamental span resonance at high frequencies ($\Omega \approx 160$) to which they are tuned. In fact, the entire transmissibility curve differs remarkably little from that of the simple mounting system.

Note that it is a relatively simple matter to examine the effect of loading each of the single- and four-span foundation beams considered in the foregoing by four lumped masses M_a. The appropriate expressions for transmissibility follow directly from those given earlier for foundation beams with attached dynamic absorbers. Thus, in these expressions, it is only necessary to equate the natural frequency of the absorbers to infinity ($\Gamma^* = 1$). A mass-loaded four-span foundation beam is shown, for example, in Fig. 17.

Calculations of the transmissibility across mounting systems with mass-loaded single- and four-span foundation beams are shown in Fig. 18 as the solid- and chain-line curves for which the mass ratio $\gamma_a = 4M_a/M_b = 2.5$. The antivibration mounts have average spacing ($h_1 = 0.25a$, $h_2 = 0.75a$) or, equivalently, are located centrally on each of the foundation spans, as in Fig. 17 ($h_1 = 0.25a$). For comparison, the dashed-line curve shows the transmissibility across the mounting system of Fig. 16. This system utilizes four dynamic absorbers for which $\gamma_a = 4M_a/M_b = 0.25$; that is, the total added mass is only one-tenth of that employed when the companion curves of Fig. 18 were calculated. Here, in addition to the attached dynamic absorbers, the mount spacing is carefully adjusted to avoid essentially all evidence of the transmissibility peak at the second mode of foundation vibration where $\Omega \approx 54$ ($h_1 = 0.49a$ and $h_2 = 0.98a$).

The solid- and chain-line curves demonstrate how the loading masses M_a shift the foundation resonances, and the corresponding transmissibility peaks,

to lower frequencies. Such a shift is always evident when a structure is mass loaded.[1] The shift, which is substantial here because the masses M_a total one-quarter of the machine mass, has the detrimental effect of increasing peak levels of transmissibility at the lower resonances of the foundation beams; for example, the peaks at the fundamental resonances of the single- and four-span foundation beams are increased by 10 and by 15 dB (compare with the dashed- and chain-line curves of Fig. 14, respectively). However, the mechanical impedance of the masses M_a increases in proportion to frequency ω and, at higher frequencies, predominates the beam impedance, which increases essentially as $\sqrt{\omega}$. The overall levels of the transmissibility curves then fall off rapidly. Note that, as far as the single-span beams are concerned, the added mass would be more effective in blocking force transmission at high frequencies if it were concentrated into fewer parts on each beam. Thus, if the mass is separated into too many parts, it merely serves to increase the mass density of the beam rather than to act as an impedance discontinuity--except at very high frequencies above the range of importance here. If, for example, the single-span beams support only two lumped masses and two anti-vibration mounts placed at one-quarter of the beam length from each termination--then in Fig. 18, for the same added mass as involved when the solid-line curve was calculated, the transmissibility peaks at the second ($\Omega \approx 32$), third, and fourth resonances of the foundation beams would drop by an average of 8 dB, although the peak at the fundamental resonance would change very little in magnitude and frequency ($\Omega \approx 6$).[6]

4.13 Compound Mounting of Machine with Four Mounts per Side on Single-Span Beams

This mounting system is pictured in Fig. 19 where both stages of the compound system are supported by four mounts. The lower four mounts are arbitrarily but symmetrically located in pairs about the beam center. An

expression for the transmissibility across the system can be derived as follows:

$$T = \left|\frac{4\tilde{F}_2}{\tilde{F}_1}\right| = \left|\sum_{m=1,3,5,\ldots} \left[\frac{(\beta^*)^4}{(\beta^*)^4 - 1}\right] \frac{4\theta_m}{(n_m a)} \varepsilon^* \left[\varphi_m(h_1) + \alpha^* \varphi_m(h_2)\right]\right| \quad , \tag{92}$$

where θ_m, β^*, $(n_m a)$ and $\varphi_m(h_i)$ are defined by Eqs. (58), (64), (59) - (61), and (57). In addition,

$$\varepsilon^* = \beta(\beta E^* - \beta B^* - \Gamma^*)/[\xi^*(1 + \beta) - \beta\xi^*\lambda(\Omega^*)^2 - 2\beta(A^* + E^*) + 4(\beta B^* + \Gamma^*)] \quad , \tag{93}$$

$$\alpha^* = (\beta A^* - \beta B^* - \Gamma^*)/(\beta E^* - \beta B^* - \Gamma^*) \quad , \tag{94}$$

and

$$\xi^* = [(2 - \beta A^* + \Gamma^*)(\beta E^* - \beta B^* - \Gamma^*) + (2 - \beta B^*)(\beta A^* - \beta B^* - \Gamma^*)] \quad . \tag{95}$$

In these equations, the quantity β is a simple dimensionless constant--it should not be confused with the complex quantity β^* of Eq. (92). The complex quantities A^*, B^*, and E^* are defined by Eqs. (47), (48), and (51). In addition,

$$\gamma = M/2M_b \quad , \tag{96}$$

$$\lambda = (1 + \beta)/(2 + \beta) \quad , \tag{97}$$

$$\beta = M_2/M_1 \quad , \tag{98}$$

$$\Gamma^* = -4(\Omega^*)^2\beta/(2 + \beta) = -\frac{4\Omega^2}{(1 + j\delta_K)} \frac{\beta}{(2 + \beta)} \quad , \tag{99}$$

and

$$na = 2.36502\ (\Omega/\Xi)^{\frac{1}{2}} \quad , \tag{100}$$

where $\Xi = \omega_1/\omega_o$ in which ω_1 is the fundamental resonant frequency of the unloaded foundation beams and ω_o is the reference frequency of the compound system [Eq. (23)].

Representative calculations of transmissibility T made from Eq. (92) are plotted in Fig. 20 as a function of the frequency ratio $\Omega = \omega/\omega_o$. The three solid-line curves refer to values of $\beta = 0.1$, 0.2, and 1.0; for comparison, the dashed-line curve shows the transmissibility across the simple mounting system ($\beta = 0$). The mass and frequency ratios $\gamma = \Xi = 10$. The mount spacing is such that $h_1 = 0.25a$ and $h_2 = 0.75a$. The performance of the compound mounting systems is clearly superior to that of the simple mounting system and becomes more so as frequency increases above the secondary resonant frequencies ω_2 of the compound systems.

4.1.4 Machine with Four Mounts per Side Supported by Floating Foundation Beams of Single Span

When particularly low levels of transmitted force are required at high frequencies, and the use of additional lumped masses to load the foundation beams is not acceptable or sufficiently effective, the mounting system of Fig. 21 can be advantageously employed. Here, additional damped springs of stiffness K_F support each end of the foundation beams to produce a so-called floating foundation. The mounts that support the machine are again located symmetrically about the beam centers, but their position is otherwise arbitrary.

An expression for the transmissibility across the mounting system of Fig. 21 can be derived in terms of the normal modes of vibration of the foundation as follows[11]:

$$T = \left|\frac{4\tilde{F}_2}{\tilde{F}_1}\right| = \left|\frac{(S^*Y^* + W^*X^*)}{2\{Y^*[1 + 2(\Omega^*)^2(P^* - 1)] + X^*[1 + 2(\Omega^*)^2 Q^*]\}}\right| \quad , \tag{101}$$

where

$$P^* = \gamma \sum_{m=1,3,5,\ldots}^{\infty} \frac{\varphi_m^2(h_1)}{\xi^*[(\beta^*)^4 - 1]} \quad , \tag{102}$$

$$Q^* = \gamma \sum_{m=1,3,5,\ldots}^{\infty} \frac{\varphi_m(h_1)\varphi_m(h_2)}{\xi^*[(\beta^*)^4 - 1]} \quad , \tag{103}$$

$$S^* = 2 \sum_{m=1,3,5,\ldots}^{\infty} \frac{\Delta_m \varphi_m(h_1)}{(n_m a)\Psi_m} \left[\frac{(\beta^*)^4}{(\beta^*)^4 - 1}\right] \quad , \tag{104}$$

$$W^* = 4 \sum_{m=1,3,5,\ldots}^{\infty} \frac{\Delta_m \varphi_m(h_2)}{(n_m a)\Psi_m} \left[\frac{(\beta^*)^4}{(\beta^*)^4 - 1}\right] \quad , \tag{105}$$

$$X^* = (P^* - Q^* - 1) \quad , \tag{106}$$

and

$$Y^* = (R^* - Q^* - 1) \quad . \tag{107}$$

In these equations, the mass ratio γ is given by Eq. (96), β^* is given by Eqs. (64) - (66) in terms of α , where

$$\alpha = N_R \, (\Omega/\Xi)^{\frac{1}{2}} \tag{108}$$

and

$$R^* = \gamma \sum_{m=1,3,5,\ldots}^{\infty} \frac{\varphi_m^2(h_2)}{\xi^*[(\beta^*)^4 - 1]} \quad , \tag{109}$$

$$\varphi_m(h_i) = [(\cosh n_m h_i + \cos n_m h_i) - \theta_{m1} \sinh n_m h_i - \theta_{m2} \sin n_m h_i] \qquad (i = 1,2) \tag{110}$$

$$\Psi_m = [1 - 3\Delta_m/(n_m a) + \Delta_m(\theta_{m1} + \theta_{m2})] \quad , \tag{111}$$

$$\Delta_m = - 6 \kappa/(n_m a)^3 \quad , \tag{112}$$

$$\xi^* = - 2 \Psi_m (\Omega^*)^2 \quad , \tag{113}$$

and

$$\Omega^* = \Omega/(1 + j\delta_K)^{\frac{1}{2}} \quad , \tag{114}$$

where h is some fraction of the beam half-length a, and δ_K is the damping factor of each antivibration mount. In addition,

$$\theta_{m1} = (\cosh 2 n_m a - \cos 2 n_m a + 2\Delta_m \sin 2 n_m a)/(\sinh 2 n_m a - \sin 2 n_m a) \quad , \tag{115}$$

$$\theta_{m2} = (\cosh 2 n_m a - \cos 2 n_m a + 2\Delta_m \sinh 2 n_m a)/(\sinh 2 n_m a - \sin 2 n_m a) \quad , \tag{116}$$

$$\kappa = (K_F/K_S) \quad , \tag{117}$$

and

$$\Omega = \omega/\omega_o \quad , \tag{118}$$

where

$$\omega_o = (8K/M)^{\frac{1}{2}} \quad . \tag{119}$$

Here, K is the stiffness of each antivibration mount, K_F is the stiffness of each mount that supports the floating foundation beams, and K_S is the static stiffness of a simply supported beam that is loaded at its midpoint and that has the same dimensions as the two foundation beams under consideration. The values of $n_m a$, which depend here upon the value of the stiffness ratio κ , are the roots of the equation

$$(\sinh na \cos na + \cosh na \sin na) = [12\kappa/(na)^3](\cosh na \cos na) \quad . \tag{120}$$

The roots must be obtained numerically although, when m is very large ($m > 30$) they can be calculated from the equation

$$n_m a = (4m - 5)(\pi/4) \quad . \tag{121}$$

The first thirty roots of Eq. (120) that have been determined when $\kappa = 3$ and $\kappa = 10$, for example, are listed in Tables II and III. In Eq. (108), the value of N_R also depends upon the value of κ , since N_R corresponds to that value of α for which the first resonance of the foundation beams occurs (at the frequency ω_1) when the unloaded beams are supported by a mount stiffness $K_F = \kappa K_S$ at each end. When $\kappa = 3$ and 10, for example, $N_R = 1.47432$ and 1.53953. Finally, in Eq. (108), the frequency ratio

$$\Xi = \omega_1/\omega_o \quad . \tag{122}$$

The normal modes of interest are those of each beam and its supporting springs considered as an entity. The relevant normal functions are specified by

Table II. The first thirty values of $n_m a$ for a floating foundation beam supported at each end by an antivibration mount for which $\kappa = 3$ (Ref. 14).

m	$n_m a$	m	$n_m a$	m	$n_m a$
1	1.47432	11	30.63116	21	62.04653
2	3.22144	12	33.77259	22	65.18811
3	5.61079	13	36.91407	23	68.32970
4	8.66780	14	40.05559	24	71.47128
5	11.79207	15	43.19712	25	74.61287
6	14.92801	16	46.33867	26	77.75446
7	18.06722	17	49.48023	27	80.89604
8	21.20764	18	52.62180	28	84.03763
9	24.34859	19	55.76337	29	87.17922
10	27.48980	20	58.90495	30	90.32081

Table III. First thirty values of $n_m a$ for a floating foundation beam supported at each end by an antivibration mount for which $\kappa = 10$ (Ref. 11).

m	$n_m a$	m	$n_m a$	m	$n_m a$
1	1.53953	11	30.63262	21	62.04671
2	3.92195	12	33.77368	22	65.18826
3	5.89140	13	36.91491	23	68.32983
4	8.73788	14	40.05624	24	71.47140
5	11.81867	15	43.19764	25	74.61297
6	14.94088	16	46.33909	26	77.75455
7	18.07442	17	49.49058	27	80.89612
8	21.21208	18	52.62209	28	84.03770
9	24.35152	19	55.76362	29	87.17929
10	27.49183	20	58.90516	30	90.32087

Eq. (110) in terms of a stiffness ratio $\kappa = K_F/K_S$. Values of a parameter $n_m a$, which specify the corresponding natural frequencies of the floating foundation, and which depend upon the values selected for κ have to be determined numerically as the roots of Eq. (120).

In the analysis of the mounting system, the ends of the foundation beams have been assumed to exert zero bending moment on the supporting springs (as for a simply supported termination) and to share with the springs a common vertical displacement and shearing force. The damping of the foundation has also been considered. However, it is necessary to assign the same damping factor δ_E to both the beams and their supporting springs because they were

together viewed as an entity when the normal modes of foundation vibration were established. In the calculations to be discussed, the damping factor $\delta_E = 0.01$ and the stiffness ratio $\kappa = 3$.

One calculation of the transmissibility across the mounting system is plotted in Fig. 22 as the chain-line curve for which the antivibration mounts beneath the item of machinery have the same average spacing as that employed in the previous calculations. The dashed-line curve is reproduced here from Fig. 14 to show the transmissibility observed, for the same mount spacing, when the foundation beams were clamped rigidly at each end. Note that the transmissibility peaks at the third and fourth resonances of the foundation beams are beneficially absent from the curve calculated for the mounting system of Fig. 21.

To obtain the solid-line transmissibility curve of Fig. 22, it is necessary to adjust the spacing of the upper mounts in Fig. 21 until $h_1 = 0.35a$ and $h_2 = 0.869a$. Moreover, if a different stiffness K_F is chosen for the lower springs that support the foundation beams, and if evidence of the second mode of vibration of the floating foundation is to be kept from the transmissibility curve, then the position of the upper mounts must again be altered. For example, if K_F is increased until the stiffness ratio $\kappa = K_F/K_S = 10$, the upper mounts must be relocated where $h_1 = 0.364a$ and $h_2 = 0.98a$.

Note that the antivibration mounts have always been placed symmetrically about the midpoints of both the clamped and the floating foundation beams considered here, or they have been located at midspan on the multispan beams considered. In this way, only the symmetrical beam modes have been excited. This is an advantage because, if the mount location had been chosen otherwise, the antisymmetric as well as the symmetric beam modes would be excited, and essentially twice the number of foundation resonances and associated peaks would be observed in the preceding transmissibility plots than are presently apparent.

4.1.5 Machine with Four Mounts per Side with Floating Foundation Beam to which Are Attached Lumped Masses of Dynamic Vibration Absorbers at Each Mount Location

The transmissibility T across the "compound" system of Fig. 23 can be stated as follows:

$$T = \left|\frac{4\tilde{F}_2}{\tilde{F}_1}\right| = \left|\frac{C^*(\theta^* Y^* + H^*) + D^*(\theta^* X^* - G^*)}{A^*(\theta^* Y^* + H^*) + B^*(\theta^* X^* - G^*)}\right| \quad , \tag{123}$$

where

$$X^* = (P^* - Q^* - 1) \quad , \tag{124}$$

$$Y^* = (R^* - Q^* - 1) \quad , \tag{125}$$

and

$$A^* = 2\{\theta^*[1 + 2(\Omega^*)^2(P^* - 1)] - 2(\Omega^*)^2[(Q^*)^2(P^* - \Phi^*) - (P^*)^2(R^* + \Phi^*)]\} \quad , \tag{126}$$

$$B^* = 2\{\theta^*[1 + 2(\Omega^*)^2 Q^*] - 2(\Omega^*)^2 Q^*[(Q^*)^2 - P^* R^* - \Phi^*(P^* + R^*)]\} \quad , \tag{127}$$

$$C^* = \{\theta^* S^* + W^* Q^* \Phi^* - S^*[(Q^*)^2 - P^*(R^* + \Phi^*)]\} \quad , \tag{128}$$

$$D^* = \{\theta^* W^* + S^* Q^* \Phi^* - W^*[(Q^*)^2 - P^*(R^* + \Phi^*)]\} \quad , \tag{129}$$

$$G^* = \{(P^* - Q^*)[(Q^*)^2 - P^* R^*] - \Phi^*[(P^*)^2 + (Q^*)^2 - Q^*(P^* + R^*)]\} \quad , \tag{130}$$

and

$$H^* = \{(Q^* - R^*)[(Q^*)^2 - P^* R^*] - \Phi^*[(R^*)^2 + (Q^*)^2 - Q^*(P^* + R^*)]\} \quad . \tag{131}$$

Here P^*, Q^*, S^*, and W^*, X^*, Y^* are as defined by Eqs. (102) - (107), R^* and Ω^* are given by Eqs. (109) and (114), and

$$\theta^* = [(Q^*)^2 - (P^* + \Phi^*)(R^* + \Phi^*)] \quad . \tag{132}$$

All other parameters on which the complex quantities P^*, Q^*, R^*, S^*, and W^*, X^*, Y^* depend are as previously defined; in particular,

$$\alpha = N_R(\Omega/\Xi)^{\frac{1}{2}} \quad , \tag{133}$$

where $\Omega = \omega/\omega_o$, $\Xi = \omega_1/\omega_o$, and $N_R = 1.47432$ or 1.53953 when $\kappa = 3$ or 10, respectively. Finally, the quantity

$$\Phi^* = -\frac{(K^*/j\omega)}{Z} \quad , \tag{134}$$

where appropriate substitution has to be made for the mechanical impedance Z of the particular devices that are attached to the intermediate beams at each mount location. For example, when the beams are loaded by lumped masses M_a, as in Fig. 23, then $Z = j\omega M_a$ and

$$\Phi^* = \frac{K^*}{\omega^2 M_a} = \frac{(\gamma/\gamma_a)}{(\Omega^*)^2} \quad , \tag{135}$$

where $\gamma = M/2M_b$ and $\gamma_a = 4M_a/M_b$. Alternatively, when dynamic absorbers are attached to the beams, as in Fig. 24, then

$$Z = j\omega M_a \Gamma^* \tag{136}$$

and

$$\Phi^* = \frac{(\gamma/\gamma_a)}{(\Omega^*)^2 \Gamma^*} \quad , \tag{137}$$

where

$$\Gamma^* = \left[\frac{1 + 2j(\omega/\omega_a)\delta_R}{1 - (\omega/\omega_a)^2 + 2j(\omega/\omega_a)\delta_R} \right] \quad . \tag{138}$$

Design parameters of the absorbers are the damping ratio δ_R and tuning ratio (ω_a/ω_1), which is related to the frequency ratio (ω/ω_a) of Eq. (138) as follows:

$$\frac{\omega}{\omega_a} = \frac{(\Omega/\Xi)}{\omega_a/\omega_1} \tag{139}$$

Appropriate values of (ω_a/ω_1) and δ_R are those listed in Table I for a single-span beam with clamped terminations. Even though the terminations differ in the two cases, the values of Table I yield very satisfactory results in the present situation.

Representative calculations of transmissibility of the compound system of Fig. 23 are plotted in Fig. 25 as the three solid-line curves for which "β" = 0.1, 0.2, and 1.0. These calculations utilize the mass and frequency ratios $\gamma = \Xi = 10$, and average spacing ($h_1 = 0.25a$ and $h_2 = 0.75a$) of the upper mounts and, hence, of the loading masses M_a. The upper mounts, the intermediate beams, and the lower mounts share a common value of the damping factors $\delta_K = \delta_E = 0.05$. The curves of Fig. 25 were obtained for a common value of $M/2M_b = 10$, the choice of which is equivalent to the adoption of a mass ratio "β" = 0.1. Because it is generally not feasible to generate such large values of "β" as 0.2 and 1.0 by making the intermediate beams uniformly more massive (in the absence of the masses M_a), the choice of values of the mass ratios $\gamma_a = 4M_a/M_b = 1.0$ and 9 effectively yields the values of "β" = 0.2 and 1.0.

In Fig. 25 each curve exhibits three transmissibility peaks at frequencies that are essentially equal to the resonant frequency $\omega_o = (8K/M)^{\frac{1}{2}}$ and to the initial and second resonant frequencies ω_1 and ω_2 of the intermediate beams on their lower mounts of stiffness K_F. As the loading masses M_a and, hence, the values of "β" are increased, ω_1 and ω_2 are shifted to progressively lower frequencies. Above ω_1--the frequency of the "secondary" resonance of the compound system--the levels of the transmissibility curves fall off markedly and lie appreciably below the level of the dashed-line curve for the simple mounting system, except at frequencies in the vicinity of ω_2. The advantages of using large "intermediate" masses to achieve especially low values of transmissibility at high frequencies are again clearly apparent. Moreover, improved high-frequency performance can be obtained through judicious location of the upper mounts of the system. Thus, although the transmissibility peaks at the initial resonance of the intermediate beams are relatively insensitive to mount location, excitation of the second beam resonance can be avoided and evidence of it eliminated entirely from the transmissibility curves. This is true, for example, if the value $h_2 = 0.869a$ is selected in Fig. 33, and if the consecutive values of $h_1 = 0.350a$, $0.437a$, and $0.615a$ are employed when "β" = 0.1, 0.2, and 1.0, respectively. Thus, if the mount locations specified here for the compound system with "β" = 0.2 (namely, $h_1 = 0.437a$ and $h_2 = 0.869a$) are adopted in place of the average spacing utilized hitherto, the transmissibility across the system becomes that shown by the chain-line curve of Fig. 25. No evidence remains in this curve of the significant peak observed previously at the second resonance of the intermediate beams where $\Omega \approx 35$; rather, transmissibility now falls off monotonically at all frequencies above ω_1, decreasing by more than 27 dB in the octave $10 < \Omega < 20$.

Representative calculations of the transmissibility across the mounting system of Fig. 24 are plotted in Fig. 26 for compound systems with $\gamma = M/2M_b = 10$. The dashed-line curve shows the transmissibility across the system of Fig. 23 with $M_a = 0$ so that the mass ratio "β" = 0.1. The upper mounts of the system have average spacing; their damping factor $\delta_K = 0.05$--whereas the lower mounts and the intermediate beams share the damping factor $\delta_E = 0.01$. The solid-line curve shows how the resonance of the intermediate beams at the frequency ω_2 ($\Omega \approx 50$) can be avoided simply by locating the upper mounts where $h_1 = 0.350a$ and $h_2 = 0.869a$. The chain-line curve shows how the "secondary" resonance of the system--namely, the initial resonance of the intermediate beams at the frequency ω_1 ($\Omega \approx 10$)--can be suppressed effectively (essentially by 20 dB) if dynamic absorbers are attached to the intermediate beams in the manner of Fig. 24. Here, the small absorber mass ratio $\gamma_a = 4M_a/M_b = 0.25$, so that $\omega_a/\omega_1 = 0.880$ and $\delta_R = 0.226$, as specified in Table I. Note that, because the favorable mount spacing has been maintained, excitation of the second beam resonance at the frequency ω_2 ($\Omega \approx 50$) has again been virtually avoided. Also note that, for all practical purposes, the values of transmissibility above ω_o become continually smaller as frequency increases into the high-frequency region, where very large uninterrupted reductions of transmitted force have been achieved.

4.2 Platelike Foundations

Considered now is the resilient mounting of a vibrating item of machinery of mass M on platelike substructures that have been modeled as thin, simply supported, square, rectangular, or circular plates with small internal damping and mass M_p. Also considered are plates that have been modified by the attachment of dynamic vibration absorbers or lumped masses at each mount location--or by the introduction of rigid cross members, which divide the square and

rectangular plates into four separate quadrants that are free to vibrate independently of one another.

The item of machinery is supported either by eight or by four antivibration mounts that are arbitrarily, but symmetrically, located with respect to the plate centers. The mounts have complex stiffnesses K^* and small internal damping factors that are governed by Eq. (1). The frequency dependence of K and δ_K is again assumed to be negligible.

A vibratory force $\tilde{F}_1$ acts vertically on the mounted item to produce a total vertical force $\tilde{F}_2$ at the plate boundaries. The force $\tilde{F}_2$ comprises four discrete forces, one at each plate corner, plus a distributed force along the four plate sides. For each of the plate configurations mentioned in the foregoing, transmissibility $T = |\tilde{F}_2/\tilde{F}_1|$ has been calculated in terms of a frequency ratio $\Omega = \omega/\omega_o$ where ω is again the impressed frequency and ω_o is the natural frequency of the mounting system calculated as though the platelike substructures were ideally rigid.

4.2.1 Square Plates

An item of machinery supported by eight identical antivibration mounts on a rectangular plate of mass M_p and sides of lengths a and μa is shown in Fig. 27. For a square plate, the parameter $\mu = 1.0$. The symmetric mount locations are specified by coordinates (h_{1x}, h_{1y}), (h_{2x}, h_{2y}) that describe the distance of two adjacent mounts on one side of the machine from the near plate corner, which is taken as the coordinate origin.

The force transmissibility across the mounting system can be expressed as follows[26]:

$$T = \left| \frac{U^* V^*}{[1 - (\Omega^*)^2 - W^*]} \right| , \qquad (140)$$

where

$$U^* = \sum_{k=1,3,5,\ldots}^{\infty} \sum_{m=1,3,5,\ldots}^{\infty} \frac{16(\beta^*)^4}{\pi^2 km\lambda^*} \left[\varphi_{k,m}(h_{1x},h_{1y}) + \Gamma^* \varphi_{k,m}(h_{2x},h_{2y})\right] \quad , \tag{141}$$

$$V^* = \frac{(1 - B^* + C^*)}{2[(1 + A^*)(1 + C^*) - (B^*)^2]} \quad , \tag{142}$$

$$W^* = \frac{(A^* + 2B^* + C^*) + 2[A^*C^* - (B^*)^2]}{2[(1 + A^*)(1 + C^*) - (B^*)^2]} \quad , \tag{143}$$

and

$$(\Omega^*)^2 = \Omega^2/(1 + j\delta_K) = (\omega/\omega_o)^2/(1 + j\delta_K) \quad . \tag{144}$$

In these equations,

$$A^* = \sum_{k=1,3,5,\ldots}^{\infty} \sum_{m=1,3,5,\ldots}^{\infty} \frac{2\gamma\varphi_{k,m}^2(h_{1x},h_{1y})}{\lambda^*(\Omega^*)^2} \quad , \tag{145}$$

$$B^* = \sum_{k=1,3,5,\ldots}^{\infty} \sum_{m=1,3,5,\ldots}^{\infty} \frac{2\lambda\varphi_{k,m}(h_{1x},h_{1y})\varphi_{k,m}(h_{2x},h_{2y})}{\lambda^*(\Omega^*)^2} \quad , \tag{146}$$

$$C^* = \sum_{k=1,3,5,\ldots}^{\infty} \sum_{m=1,3,5,\ldots}^{\infty} \frac{2\gamma\varphi_{k,m}^2(h_{2x},h_{2y})}{\lambda^*(\Omega^*)^2} \quad , \tag{147}$$

$$\Gamma^* = \left[\frac{1 + A^* - B^*}{1 - B^* + C^*}\right] \quad , \tag{148}$$

$$\varphi_{k,m}(h_{ix},h_{iy}) = \sin k\pi(h_i x/a)\sin m\pi(h_i y/\mu a) \quad , \quad (i = 1,2) \tag{149}$$

$$\lambda^* = [(\beta^*)^4 - 1] \quad , \tag{150}$$

and

$$\beta^* = \frac{n_{k,m}a}{n^* a} = \frac{\pi[k^2 + (m/\mu)^2]^{\frac{1}{2}}}{(p + jq)} \quad , \tag{151}$$

$$\gamma = M/M_p \quad . \tag{152}$$

In equation (151), p and q are given by Eqs. (65) and (66), where $\alpha = na$, provided that the damping factors δ_E and δ_G associated with the Young's modulus and shear modulus deformations of the plate material are equal, as may realistically be assumed.[1,25,26] Finally, the frequency ratio Ω and the dimensionless product na are related as follows:

$$\Omega = (\tfrac{1}{2}\, na)^2 \Xi / N_{R1}^2 \quad , \tag{153}$$

where

$$N_{R1} = \pi(1 + \mu^2)^{\frac{1}{2}}/2\mu \tag{154}$$

is the value taken by $(\frac{1}{2}\, na)$ at the fundamental resonant frequency ω_{11} of the unloaded plate, and

$$\Xi = \omega_{11}/\omega_o \quad . \tag{155}$$

Odd integral multiples of k and m appear in the summations of Eqs. (141) and (145) - (147) because only the symmetrical plate modes contribute

to plate transmissibility.[25,27,28] Whereas forces are transmitted to the plate boundaries when the antisymmetric modes are excited (k and m even) the net upward and downward components of these forces counter one another exactly. Values of k and m through a range of at least 1-99 have been employed in all summations evaluated.

When the item of machinery is supported by only four antivibration mounts, as in Fig. 27(b), $h_{1x} = h_{2x}$, and $h_{1y} = h_{2y}$, so that Eqs. (145) - (147) for A^*, B^* and C^* become identical; and the expression for transmissibility reduces to

$$T = \left| \frac{T^*}{[1 - (\Omega^*)^2 - \gamma\xi^*]} \right| \quad , \tag{156}$$

where

$$T^* = \sum_{k=1,3,5,\ldots}^{\infty} \sum_{m=1,3,5,\ldots}^{\infty} \frac{16(\beta^*)^4 \varphi_{k,m}(h_x,h_y)}{\pi^2 km\lambda^*} \tag{157}$$

and

$$\xi^* = \sum_{k=1,3,5,\ldots}^{\infty} \sum_{m=1,3,5,\ldots}^{\infty} \frac{4\varphi_{k,m}^2(h_x,h_y)}{\lambda^*} \quad . \tag{158}$$

Note that, for the system of Fig. 27(a), the natural mounting frequency ω_o is defined as

$$\omega_o = (8K/M)^{\frac{1}{2}} \quad ; \tag{159}$$

whereas, for the system of Fig. 27(b),

$$\omega_o = 2(K/M)^{\frac{1}{2}} \quad . \tag{160}$$

Plotted in Fig. 28 are the results of transmissibility calculations made from Eq. (140) for a vibrating machine supported by eight mounts on a square plate ($\mu = 1.0$) having the small damping factors $\delta_E = \delta_G = 0.01$. The mounts are uniformly spaced such that $h_{1x} = 0.2a$, $h_{2x} = 0.4a$, and $h_{1y} = h_{2y} = a/3$; here, and subsequently, the mount damping factors $\delta_K = 0.05$. The mass and frequency ratios $\gamma = M/M_P = 4$ and $\Xi = \omega_{11}/\omega_o = 4$. The transmissibility when the plate is ideally rigid is shown by the dashed-line curve. Note that the first transmissibility peak in the solid-line curve occurs at a smaller value of the frequency ratio $\Omega = \omega/\omega_o$ than unity because the effective stiffness of the mounts is reduced by the plate flexibility. Again, the second peak occurs at a greater value of Ω than 4 because the natural frequencies of the plate are shifted to higher frequencies by the springlike constraint exerted on it by the mounts.

The transmissibility curve of Fig. 28 is characterized by many resonances as compared to curves that have been calculated for an item of machinery supported by beamlike and modified beamlike substructures (Sec. 4.1). Furthermore the solid-line curve of Fig. 28 is typical of many other curves that have been calculated for a variety of mount locations. For example, no advantage exists to deploying the eight mounts in circular configurations of different radii and equal angular spacings about the plate center. Nor can customary linear mount configurations be found that provide noticeably reduced numbers or levels of transmissibility peaks.

By contrast, judicious choice of mount locations is possible when an item of machinery is supported by only four mounts, and results superior to those of Fig. 28 can be obtained. Unfortunately, the use of other, less favorable mount locations can then greatly increase the extent to which the plate resonances are excited. This is evident in Fig. 29, which relates to the same square plate as before and to four mounts having symmetrical locations specified by $h_x/a = h_y/a = 0.25$. The mass and frequency ratios $\gamma = \Xi = 4$ remain unchanged in value.

The transmissibility curve is now far more "spiky" than in Fig. 28, and the plate will respond more strongly than before to the amplitudes of the disturbing frequencies from the mounted item. However, by contracting the mount separation until $h_x/a = h_y/a = 1/3$, the transmissibility curve of Fig. 30 is obtained with a smaller density of resonances; in fact, this judicious choice of mount locations has halved the number of plate resonances that are excited. Thus, excitation by an impressed force of any mode of plate vibration, other than the first, can be avoided[28] if the force is located at any point on a nodal line of the particular mode of concern. This fact has been used to advantage in the present situation, where each of the four mounts is located on nodal lines of the [(3,1), (1,3)], (3,3), [(5,3), (3,5)], [(7,3), (3,7)], ..., modes, which are no longer excited; rather, only the following sequence of symmetrical modes is observed: (1,1), [(5,1), (1,5)], [(7,1), (1,7) (5,5)], [(7,5), (5,7)], ...

4.2.2 Circular Plates

The possibility has been examined of mounting machinery on circular plate-like floor areas. Such an area, for example, could be supported around its perimeter by a rigid circular rib and be separated by an expansion joint from the adjacent floor areas of the square or rectangular machinery room in which it is located. This situation is modeled in Fig. 31(a), where a simply supported circular plate is excited symmetrically by four, equal, in-phase vibratory forces. The forces are transmitted from an item of machinery of mass M by mounts of equal stiffness that are located on the plate at equal distances $\lambda a'$ from the plate center, where a' is the plate radius (and, thus, the half-length of the sides of the circumscribing square). The parameter λ, which should not be confused with the complex quantity of Eq. (150) is chosen such that $0 < \lambda < 1.0$.

The force transmissibility T across the mounting system to the plate boundaries is governed by the equation[25]

$$T = |\Psi^*/[1 - (\Omega^*)^2 + \theta^*]| \quad , \tag{161}$$

where

$$\theta^* = \gamma(n^*a')\Phi^*/\lambda \quad , \tag{162}$$

$$\Psi^* = \left[\frac{(J_{o\lambda}I_o + I_{o\lambda}J_o) - \phi_a^*,(J_{o\lambda}I_1 + I_{o\lambda}J_1)}{2J_oI_o - \phi_a^*,(J_oI_1 + J_1I_o)}\right]_{(n^*a')} \quad , \tag{163}$$

and Ω^* is again given by Eq. (144) in which

$$\Omega = (na')^2\Xi/(2.2325)^2 \quad . \tag{164}$$

As before, $\Xi = \omega_{11}/\omega_o$, where ω_{11} is now the fundamental resonant frequency of the circular plate of mass M_p. In addition, $\gamma = M/M_p$, and

$$\Phi^* = R^*/S^* \quad , \tag{165}$$

where

$$R^* = \lambda\{2\Lambda\phi_a^*,(J_{o\lambda}I_{o\lambda}) - (n^*a')(J_{o\lambda}Y_{o\lambda} + \Lambda K_{o\lambda}I_{o\lambda})[\phi_a^*,(J_1I_o + J_oI_1) - 2J_oI_o]$$

$$+ (n^*a')(J_{o\lambda}^2)[\phi_a^*,(Y_1I_o + I_1Y_o) - 2Y_oI_o] + \Lambda(n^*a')(I_{o\lambda})^2[\phi_a^*,(J_1K_o - K_1J_o) - 2J_oK_o]\}_{(n^*a')} \tag{166}$$

and

$$S^* = -4\Lambda[\phi^*_{a'}(J_1 I_o + J_o I_1) - 2J_o I_o]_{(n^* a')} \quad . \tag{167}$$

In these equations, such abbreviations as J_o, I_1, $Y_{o\lambda}$, and $K_{o\lambda}$ have been used to represent the ordinary and modified Bessel functions $J_o(n^* a')$, $I_1(n^* a')$, $Y_o(\lambda n^* a')$, and $K_o(\lambda n^* a')$; in addition,

$$\Lambda = 2/\pi \tag{168}$$

and

$$\phi^*_{a'} = (1 - \nu)/(n^* a') \quad . \tag{169}$$

where ν is Poisson's ratio. All Bessel functions have the complex argument $n^* a'$, a dimensionless product that is given by Eqs. (65) and (66) in which the quantity α is replaced by na', where a' is currently the plate radius.

Selection of the values $\lambda = 0.4714$ and 0.7071 yields mount locations that are congruent to those utilized on the square plates considered in Figs. 30 and 29, where $h_x/a = h_y/a = 1/3$ and $1/4$, respectively. For example, the solid-line transmissibility curve of Fig. 32 has been calculated from Eq. (161) with the mass and frequency ratios $\gamma = \Xi = 4$ and the plate damping factors $\delta_E = \delta_G = 0.01$, as before, and with mount locations specified by the value $\lambda = 0.7071$. Although these mount locations were previously associated with a pronounced resonant response of the square plate considered in Fig. 29, only one-third of the number of resonant peaks is now in evidence. Moreover, the dashed-line curve of Fig. 32 shows how the mount spacing can be contracted to avoid the excitation of the second symmetrical plate resonance; thus, because the mounts now lie on the single nodal circle (for which $\lambda = 0.4414$) accompanying this resonance, the normally anticipated transmissibility peak ($\Omega \approx 25$) has been replaced by a broad trough of significantly lower level.

To conclude, it should be recognized that an effective example has been considered in the foregoing, and that the overall reduction in the number of plate resonances would be much smaller had comparison been made, for example, between transmissibility curves calculated (1) for the judicious mount locations chosen on the square plate of Fig. 30, and (2) for the corresponding locations (λ = 0.4714) on the circular plate. This is not because the adoption of the circular plate would be ineffective but, rather, because the judicious choice of mount locations had proved extremely effective in the first instance.

4.2.3 Quadrant Plates

The possibility of mounting machinery on divided plates has also been examined. Thus, in Fig. 31(b) a rectangular plate is cut by expansion joints into four identical quadrants that are supported by ideally rigid cross members. Each quadrant is assumed to have simply supported boundaries, to be free to vibrate independently of the other three quadrants, and to be driven solely by the force transmitted by a single antivibration mount. The four impressed forces of Fig. 31(b) are assumed to have equal magnitude and phase, as in Fig. 31(a) and Sec. 4.2.2, and to be symmetrically located. Because the quadrants have a fundamental resonant frequency that is four times higher than that of the undivided plate, the vibration levels and the transmitted forces at this fundamental resonance, and at higher resonances, will be reduced significantly because the antivibration mounts will have greater effectiveness at these higher frequencies.

If transmissibility T is defined as the total magnitude of the output forces at the boundaries of the quadrants divided by a force $\tilde{F}_1$ impressed as in Fig. 27(b), and if the quadrant sides have the lengths a' = a/2 and μa' = μa/2, then it can be verified that

$$T = \left| \frac{(T^*)'}{[1 - (\Omega^*)^2 - \gamma(\xi^*)']} \right| \quad , \tag{170}$$

where $(T^*)'$ and $(\xi^*)'$ are given by Eqs. (157) and (158) in which β^* and $\varphi_{k,m}(h_x,h_y)$ have been replaced by

$$(\beta^*)' = \frac{\pi[k^2 + (m/\mu)^2]^{\frac{1}{2}}}{(n^* a')} \tag{171}$$

and

$$\varphi_{k,m}(h_{x'},h_{y'}) = \sin k\pi(h_{x'}/a') \sin m\pi(h_{y'}/\mu a') \quad . \tag{172}$$

In Eq. (172), the coordinates $h_{x'}$ and $h_{y'}$ describe the distance of the mounting point on the lower left-hand quadrant plate of Fig. 31(b) from the near plate corner. In addition, the summations of Eq. (158) now encompass every integral value of k,m = 1,2,3,..., the parameter Ω^* is defined by Eq. (144) in which

$$\Omega = \frac{(na')^2 \Xi}{N_{R1}^2} \quad , \tag{173}$$

and $\gamma = M/M_p$. Here, as before, the mass M_p, the quantity N_{R1} Eq. (154) , and the frequency ratio $\Xi = \omega_{11}/\omega_o$, relate to the <u>undivided</u> plate having sides of lengths a and μa. Finally, the parameter $n^* a'$ in Eq. (171) is specified by Eqs. (65) and (66) in which the parameter α is given by Eq. (67) in which a is replaced by a' = a/2.

Transmissibility calculations that have been made from Eq. (170) for a square plate (μ = 1.0) having square quadrants are plotted in Fig. 33. For both curves of this figure, the mass and frequency ratios $\gamma = \Xi = 4$; the plate damping factors $\delta_E = \delta_G = 0.01$, as in all previous plate calculations. The

mounts are also located as they were on the undivided plates. Thus, the solid- and dashed-line curves have been calculated for $h_{x'}/a' = h_{y'}/a' = 1/2$ and 2/3--values for which the mount locations match those utilized in Figs. 29 and 30, respectively. The fundamental resonance of the quadrant plates is seen to occur at a frequency that is essentially four times higher than that of the fundamental plate resonance evident in the prior figures; namely, it occurs where $\Omega \approx 16$, as expected. Moreover, for both mount locations, the quadrant-plate resonances excited are only one-third as numerous as the resonances evident in Figs. 29 and 30 through the same frequency range of calculation.

The judicious mount locations of Fig. 30 have remained equally effective in Fig. 33 and have resulted in the appearance in the dashed-line curve of only three quadrant-plate resonances, except for minute responses from the [(2,1), (1,2)], (2,2) modes where $\Omega \approx 40$ and 64. (These modes, which are nonsymmetrical, would not be excited were the quadrant plates unconstrained by the antivibration mounts.) Effectively, then, only the (1,1), [(5,1), (1,5)], and [(7,1), (1,7), (5,5)] modes of the quadrant plates give rise to resonances in the dashed-line curve of Fig. 33, and the excitation of the [(3,1), (1,3)], (3,3), and [(5,3), (3,5)] modes at intervening frequencies has been avoided because the antivibration mounts have been located at points on nodal lines of these modes. Although the predicted performance of the quadrant plates does require that the supporting cross members [Fig. 31(b)] remain rigid at all frequencies, the use of such plates appears to represent one effective approach to mounting machinery on platelike floor areas.

4.2.4 Rectangular Plates

Rectangular plates that have identical aspect ratios $\mu = 0.5$ are considered in this section. The effectiveness of mounting machinery on quadrant plates is illustrated again in Fig. 34. The value of attaching dynamic vibration absorbers

or lumped masses to undivided plates at each mount location is demonstrated subsequently.

The transmissibility curves of Fig. 34 have been determined for new values of the mass and frequency ratios $\gamma = M/M_p = 6$ and $\Xi = \omega_{11}/\omega_o = 5$, and for values of the mount and plate damping factors $\delta_K = 0.05$ and $\delta_\Xi = \delta_G = 0.01$ that will be utilized throughout this section. The solid-line curve relates to the mounting configuration of Fig. 27(a), where eight antivibration mounts are uniformly spaced beneath the item of machinery such that $h_{1x} = 0.2a$, $h_{2x} = 0.4a$, and $h_{1y} = h_{2y} = \mu a/3 = a/6$. The dashed-line curve shows how the number of transmissibility peaks can be reduced significantly if four antivibration mounts are deployed on the quadrant plates of Fig. 31(b) such that $h_{x'} = 2a'/3$, $h_{y'} = 2\mu a'/3 = a'/3$. For these judicious mount locations, the (3,1), (1,3), (3,3), (5,3), ..., modes of the quadrant plates ($\mu = 1/2$) are not excited.

For the undivided plate, the fundamental resonance that occurs at the frequency ω_{11} is the most pronounced and potentially the most troublesome plate resonance encountered. Here, in Fig. 34, the severe loss in isolation observed at the frequency ω_{11} has been mitigated by the introduction of the quadrant plates. Thus, the transmissibility peak at the fundamental resonance of the quadrants ($\Omega \approx 20$) lies some 13.5 dB beneath the peak at the fundamental resonance of the undivided plate ($\Omega \approx 6$) even though it remains essentially as "abrupt" as before.

Peak values of transmissibility can also be reduced effectively by attaching dynamic vibration absorbers to the undivided plate, for example, at all four mount locations. One such dynamic absorber is shown in the broken area of Fig. 35(a). The four dynamic absorbers have identical design, and each comprises a lumped mass M_a that is connected by a spring of stiffness K_a and a dahspot of coefficient of viscosity η_a to the plate, the motion of which is excessive at some resonant frequency that, in this instance, is taken to be ω_{11}. The absorbers

are tuned to resonate at a frequency neighboring ω_{11} at which their motion becomes relatively large, whereas the motion of the plate and the force transmitted to its boundaries are minimized. The absorbers have natural frequencies $\omega_a = (K_a/K_a)^{\frac{1}{2}}$ and damping ratios $\delta_R = (\eta_a/\eta_{ac}) = (\omega_a \eta_a/2K_a)$, where η_{ac} is the value of the coefficient of viscosity required to damp the absorbers critically.[1]

The transmissibility across the mounting system of Fig. 35(a) can be expressed as follows:[25]

$$T = \left| \frac{T^*}{\{[1 - (\Omega^*)^2](1 - \gamma_a \xi^* \theta^*) - \gamma \xi^*\}} \right| \quad , \tag{174}$$

where Ω^*, γ, T^*, and ξ^* are given by Eqs. (144), (152), (157), and (158), and

$$\theta^* = \frac{(1 + j\Delta_a)}{[1 - \Omega_m^2(\omega_{11}/\omega_a)^2 + j\Delta_a]} \quad . \tag{175}$$

In these equations,

$$\gamma_a = 4M_a/M_P \quad , \tag{176}$$

$$\Delta_a = 2(\omega_{11}/\omega_a)\Omega_m \delta_R \quad , \tag{177}$$

and

$$\Omega_m = \frac{\omega}{\omega_{11}} = \frac{\omega/\omega_o}{\omega_{11}/\omega_o} = \frac{\Omega}{\Xi} \quad , \tag{178}$$

where Ω and Ξ are again related by Eq. (153). The so-called tuning ratio ω_a/ω_{11} and the damping ratio δ_R are design parameters of the dynamic absorbers, and the choice of suitable values for them is important if the full effectiveness

of the absorbers is to be realized. The values chosen in this situation are those determined previously for a single absorber[29] attached to the midpoint of a rectangular plate that is driven centrally by a vibratory point force (Table IV). Although four dynamic absorbers are now attached to the plate that is driven simultaneously by four noncentral point forces, the absorber tuning and damping ratios established previously[29] have been found to yield very satisfactory results in the present situation. (Note that the tuning and damping ratios should relate to an absorber of mass M_a not $4M_a$. For example, if $\gamma_a = 4M_a/M_p = 0.2$, the appropriate values of $\omega_a/\omega_{11} = 0.869$ and $\delta_R = 0.268$ are those listed in Table IV for an absorber of mass $M_a = 0.05 \times M_p$ that is attached to a rectangular plate of aspect ratio $\mu = 1/2$.

The effectiveness of the dynamic absorbers is illustrated in Fig. 36, where the dashed-line curve relates to the transmissibility across the mounting system of Fig. 27(b) supported by a rectangular plate for which $\gamma = 6$, $\Xi = 5$, and $\mu = 1/2$. The four antivibration mounts are again located judiciously where $h_x/a = h_y/\mu a = 1/3$. The solid-line curve predicts the transmissibility across a duplicate mounting system to which four dynamic absorbers are attached in the manner of Fig. 35(a). The absorbers have the mass ratio $\gamma_a = 0.2$, so that the appropriate values of ω_a/ω_{11} and δ_R are those specified in the foregoing. Although each absorber has only 5% of the plate mass, the absorbers are highly effective in suppressing the fundamental plate resonance to which they are tuned. In fact, the transmissibility peak where $\Omega \approx 6$ has essentially been suppressed by a factor of 10 in magnitude. Moreover, as observed previously for foundation beams with clamped terminations, the relatively large damping ratio of the absorbers is also markedly effective in suppressing the plate resonances at higher frequencies, particularly those adjoining ω_{11}. It is encouraging that the practical design of absorbers to suppress resonant floor motion has been discussed in Refs. 30 and 31.

Table IV. Optimum values of the frequency ratio $(\omega_a/\omega_{11})_{opt}$, and of the damping ratio $(\delta_R)_{opt}$, and the corresponding values of $(T)_{max}$ for dynamic absorbers tuned to the fundamental resonance ω_{11} of three simply supported plates (Ref. 29).

	μ = 1/2			μ = 1/3			μ = 1.0		
M_a/M_P	$(\omega_a/\omega_{11})_{opt}$	$(\delta_R)_{opt}$	(T_{max})	$(\omega_a/\omega_{11})_{opt}$	$(\delta_R)_{opt}$	$(T)_{max}$	$(\omega_a/\omega_{11})_{opt}$	$(\delta_R)_{opt}$	$(T)_{max}$
0.025	0.932	0.192	7.010	0.941	0.200	7.125	0.928	0.189	6.977
0.05	0.869	0.268	5.026	0.880	0.292	5.155	0.865	0.260	4.990
0.1	0.760	0.369	3.592	0.763	0.424	3.712	0.758	0.350	3.564
0.25	0.537	0.520	2.322	0.611	0.600	2.994	0.547	0.482	2.316

Next, it is instructive to consider plates that are mass loaded at each mount location, as in Fig. 35(b). The transmissibility in this case follows readily from Eq. (174) when it is recognized that the dynamic absorbers of Fig. 35(a) will degenerate into lumped masses M_a if the absorber springs or dampers are made infinitely stiff or viscous. In either case, the parameter $\theta^* = 1.0$ in Eq. (175). No other modification is required. Representative calculations of transmissibility appear in Fig. 37, where the dashed-line curve shows the transmissibility across the basic mounting system of Fig. 27(b) for which $\mu = 1/2$. Once again, $\gamma = \Xi = 4$, and the antivibration mounts are judiciously located where $h_x/a = h_y/\mu a = 1/3$. The transmissibility across an identical mounting system to which lumped masses have been added at each mount location, as in Fig. 35(b), is shown by the solid-line curve. The total added mass is equal to that of the mounted item of machinery; namely, $\gamma_a = 4M_a/M_p = 4$. Use of such heavy mass loading is necessary if the overall level of the transmissibility curve is to be reduced significantly. For a value of $\gamma_a = 1.0$, the resultant transmissibility curve would lie approximately halfway between the solid- and dashed-line curves at frequencies above the fundamental plate resonance ($\Omega \approx 3$). Adoption of a mass ratio as small as 0.2--that of the dynamic absorbers used previously--would be ineffectual in reducing transmissibility much below the level of the dashed-line curve, except at very high frequencies where the impedance of the loading masses M_a would eventually predominate the plate impedance.

The masses M_a shift the plate resonances and the accompanying transmissibility peaks to lower frequencies as the solid-line curve ($\gamma_a = 4$) of Fig. 37 indicates. Such a frequency shift, which is always apparent when a structure is mass loaded,[1,14,29] has the detrimental effect here of increasing the level of the transmissibility peak at the frequency ω_{11} of the

fundamental plate resonance. However, at higher frequencies, adoption of the substantial mass ratio has provided very large reductions in transmissibility. In fact, no transmissibility peaks are evident (within the decibel range considered) once the frequency ratio $\Omega > 88$. Although the use of quadrant plates would yield considerably fewer transmissibility peaks than presently appear in the dashed-line curve of Fig. 37, it should be recognized that, for the quadrant plates, the transmissibility would follow the level of the dashed-line curve rather than the greatly reduced level of the solid-line curve for the mass-loaded plate of Fig. 35(b).

4.2.5 Compound Mounting of Machine with Four Mounts on Rectangular Plate

Finally, the performance of the compound mounting system has been analyzed when it is supported by four antivibration mounts on a simply supported rectangular plate. The relevant transmissibility equation is as follows:

$$T = \left| \frac{\displaystyle\sum_{k=1,3,5,\ldots}^{\infty} \sum_{m=1,3,5,\ldots}^{\infty} \frac{16}{\pi^2 km} \left[\frac{(\beta^*)^4}{(\beta^*)^4 - 1}\right] \varphi_{k,m}(h_x,h_y)}{1 - 2\lambda(\Omega^*)^2 + \frac{\lambda\beta}{(2+\beta)}(\Omega^*)^4 - \gamma(1+\beta)R^* \displaystyle\sum_{k=1,3,5,\ldots}^{\infty} \sum_{m=1,3,5,\ldots}^{\infty} \frac{4\varphi^2_{k,m}(h_x,h_y)}{[(\beta^*)^4 - 1]}} \right| , \tag{179}$$

where λ, β, Ω^*, $\varphi_{k,m}(h_x,h_y)$ and β^* are given by Eqs. (97), (98), (144), (149), and (151), respectively. In addition,

$$R^* = \left[1 - \frac{\beta}{(2+\beta)}(\Omega^*)^2\right] \tag{180}$$

and

$$\gamma = M_1/M_p \quad , \tag{181}$$

where M_1 is the machine mass. Also, in Eq. (144),

$$\Omega = \left(\frac{na}{2}\right)^2 \frac{\Xi}{N_{R1}^2} \quad , \tag{182}$$

where

$$N_{R1} = \left(\frac{\pi}{2\mu}\right) (1 + \mu^2)^{\frac{1}{2}} \quad . \tag{183}$$

Representative calculations of the performance of the compound mounting system are illustrated in Fig. 38, the solid-line curves of which relate to compound systems supported on a rectangular plate for which $\mu = 1/2$. The mass and frequency ratios $\gamma = \Xi = 4$, where now $\Xi = \omega_{11}/\omega_o$ in which ω_o is the reference frequency of the compound system [Eq. (23)]. In addition, in the frequency ratio $\Omega = \omega/\omega_o$, ω_o is also this reference frequency. Shown in Fig. 38 are the performances of the compound systems with mass ratios $\beta = M_2/M_1 = 0.1$, 0.2, and 1.0. For comparison, the dashed-line curve shows the performance of the simple mounting system ($\beta = 0$). For all curves, the anti-vibration mounts are favorably located where $h_x/a = h_y/\mu a = 1/3$. As before, the excellence of the performance of the compound system at high frequencies is clearly apparent, especially for the largest mass ratio $\beta = 1.0$, which attenuates greatly the magnitudes of the higher plate resonances.

ACKNOWLEDGMENTS

The assistance of Adah A. Wolfe in obtaining the curves of the figures in this report is acknowledged with gratitude. The investigation was sponsored jointly by the U. S. Naval Sea Systems Command, Ship Silencing Division, and by the U. S. Office of Naval Research.

REFERENCES

1. J. C. Snowdon, Vibration and Shock in Damped Mechanical Systems (John Wiley and Sons, Inc., New York, 1968).

2. M. Harrison, A. O. Sykes, and M. Martin, "Wave Effects in Isolation Mounts," J. Acoust. Soc. Am. 24, 62-71 (1952).

3. E. E. Ungar and C. W. Deitrich, "High-Frequency Vibration Isolation," J. Sound Vib. 4, 224-241, (1966).

4. A.Major, Vibration Analysis and Design of Foundations for Machines and Turbines (Collet's Holdings, Ltd., London, 1962).

5. L. S. Jacobsen and R. S. Ayre, Engineering Vibrations (McGraw-Hill Book Company, Inc., New York, 1958).

6. J. C. Snowdon, "Isolation and Absorption of Machinery Vibration," Acustica 28, 307-317 (1973).

7. E. G. Fischer and H. M. Forkois, "Practice of Equipment Design," contribution to Shock and Vibration Handbook, ed. by C. M. Harris and C. E. Crede (McGraw-Hill Book Company, Inc., New York, 1961) Chap. 43, pp. 43.1 - 43.40.

8. R. M. Gorman, "Design and Advantages of a Two-Stage Mounting System for Major Machines in Ship's Engine Room," Shock Vib. Bull. 35, No. 5, 227-234 (1966).

9. W. I. Young and R. J. Hanners, "Compound Two-Stage Resilient Isolation Mounting for Use in Attenuating Mechanical Vibrations," U. S. Patent 3,764,100 (October 9, 1973).

10. L. W. Foster, "One-Stage and Two-Stage Vibration Isolators As Applied to High-Speed Textile Spindles to Achieve Noise Reduction," J. Mech. Des., Trans. ASME, 100, 33-40 (1978).

REFERENCES -- CONTINUED

11. J. C. Snowdon, "Compound Mounting Systems that Incorporate Dynamic Vibration Absorbers," J. Engr. Ind., Trans. ASME, Ser. B, 97, 1204-1211 (1975).

12. W. H. Adams, R. H. Bennett, Jr., J. W. Schendel, and J. D. Van Dyke, Jr., "Cabin Engine Sound Suppressor," U. S. Patent 3,487,888 (January 6, 1970).

13. R. R. Wilson and C. A. Brebbia, "Dynamic Behavior of Steel Foundations for Turbo-Alternators," J. Sound Vib. 18, 405-416 (1971).

14. J. C. Snowdon, "Isolation of Machinery Vibration from Nonrigid Substructures Using Multiple Antivibration Mountings," contribution to Isolation of Mechanical Vibration, Impact, and Noise, edited by J. C. Snowdon and E. E. Ungar (American Society of Mechanical Engineers, New York, September, 1973) Chapter 5, pp. 102-127.

15. G. E. Warnaka, "Effect of Adhesive Stiffness on Extensional Damping," ASME Reprint No. 67-VIBR-41.

16. E. E. Ungar, "Loss Factors of Viscoelastically Damped Beam Structures," J. Acoust. Soc. Am. 34, 1082-1089 (1962).

17. T. R. Yoos, Jr., and F. C. Nelson, "Damping of Low-Frequency Vibration by Constrained Viscoelastic Layers," ASME Reprint 67-VIBR-62.

18. P. H. Allaway and P. Grootenhuis, "Unusual Techniques for the Control of Structural Vibration," Paper L36 in Proc. Fifth Intern. Congr. Acoust., Liege (Fifth ICA Committee, Liege, 1965), Pt. 1(b).

19. D. I. G. Jones, A. D. Nashif, and R. L. Adkins, "Effect of Tuned Dampers on Vibrations of Simple Structures," J. Am. Inst. Aeronaut. Astronaut., 5, 310-315 (1967).

20. D. B. Shotwell, "Application of Tuned and Damped Dynamic Absorber to Rubber-Tired Earthmoving Machines," ASME Reprint 67-VIBR-64.

REFERENCES -- CONTINUED

21. J. J. O'Leary, "Reduction in Vibration of the CH-47C Helicopter Using a Variable Tuning Vibration Absorber," Shock Vib. Bull, 40, Pt. 5, 191-202 (1969).

22. R. H. Bennett, Jr., J. D. Van Dyke, Jr., "Aircraft Cabin Noise Reduction System with Tuned Vibration Absorbers," U. S. Patent No. 3,490,556 (January 20, 1970).

23. R. L. Eshleman, "Shock and Vibration Technology with Reference to Electrical Systems," NASA Technology Utilization Monograph, NASA SP-5100, 1972.

24. J. C. Snowdon, "Mechanical Four-Pole Parameters and Their Application," J. Sound Vib. 15, 307-323 (1971).

25. J. C. Snowdon, "Resilient Mounting of Machinery on Platelike and Modified Platelike Substructures," J. Acoust. Soc. Am. 61, 986-994 (1977).

26. R. L. Kerlin and J. C. Snowdon, "Driving-Point Impedances of Cantilever Beams--Comparison of Measurement and Theory," J. Acoust. Soc. Am. 47, 220-228 (1970).

27. J. B. Ochs and J. C. Snowdon, "Transmissibility Across Simply Supported Thin Plates: I. Rectangular and Square Plates with and without Damping Layers," J. Acoust. Soc. Am. 58, 832-840 (1975).

28. J. C. Snowdon, "Forced Vibration of Internally Rectangular and Square Plates with Simply Supported Boundaries," J. Acoust. Soc. Am. 56, 1177-1184 (1974).

29. J. C. Snowdon, "Vibration of Simply Supported Rectangular and Square Plates to which Lumped Masses and Dynamic Vibration Absorbers Are Attached," J. Acoust. Soc. Am. 57, 646-654 (1975).

REFERENCES -- CONTINUED

30. K. H. Lenzen, "Vibration of Steel Joist-Concrete Slab Floors," AISC Eng. J. 3, 133-136 (1966).

31. D. L. Allen and J. C. Swallow, "Annoying Floor Vibrations--Diagnosis and Therapy," Sound Vib. Mag. 9, (3), 12-17 (1975).

FIGURE LEGENDS

Fig. 1 Simple mounting system with an ideally rigid machine (a) supported directly and (b) supported via nonrigid (multiresonant) flanges or feet.

Fig. 2 Force transmissibility across the simple mounting system of Fig. 1(a). The hatched area shows the frequency range through which force is attenuated. Mount damping factor $\delta_K = 0.05$.

Fig. 3 Transmissibility across the simple mounting system with wave effects calculated from the "long"-rod theory. Damping factor $\delta_E = 0.1$; mass ratio $\gamma = 50$, 100, and 250; natural mounting frequency = 5 Hz. (Ref. 1.)

Fig. 4 Practical example of simple mounting system with rigid mounted item supported by nonrigid (multiresonant) feet. (Ref. 4.)

Fig. 5 Force transmissibility across the simple mounting system of Fig. 1(b) with shear-beam resonances in feet of mounted item. Mass ratio $\gamma_F = 40$; stiffness ratio $\Gamma = K_F/K = 5$, 25, and 100; damping factors $\delta_K = 0.05$ and $\delta_F = 0.01$. (Ref. 6.)

Fig. 6 Compound mounting system with a mounted item of mass M_1, and an intermediate mass M_2 that is supported (a) directly, and (b) via nonrigid (multiresonant) flanges or feet.

Fig. 7 Compound mounting of 80,000 lb and 17,000 lb diesel generators on one extensive intermediate mass. (Ref. 8.)

Fig. 8 Small-scale compound mounting system with an intermediate mass M_2 comprising two cylindrical masses 10 and a spacer yoke 12 (resilient elements comprise 16. (Ref. 9.)

FIGURE LEGENDS -- CONTINUED

Fig. 9 Force transmissibility across the compound mounting system of Fig. 6(a). Mass ratio $\beta = M_2/M_1 = 0$ (simple mounting system), 0.1, 0.2, and 1.0; damping factor $\delta_K = 0.05$. (Ref. 1.)

Fig. 10 Force transmissibility across the compound mounting system of Fig. 6(a) (solid-line curve) and Fig. 6(b) (chain-line curve). Mass ratios $\beta = M_2/M_1 = 0.2$ and $\gamma_F = M_2/2M_F = 40$; stiffness ratio $\Gamma = 5$; damping factors $\delta_K = 0.05$ and $\delta_F = 0.01$. The dashed-line curve shows the transmissibility across the simple system of Fig. 1(a). (Ref. 6.)

Fig. 11 Vibrating item of machinery with eight antivibration mounts per side supported by foundation beams that have (a) single span, and (b) four spans. Antivibration mounts located in pairs at equal but otherwise arbitrary distances from center span.

Fig. 12 Force transmissibility across the mounting system of Fig. 11(a) (solid- and dashed-line curves) and Fig. 11(b) (chain-line curve). Mass ratio $\gamma = M/2M_b = 10$; frequency ratio $\Xi = \omega_1/\omega_o = 10$; damping factors $\delta_K = 0.05$ and $\delta_E = 0.01$. Mounts are located where $h_1 = 0.125a$, $h_2 = 0.375a$, $h_3 = 0.625a$, and $h_4 = 0.875a$ for the solid-line curve; $h_1 = 0.063a$, $h_2 = 0.438a$, $h_3 = 0.688a$, and $h_4 = 0.938a$ for the dashed-line curve; and $h_1 = 0.125a$ for the chain-line curve. (Ref. 14.)

Fig. 13 Vibrating item of machinery with four antivibration mounts per side supported by foundation beams that have (a) single span, and (b) four spans. Antivibration mounts located at center span or located in pairs at equal but otherwise arbitrary distances from center span.

FIGURE LEGENDS -- CONTINUED

Fig. 14 Force transmissibility across the mounting system of Fig. 13(a) (solid- and dashed-line curves) and Fig. 13(b) (chain-line curve). Mass ratio $\gamma = M/2M_b = 10$; frequency ratio $\Xi = \omega_1/\omega_o = 10$; damping factors $\delta_K = 0.05$ and $\delta_E = 0.01$. Mounts are located where $h_1 = 0.49a$ and $h_2 = 0.98a$ for the solid-line curve, and $h_1 = 0.25a$ and $h_2 = 0.75a$ for the dashed-line curve. (Ref. 14.)

Fig. 15 Force transmissibility across the mounting system of Fig. 16 (solid-line curve). For the dynamic absorbers, $\gamma_a = 4M_a/M_b = 0.25$, $\omega_a/\omega_m = 0.880$, and $\delta_R = 0.226$. In addition, the parameters $\gamma = M/2M_b = 10$, $\Xi = \omega_1/\omega_o = 10$, $\delta_K = 0.05$, and $\delta_E = 0.01$; the mounts are located where $h_1 = 0.25a$ and $h_2 = 0.75a$. For comparison, the dashed-line curve shows the transmissibility across the mounting system of Fig. 13(a) with the same mount locations but with a greater foundation damping factor $\delta_K = 0.05$. The chain-line curve shows the transmissibility across a mounting system in the configuration of Fig. 13(b) but with dynamic absorbers attached to each center-span location. For these dynamic absorbers, $\gamma_a = 4M_a/M_b = 0.25$, $\omega_a/\omega_m = 0.644$, and $\delta_R = 0.392$. (Ref. 14.)

Fig. 16 Vibrating item of machinery with four antivibration mounts per side supported by single-span foundation beams to which dynamic vibration absorbers are attached at each mount location.

Fig. 17 Vibrating item of machinery with four antivibration mounts per side supported by four-span foundation beams to which lumped masses are attached at each mount location.

Fig. 18 Force transmissibility across the mounting system of Fig. 17 (chain-line curve) for which $\gamma = M/2M_b = 10$, $\gamma_a = 4M_a/M_b = 2.5$, $\Xi = \omega_1/\omega_o = 10$,

FIGURE LEGENDS -- CONTINUED

δ_K = 0.05 and δ_E = 0.01. The solid-line curve shows, for the same location of mounts and loading masses (again, γ_a = 2.5), how the transmissibility across the mounting system changes when the foundation beams are replaced by beams of single span. The dashed-line curve shows the transmissibility across the mounting system of Fig. 16 with the same parameters as employed previously to calculate the solid-line curve of Fig. 15 (recall that γ_a = 0.25) but with the different mount locations h_1 = 0.49a and h_2 = 0.98a. (Ref. 14.)

Fig. 19 Compound mounting of a vibrating item of machinery of mass M_1 with an intermediate mass M_2 supported by single-span foundation beams. Lower four mounts located in pairs spaced at equal but otherwise arbitrary distances from center span.

Fig. 20 Force transmissibility across the compound mounting system of Fig. 19. Mass ratio $\beta = M_2/M_1$ = 0 (simple mounting system), 0.1, 0.2, and 1.0. Mass ratio $\gamma = M_1/2M_b$ = 10, frequency ratio $\Xi = \omega_1/\omega_o$ = 10, damping factors δ_K = 0.05 and δ_E = 0.01. Lower mounts are located where h_1 = 0.25a and h_2 = 0.75a.

Fig. 21 Vibrating item of machinery with four antivibration mounts per side supported by single-span floating foundation beams.

Fig. 22 Force transmissibility across the mounting system of Fig. 21 (solid- and chain-line curves) and Fig. 13(a) (dashed-line curve). Stiffness ratio $\kappa = K_F/K_S$ = 3, and the parameters $\gamma = M/2M_b$ = 10, $\Xi = \omega_1/\omega_o$ = 10, δ_K = 0.05, and δ_E = 0.01. The mounts are located where h_1 = 0.35a and h_2 = 0.869a for the solid-line curve, and h_1 = 0.25a and h_2 = 0.75a for the dashed- and chain-line curves. (Ref. 14.)

FIGURE LEGENDS -- CONTINUED

Fig. 23 Compound mounting system with a vibrating item of machinery supported by four antivibration mountings per side on intermediate beams that are also supported by an antivibration mounting at each end. The beams are loaded at the upper mount locations by equal lumped masses M_a.

Fig. 24 Compound mounting system with a vibrating item of machinery supported by four antivibration mountings per side on intermediate beams that are also supported by an antivibration mounting at each end. Identical dynamic vibration absorbers are attached to the beams at each upper mount location.

Fig. 25 Force transmissibility across the compound mounting system of Fig. 24. Mass ratios $\gamma = M/2M_b = 10$ and $\gamma_a = 4M_a/M_b = 0$, 1.0, and 9 ("β" = 0.1, 0.2, and 1.0, respectively); frequency ratio $\Xi = 10$; stiffness ratio $\kappa = 3$; damping factors $\delta_K = \delta_E = 0.05$. Upper mounts of the system are located where $h_1 = 0.25a$ and $h_2 = 0.75a$. The chain-line curve for $\gamma_a = 1.0$ ("β" = 0.2) shows how the transmissibility is altered if the mount and loading mass locations are changed to $h_1 = 0.437a$ and $0.869a$. (Ref. 11.)

Fig. 26 Force transmissibility across the compound mounting systems of Figs. 21 and 24. Mass ratio $\gamma = M/2M_b = 10$; frequency ratio $\Xi = 10$; stiffness ratio $\kappa = 3$; damping factors $\delta_K = 0.05$ and $\delta_E = 0.01$. For the dashed-line curve, the upper mounts in Fig. 21 are located where $h_1 = 0.25a$ and $h_2 = 0.75a$; for the solid-line curve, $h_1 = 0.350a$ and $h_2 = 0.869a$. For the chain-line curve, the upper mounts and the dynamic absorbers in Fig. 24 are also located where $h_1 = 0.350a$ and $h_2 = 0.869a$; the absorber mass ratio $\gamma_a = 4M_a/M_b = 0.25$; and the

FIGURE LEGENDS -- CONTINUED

absorber tuning and damping ratios $\omega_a/\omega_1 = 0.880$ and $\delta_R = 0.226$. (Ref. 11.)

Fig. 27 Rectangular plates with simply supported boundaries, mass M_p, and sides of lengths a and μa. A vibrating item of machinery of mass M is supported (a) by eight, and (b) by four, symmetrically located antivibration mounts, each of complex stiffness K^*.

Fig. 28 Force transmissibility across the mounting system of Fig. 27(a) supported by a square plate ($\mu = 1.0$). Antivibration mounts are uniformly spaced such that $h_{1x} = 0.2a$, $h_{1y} = \mu a/3 = a/3$, and $h_{2x} = 0.4a$, $h_{2y} = a/3$. Mass ratio $\gamma = M/M_p = 4$; frequency ratio $\Xi = \omega_{11}/\omega_o = 4$; mount and plate damping factors $\delta_K = 0.05$ and $\delta_E = \delta_G = 0.01$. (Ref. 25.)

Fig. 29 Force transmissibility across the mounting system of Fig. 27(b) supported by a square plate. Antivibration mounts are located such that $h_x = h_y = 0.25a$. The parameters $\gamma = \Xi = 4$, $\delta_K = 0.05$, and $\delta_E = \delta_G = 0.01$. (Ref. 25.)

Fig. 30 Force transmissibility across the mounting system of Fig. 27(b) supported by a square plate. Antivibration mounts are judiciously located such that $h_x = h_y = a/3$. The parameters $\gamma = \Xi = 4$, $\delta_K = 0.05$, and $\delta_E = \delta_G = 0.01$. (Ref. 25.)

Fig. 31 (a) A circular plate, and (b) a rectangular plate divided into quadrants. The plates have simply supported boundaries and mass M_p. The circular plate of radius a' is excited by forces from four antivibration mounts symmetrically located at a distance $\lambda a'$ from the plate center. The identical quadrant plates, which have sides of lengths a' and $\mu a'$, are likewise excited by forces from four symmetrically located antivibration mounts.

FIGURE LEGENDS -- CONTINUED

Fig. 32 Force transmissibility across a mounting system supported by four antivibration mounts on the circular plate of Fig. 31(a). For the solid-line curve ($\lambda = 0.7071$), the mount locations coincide with those utilized in the calculations of Fig. 29. For the dashed-line curve ($\lambda = 0.4414$), the mounts lie on the nodal circle of the second symmetrical plate mode, which is consequently not excited. The parameters $\gamma = \Xi = 4$, $\delta_K = 0.05$, Poisson's ratio $\nu = 1/3$, and $\delta_E = \delta_G = 0.01$. (Ref. 25.)

Fig. 33 Force transmissibility across a mounting system supported by four antivibration mounts on the quadrant plates of Fig. 31(b) when $\mu = 1.0$ (square quadrants). For the solid- and dashed-line curves ($h_{x'} = h_{y'} = a'/2$ and $2a'/3$, respectively), the mount locations coincide with those utilized in the calculations of Figs. 29 and 30. The parameters $\gamma = \Xi = 4$, $\delta_K = 0.05$, and $\delta_E = \delta_G = 0.01$. (Ref. 25.)

Fig. 34 Force transmissibility across the mounting system of Fig. 27(a) supported by a rectangular plate for which $\mu = 1/2$ (solid-line curve). Eight antivibration mounts are uniformly spaced such that $h_{1x} = 0.2a$, $h_{1y} = \mu a/3 = a/6$, and $h_{2x} = 0.4a$, $h_{2y} = a/6$. The dashed-line curve shows the force transmissibility across a mounting system supported by four antivibration mounts on the quadrant plates of Fig. 31(b) when $\mu = 1/2$. The mounts are located such that $h_{1x} = 2a'/3$, $h_{y'} = 2\mu a'/3 = a'/3$. For both curves, the parameters $\gamma = 6$, $\Xi = 5$, $\delta_K = 0.05$, and $\delta_E = \delta_G = 0.01$. (Ref. 25.)

Fig. 35 Vibrating item of machinery of mass M supported by four symmetrically located antivibration mounts, each of complex stiffness K^*, on

FIGURE LEGENDS -- CONTINUED

rectangular plates with simply supported boundaries, mass M_p, and sides of lengths a and μa. (a) Dynamic vibration absorbers of mass M_a, and (b) lumped loading masses M_a, are attached to the plates at each mount location.

Fig. 36 Force transmissibility across the mounting system of Fig. 35(a) supported by a rectangular plate for which $\mu = 1/2$ (solid-line curve). Mounts and dynamic absorbers are located where $h_x = a/3$, $h_y = \mu a/3 = a/6$. For the dynamic absorbers, $\gamma_a = 4M_a/M_p = 0.2$, $\omega_a/\omega_{11} = 0.869$, and $\delta_R = 0.268$. The parameters $\gamma = 6$, $\Xi = 5$, $\delta_K = 0.05$, and $\delta_E = \delta_G = 0.01$. The dashed-line curve shows the transmissibility across the same mounting system when the absorbers are absent ($\gamma_a = 0$). (Ref. 25.)

Fig. 37 Force transmissibility across the mounting system of Fig. 35(b) supported by a rectangular plate for which $\mu = 1/2$ (solid-line curve). Mounts and lumped masses located where $h_x = a/3$, $h_y = \mu a/3 = a/6$. The parameters $\gamma_a = 4M_a/M_p = 4$, $\gamma = \Xi = 4$, $\delta_K = 0.05$, and $\delta_E = \delta_G = 0.01$. The dashed-line curve shows the transmissibility across the same mounting system when the loading masses are absent ($\gamma_a = 0$). (Ref. 25.)

Fig. 38 Force transmissibility across a compound mounting system supported by four symmetrically located mounts on a simply supported rectangular plate for which $\mu = 1/2$. Mass ratio $\beta = 0$ (simple mounting system), 0.1, 0.2, and 1.0. Mounts are located where $h_x = a/3$, $h_y = \mu a/3 = a/6$. Mass and frequency ratios $\gamma = M_1/M_p = 4$ and $\Xi = 4$.

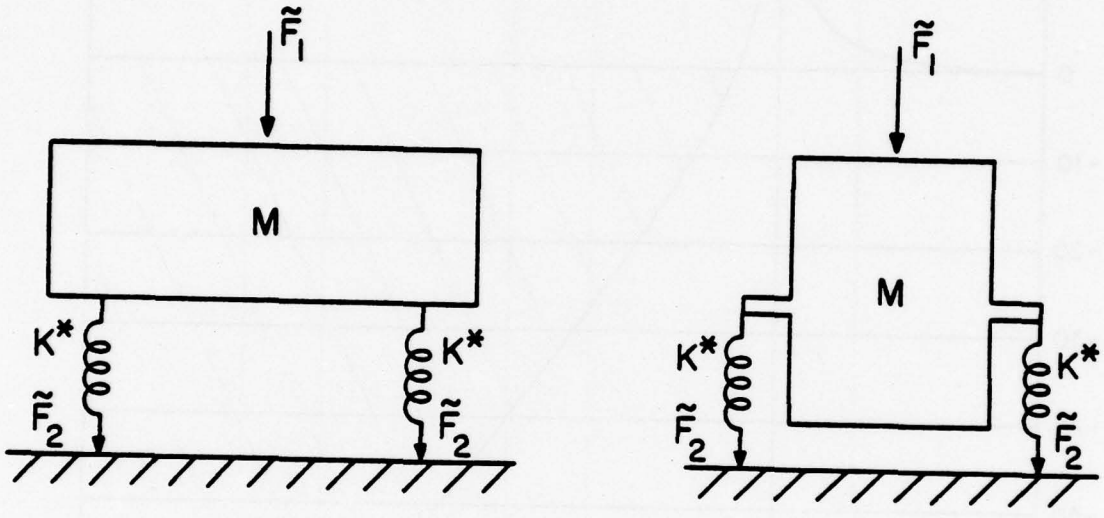

FIG. 1

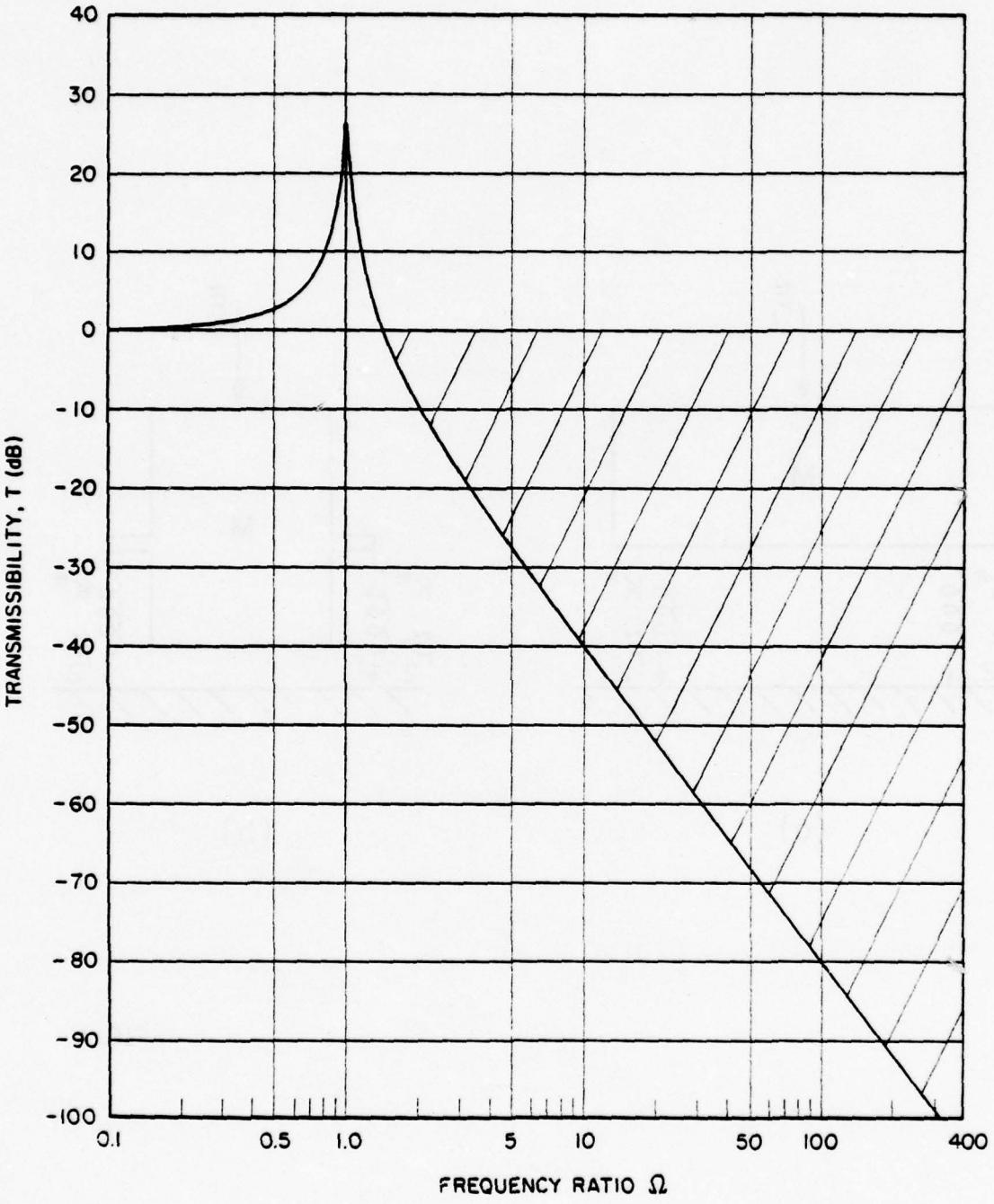
40
30
20
10
0
-10
-20
-30
-40
-50
-60
-70
-80
-90
-100
TRANSMISSIBILITY, T (dB)
0.1
0.5
1.0
5
10
50
100
400
FREQUENCY RATIO Ω

FIG. 2

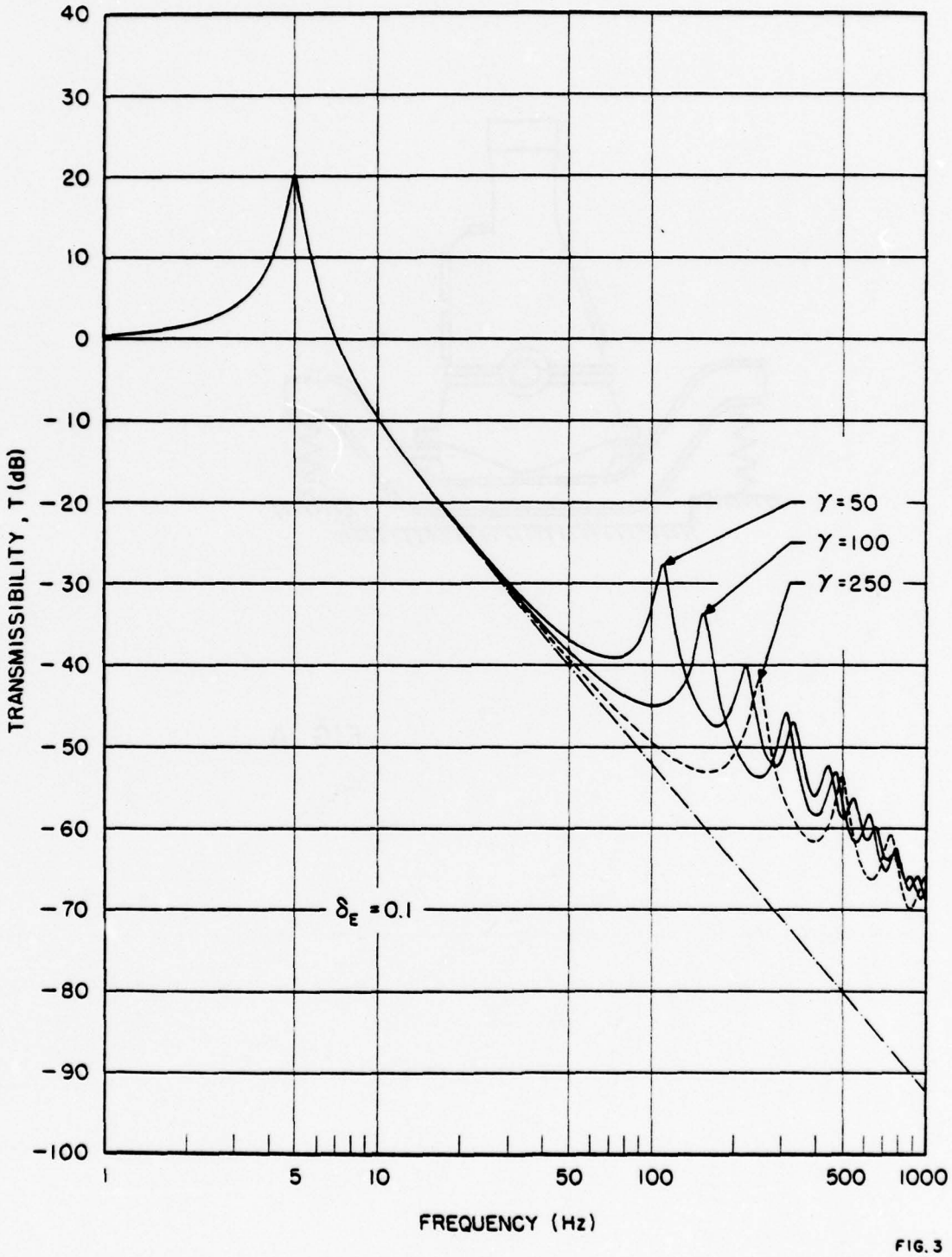
40
30
20
10
0
-10
-20
-30
-40
-50
-60
-70
-80
-90
-100
TRANSMISSIBILITY, T (dB)
1
5
10
50
100
500
1000
FREQUENCY (Hz)
γ = 50
γ = 100
γ = 250
δE = 0.1

FIG. 3

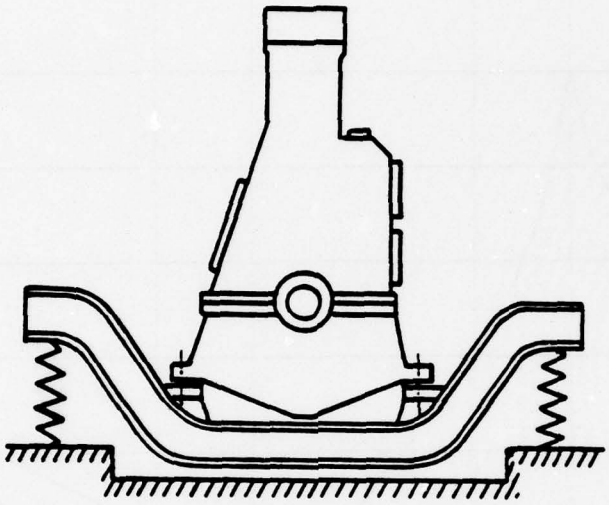

FIG. 4

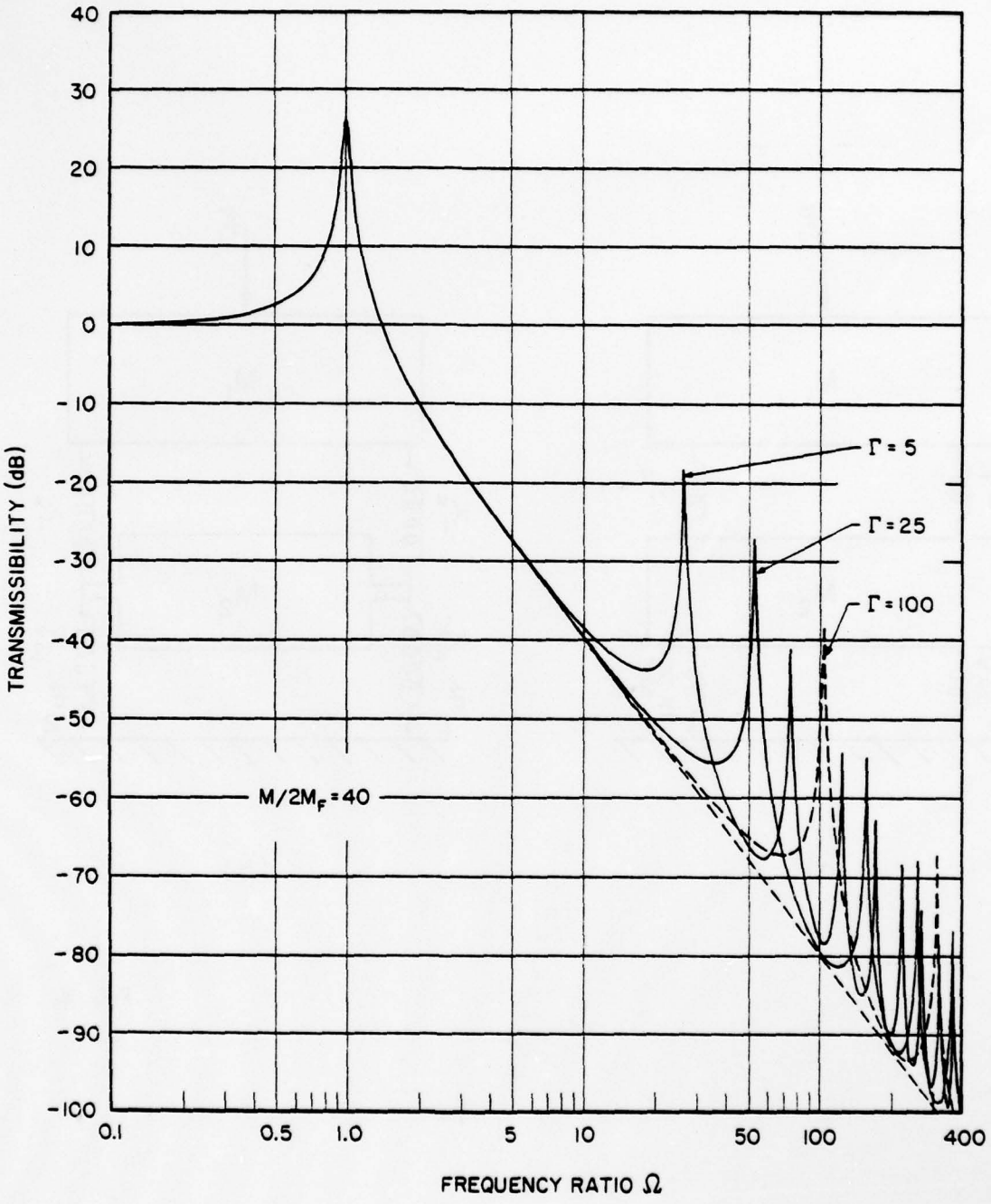
40
30
20
10
0
-10
-20
-30
-40
-50
-60
-70
-80
-90
-100
TRANSMISSIBILITY (dB)
Γ = 5
Γ = 25
Γ = 100
M/2M_F = 40
0.1
0.5
1.0
5
10
50
100
400
FREQUENCY RATIO Ω

FIG. 5

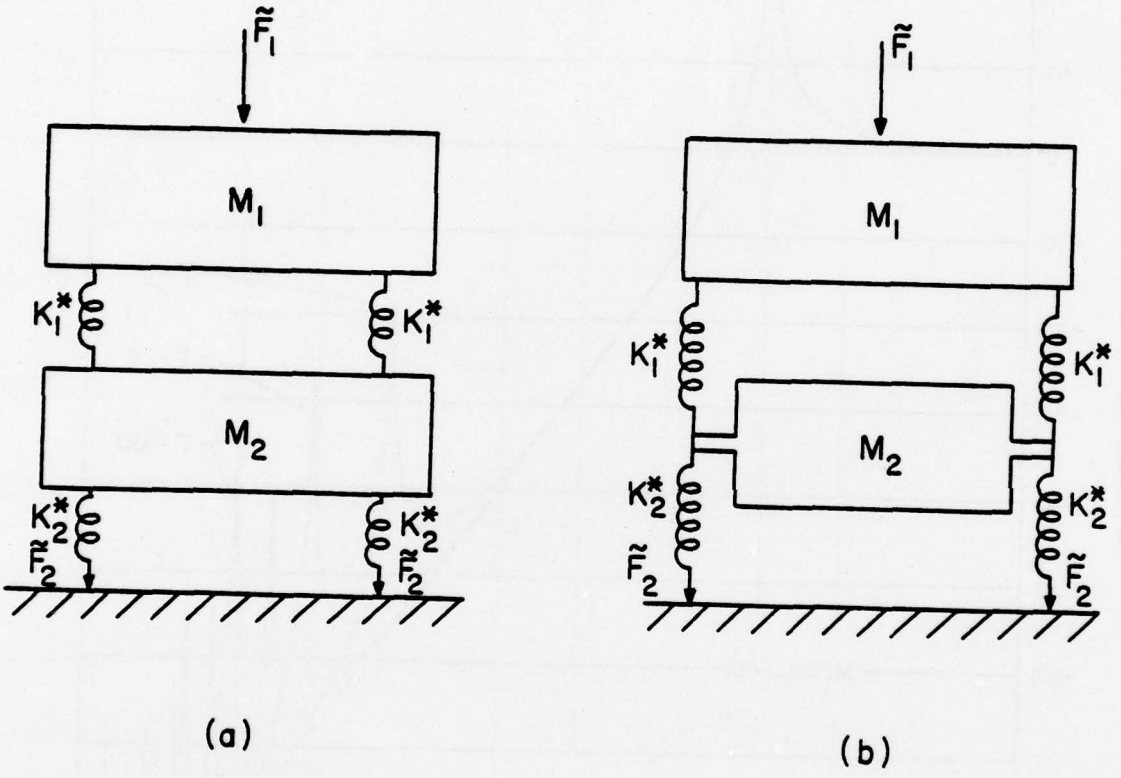
$\tilde{F}_1$
M_1
K_1^*
K_1^*
M_2
K_2^*
K_2^*
$\tilde{F}_2$
$\tilde{F}_2$
(a)
$\tilde{F}_1$
M_1
K_1^*
K_1^*
M_2
K_2^*
K_2^*
$\tilde{F}_2$
$\tilde{F}_2$
(b)

FIG. 6

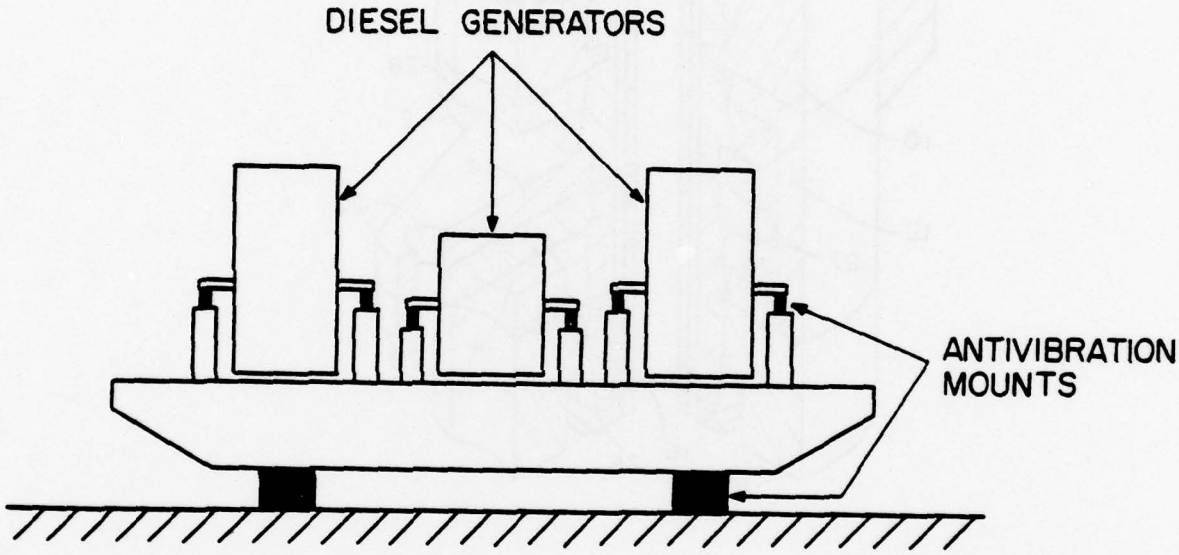

FIG. 7

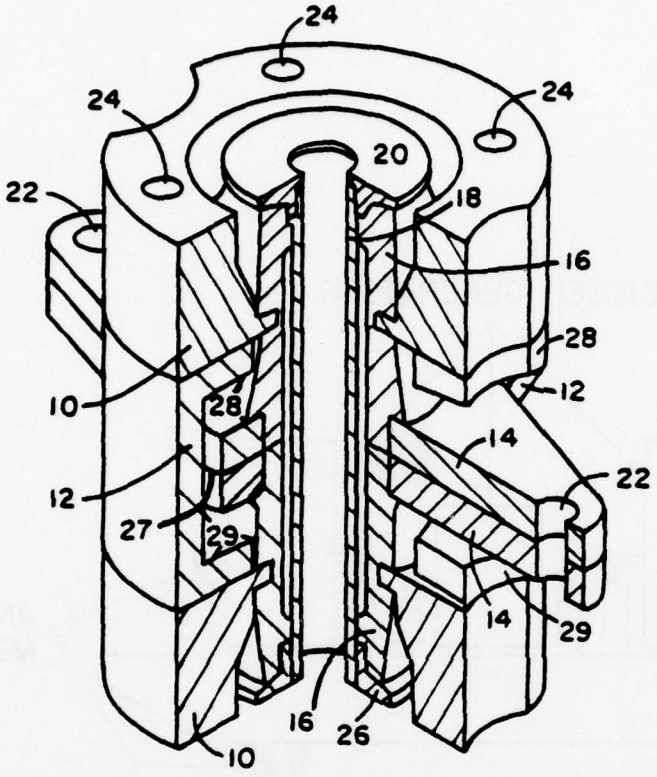

FIG. 8

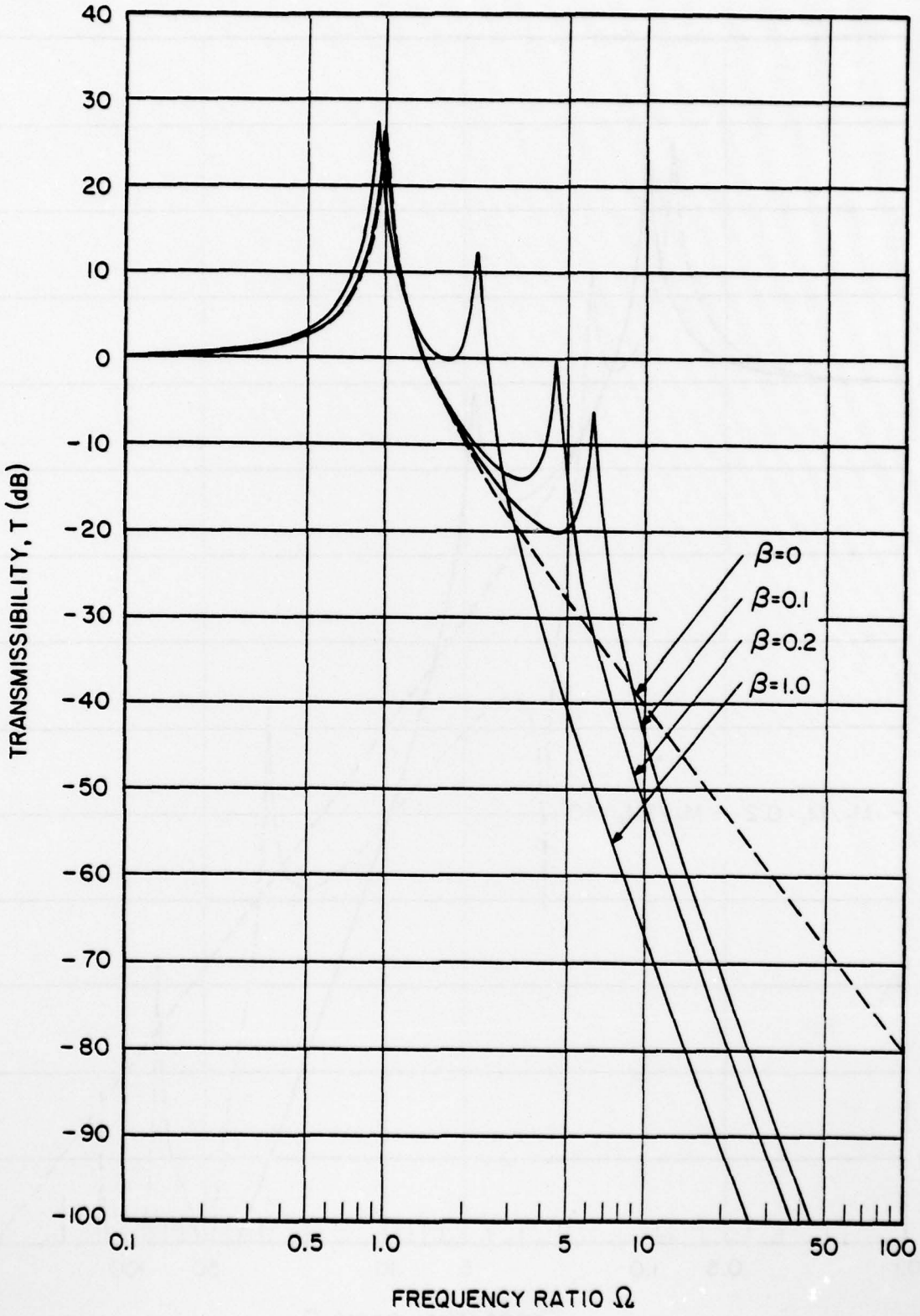
40
30
20
10
0
-10
-20
-30
-40
-50
-60
-70
-80
-90
-100
TRANSMISSIBILITY, T (dB)
0.1
0.5
1.0
5
10
50
100
FREQUENCY RATIO Ω
β=0
β=0.1
β=0.2
β=1.0

FIG. 9

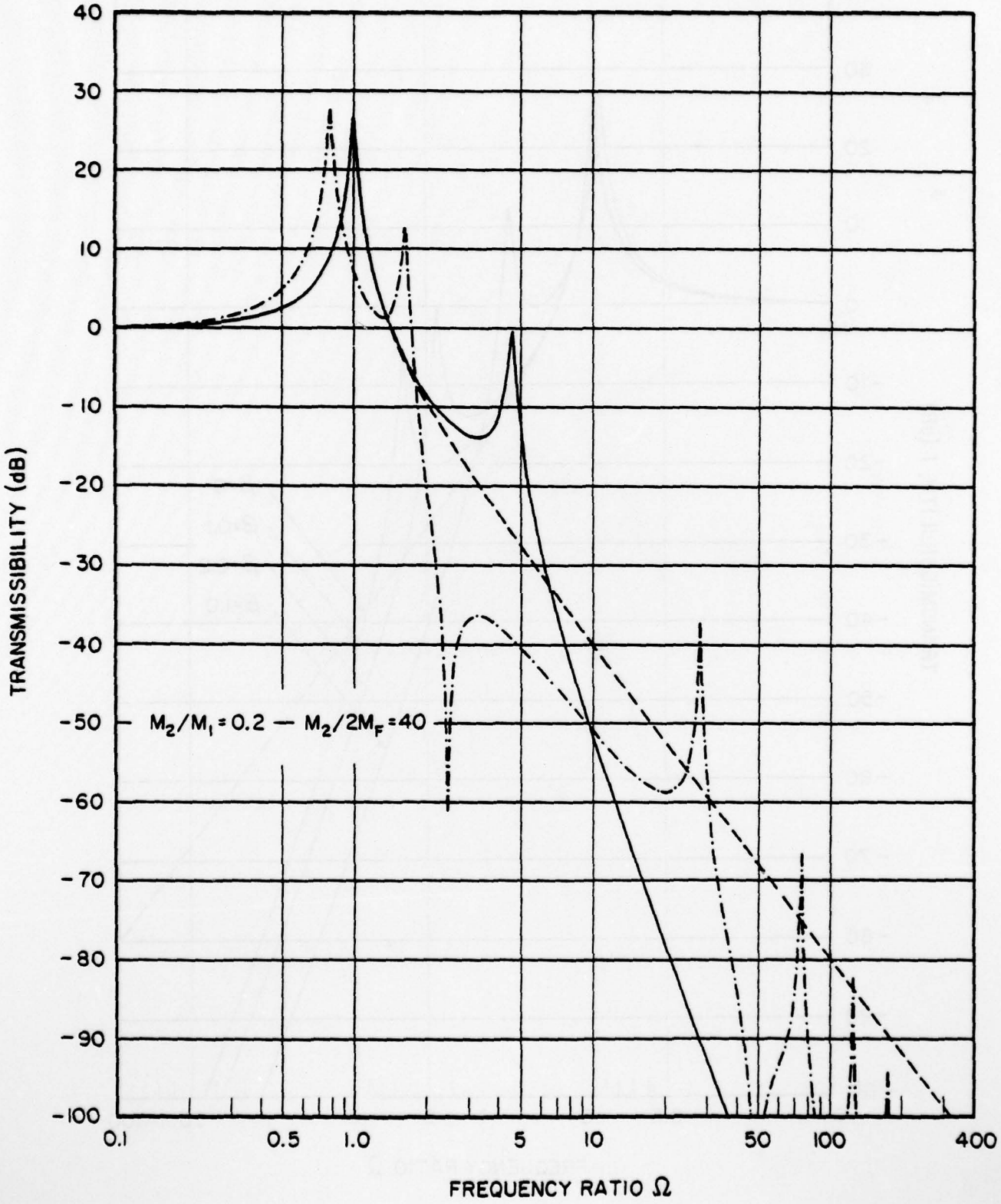
40
30
20
10
0
-10
-20
-30
-40
-50
-60
-70
-80
-90
-100
TRANSMISSIBILITY (dB)
$M_2/M_1 = 0.2$ — $M_2/2M_F = 40$
0.1
0.5
1.0
5
10
50
100
400
FREQUENCY RATIO Ω

FIG. 10

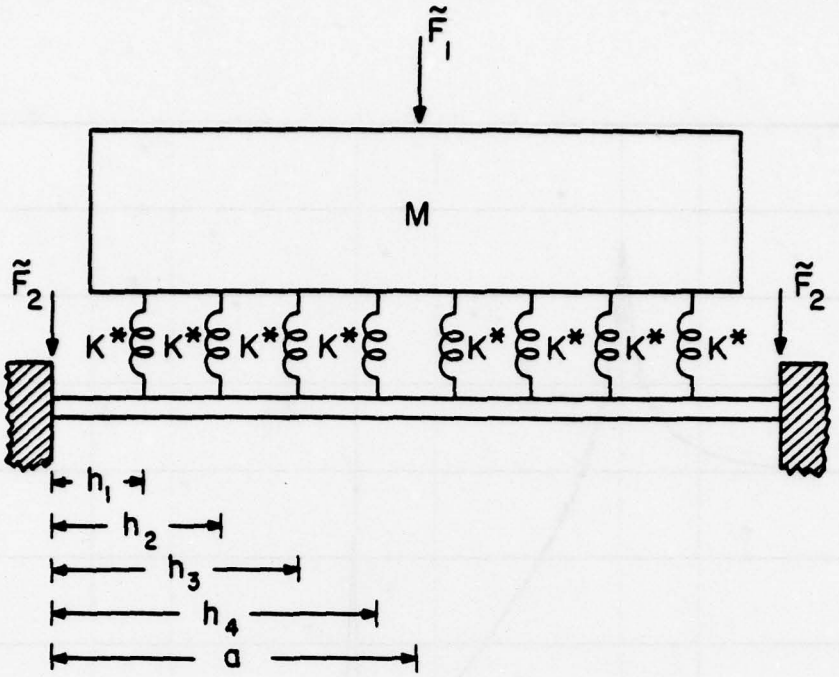
$\tilde{F}_1$
M
$\tilde{F}_2$
$\tilde{F}_2$
K* K* K* K* K* K* K* K*
h_1
h_2
h_3
h_4
a

(a)

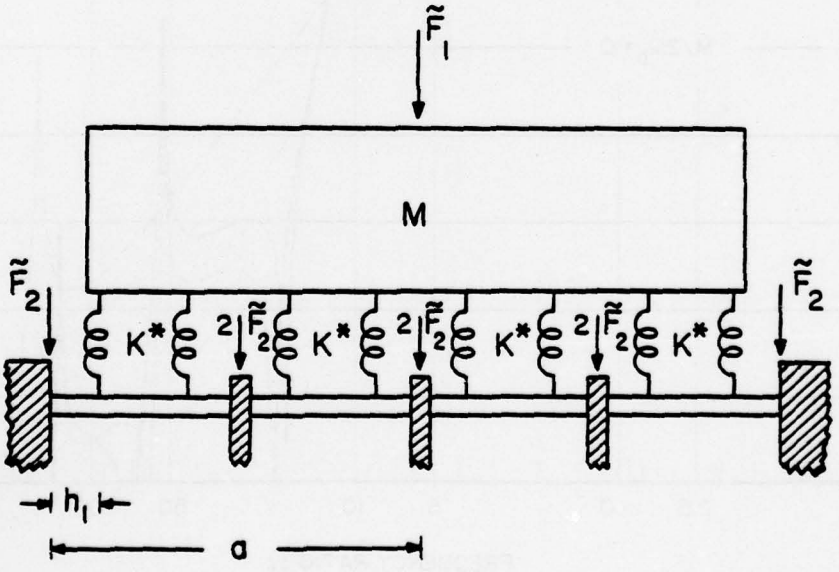
$\tilde{F}_1$
M
$\tilde{F}_2$
$\tilde{F}_2$
K* 2$\tilde{F}_2$ K* 2$\tilde{F}_2$ K* 2$\tilde{F}_2$ K*
h_1
a

(b)

FIG.11

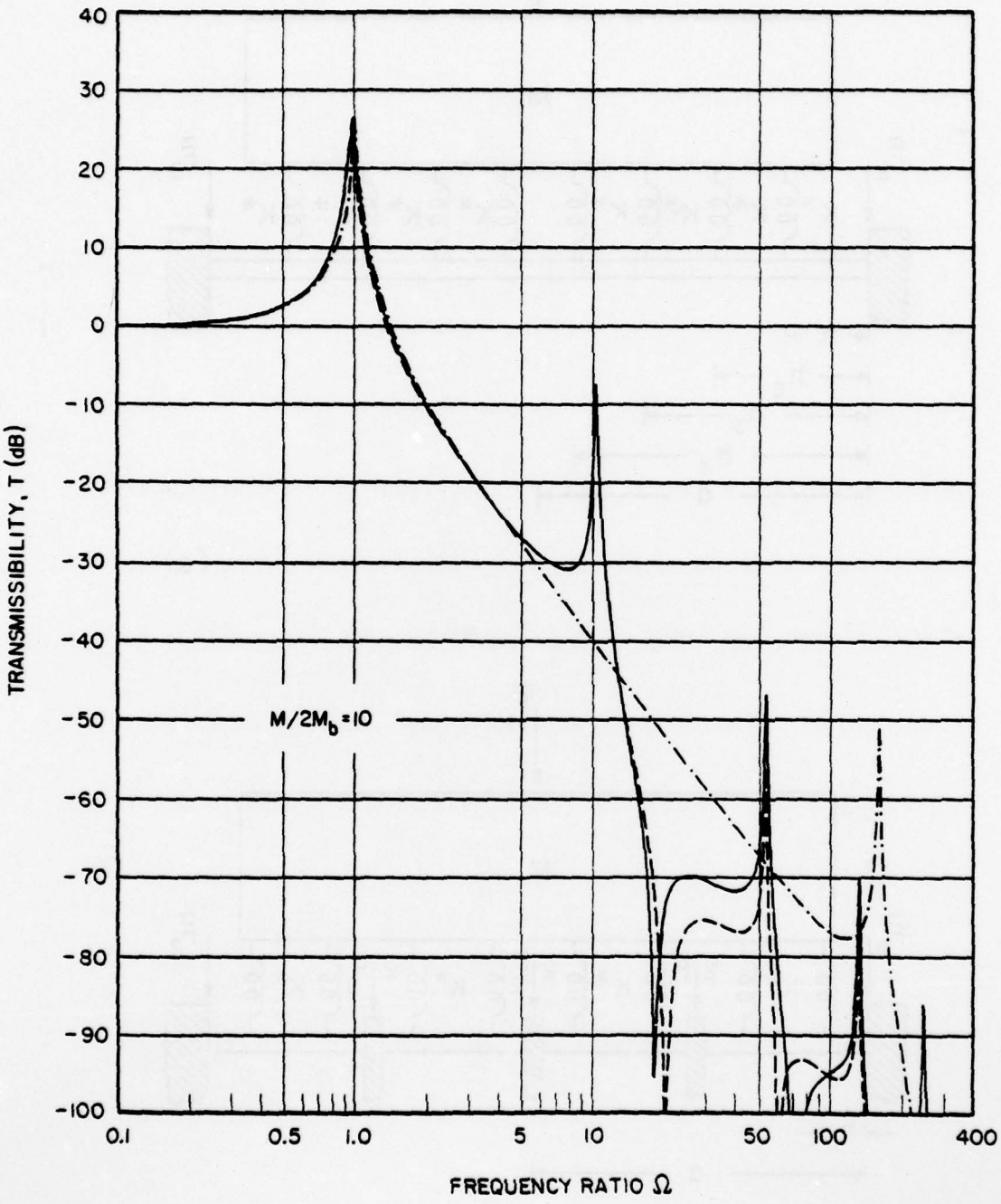
40
30
20
10
0
-10
-20
-30
-40
-50
-60
-70
-80
-90
-100
TRANSMISSIBILITY, T (dB)
M/2M_b=10
0.1
0.5
1.0
5
10
50
100
400
FREQUENCY RATIO Ω

FIG. 12

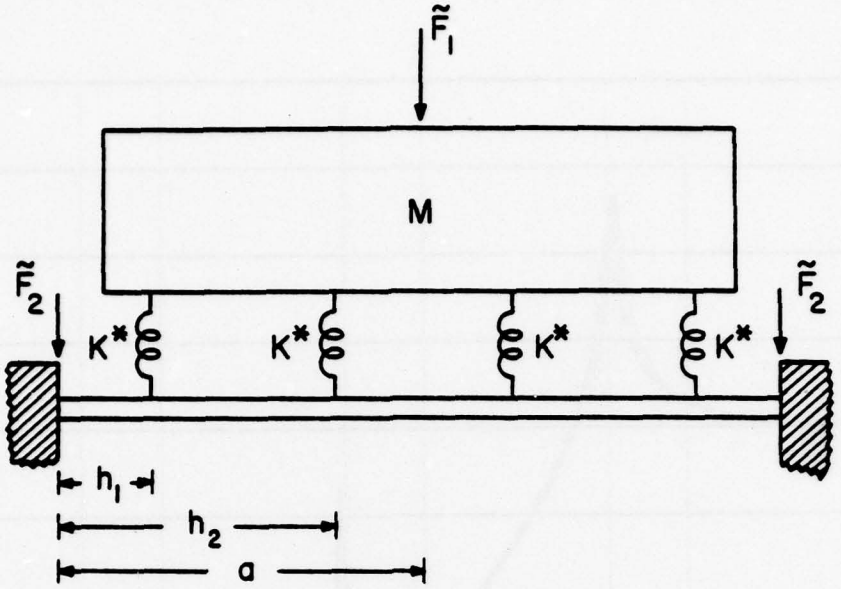
$\tilde{F}_1$
M
$\tilde{F}_2$
K*
K*
K*
K*
$\tilde{F}_2$
h_1
h_2
a

(a)

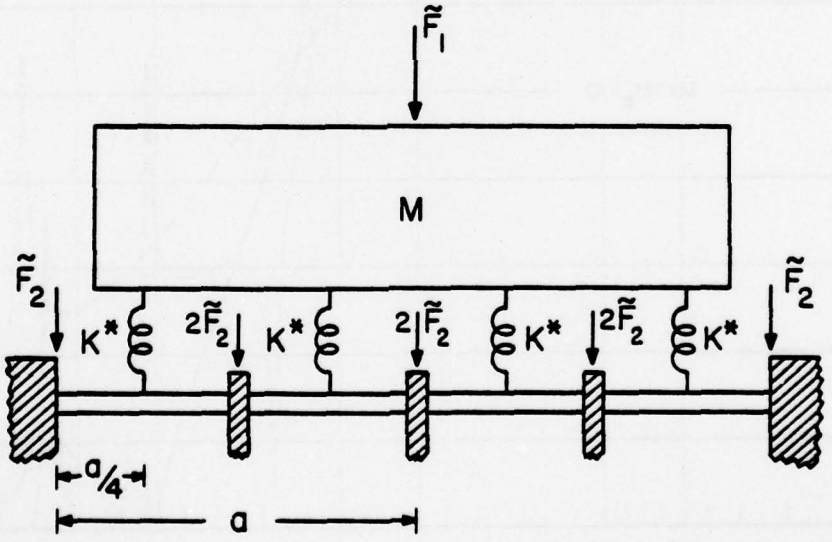
$\tilde{F}_1$
M
$\tilde{F}_2$
K*
$2\tilde{F}_2$
K*
$2\tilde{F}_2$
K*
$2\tilde{F}_2$
K*
$\tilde{F}_2$
a/4
a

(b)

FIG. 13

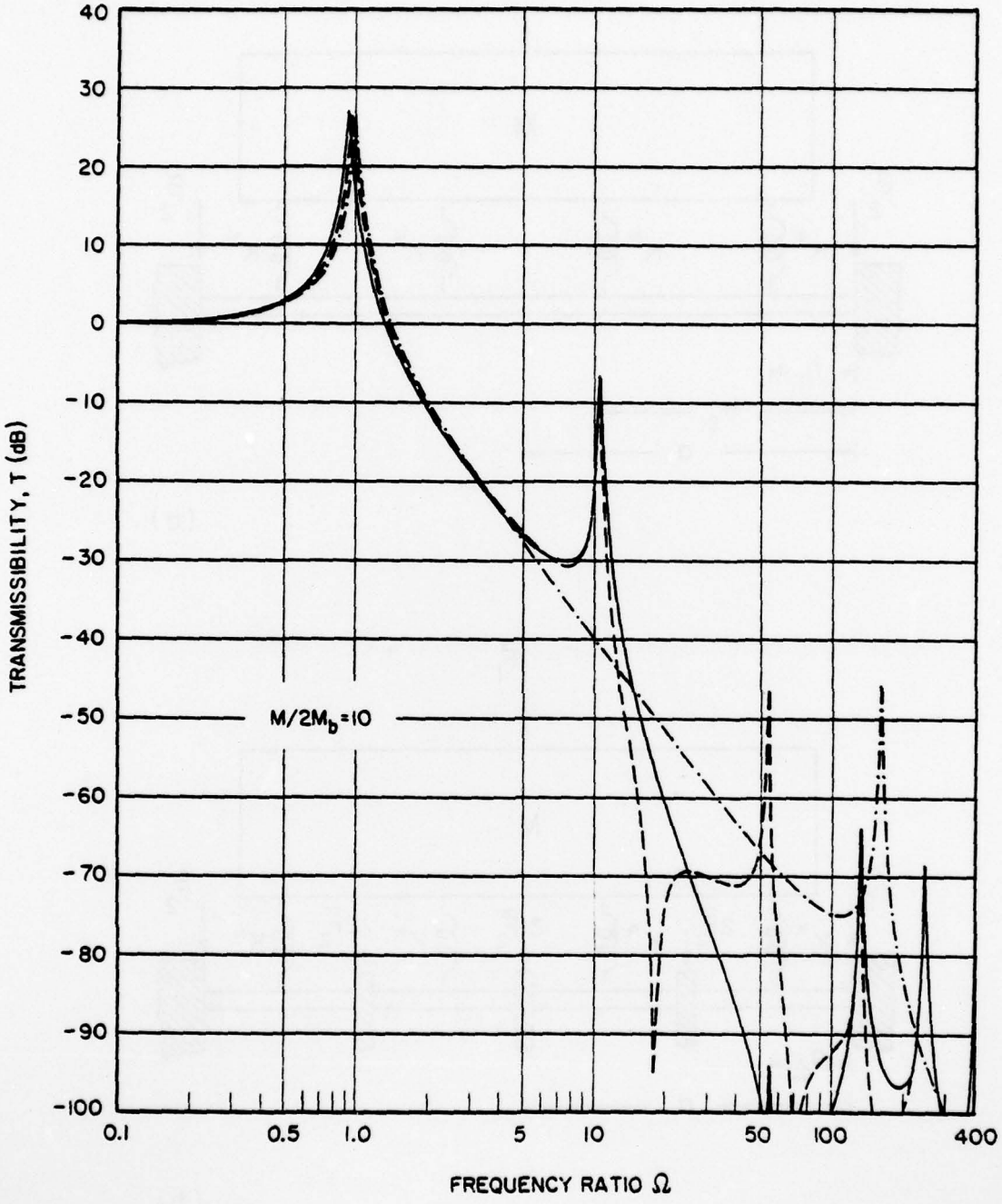
40
30
20
10
0
-10
-20
-30
-40
-50
-60
-70
-80
-90
-100
TRANSMISSIBILITY, T (dB)
M/2M_b=10
0.1
0.5
1.0
5
10
50
100
400
FREQUENCY RATIO Ω

FIG. 14

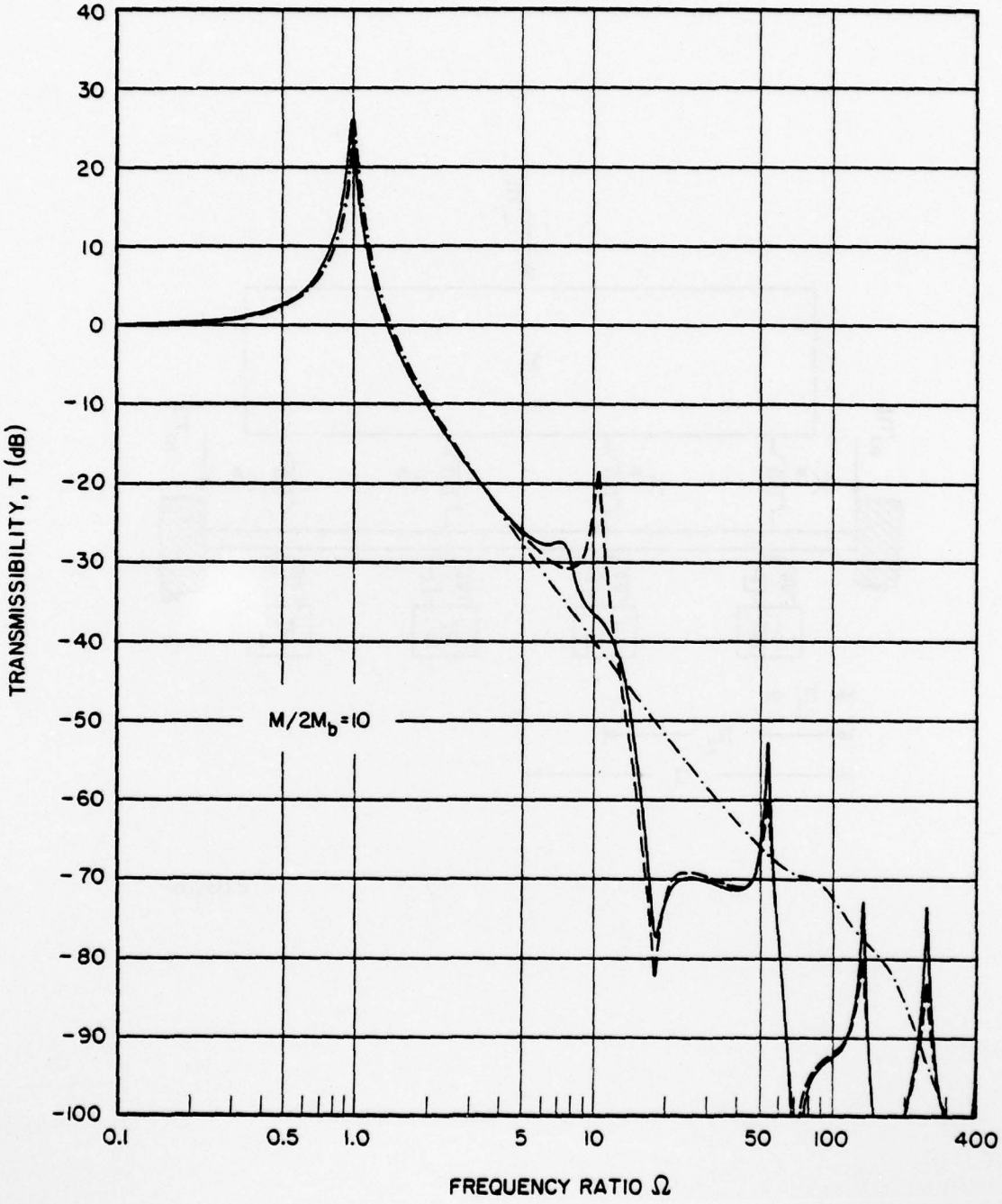
40
30
20
10
0
-10
-20
-30
-40
-50
-60
-70
-80
-90
-100
TRANSMISSIBILITY, T (dB)
M/2M$_b$=10
0.1
0.5
1.0
5
10
50
100
400
FREQUENCY RATIO Ω

FIG. 15

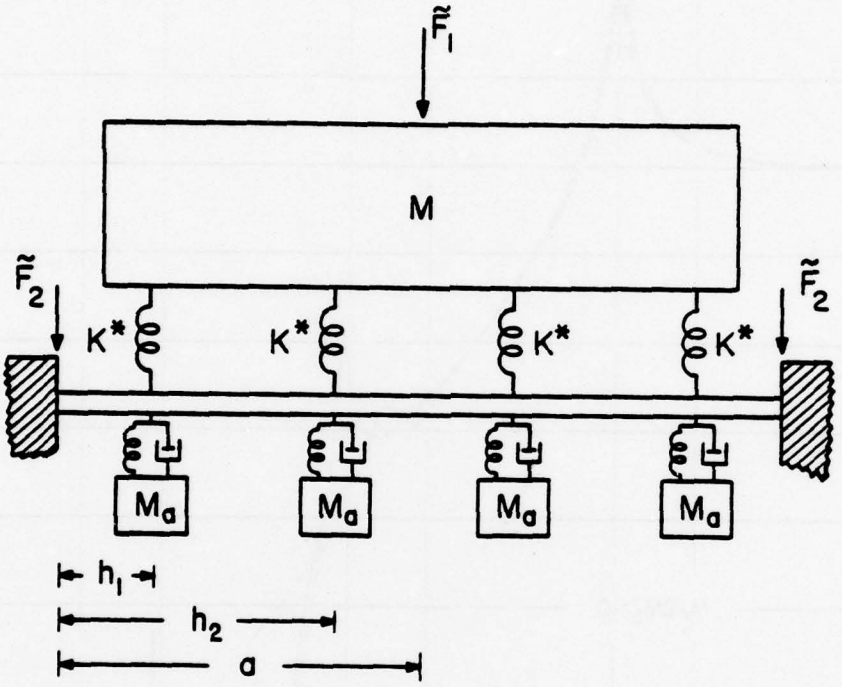

FIG.16

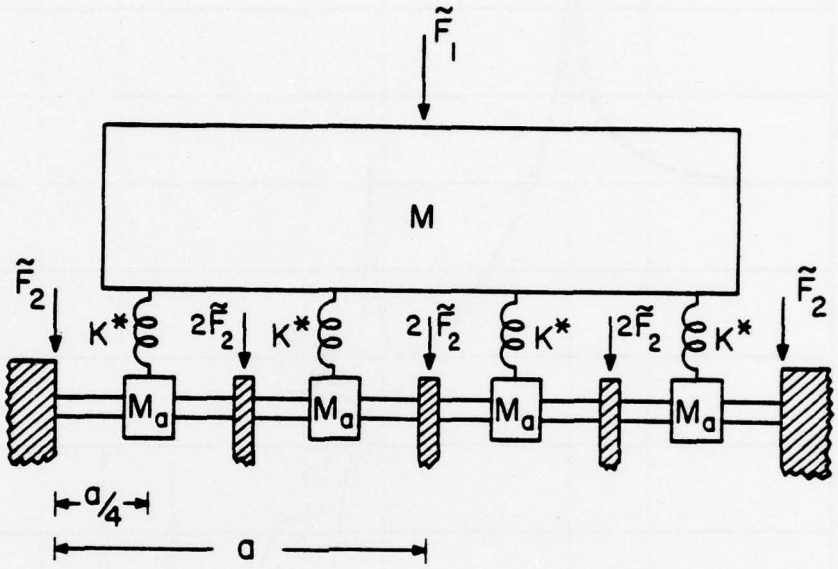
$\tilde{F}_1$
M
$\tilde{F}_2$
K*
$2\tilde{F}_2$
K*
$2\tilde{F}_2$
K*
$2\tilde{F}_2$
K*
$\tilde{F}_2$
M_a
M_a
M_a
M_a
a/4
a

FIG. 17

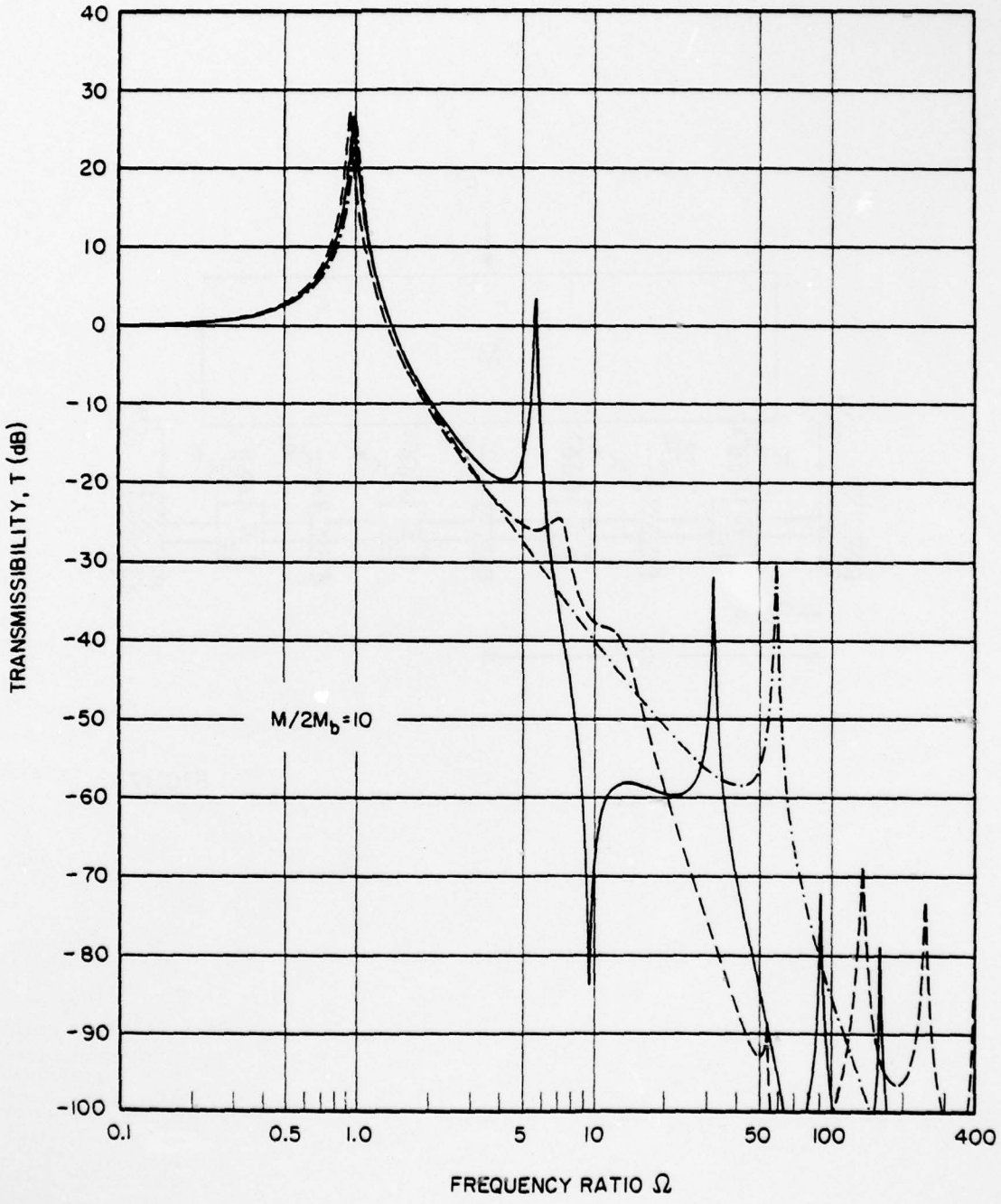
40
30
20
10
0
-10
-20
-30
-40
-50
-60
-70
-80
-90
-100
TRANSMISSIBILITY, T (dB)
M/2M_b=10
0.1
0.5
1.0
5
10
50
100
400
FREQUENCY RATIO Ω

FIG.18

AD-A074 737 PENNSYLVANIA STATE UNIV UNIVERSITY PARK APPLIED RESE--ETC F/G 20/11
VIBRATION ISOLATION ON RIGID AND NONRIGID FOUNDATIONS.(U)
JUL 79 J C SNOWDON N00024-79-C-6043
UNCLASSIFIED ARL/PSUTM-79-137 NL

2 OF 2
AD
A074737

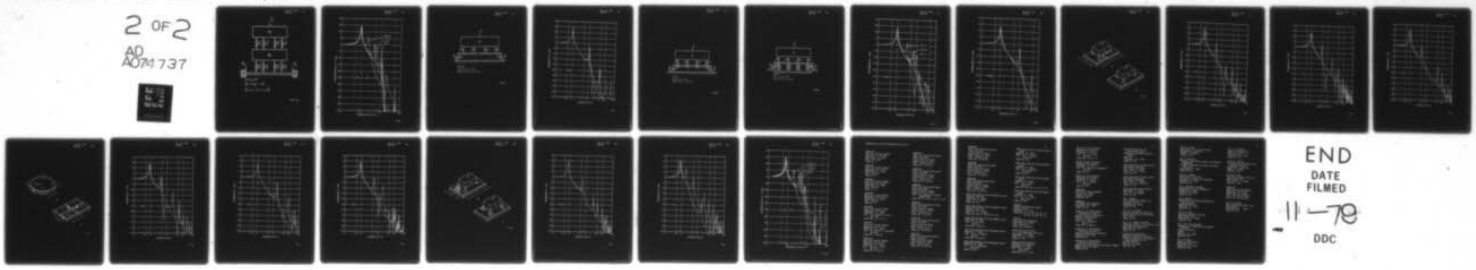

END
DATE
FILMED
11-79
DDC

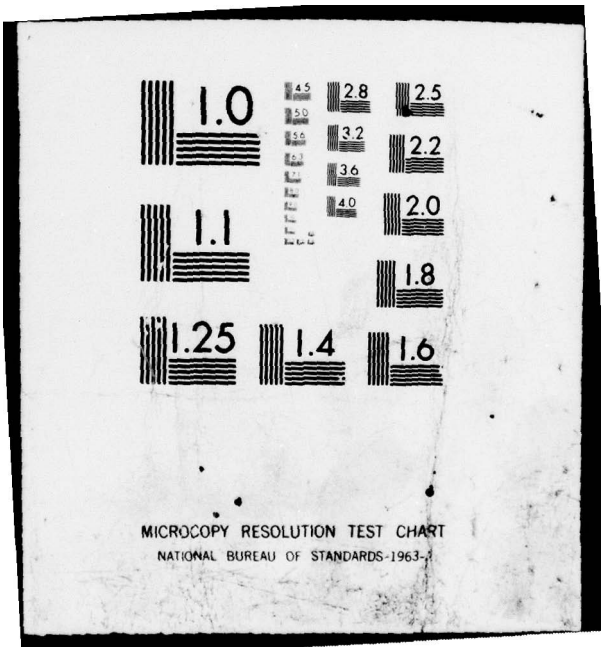
1.0
1.1
1.25
1.4
1.6
1.8
2.0
2.2
2.5
2.8
3.2
3.6
4.0
4.5
5.0
5.6
MICROCOPY RESOLUTION TEST CHART
NATIONAL BUREAU OF STANDARDS-1963-A

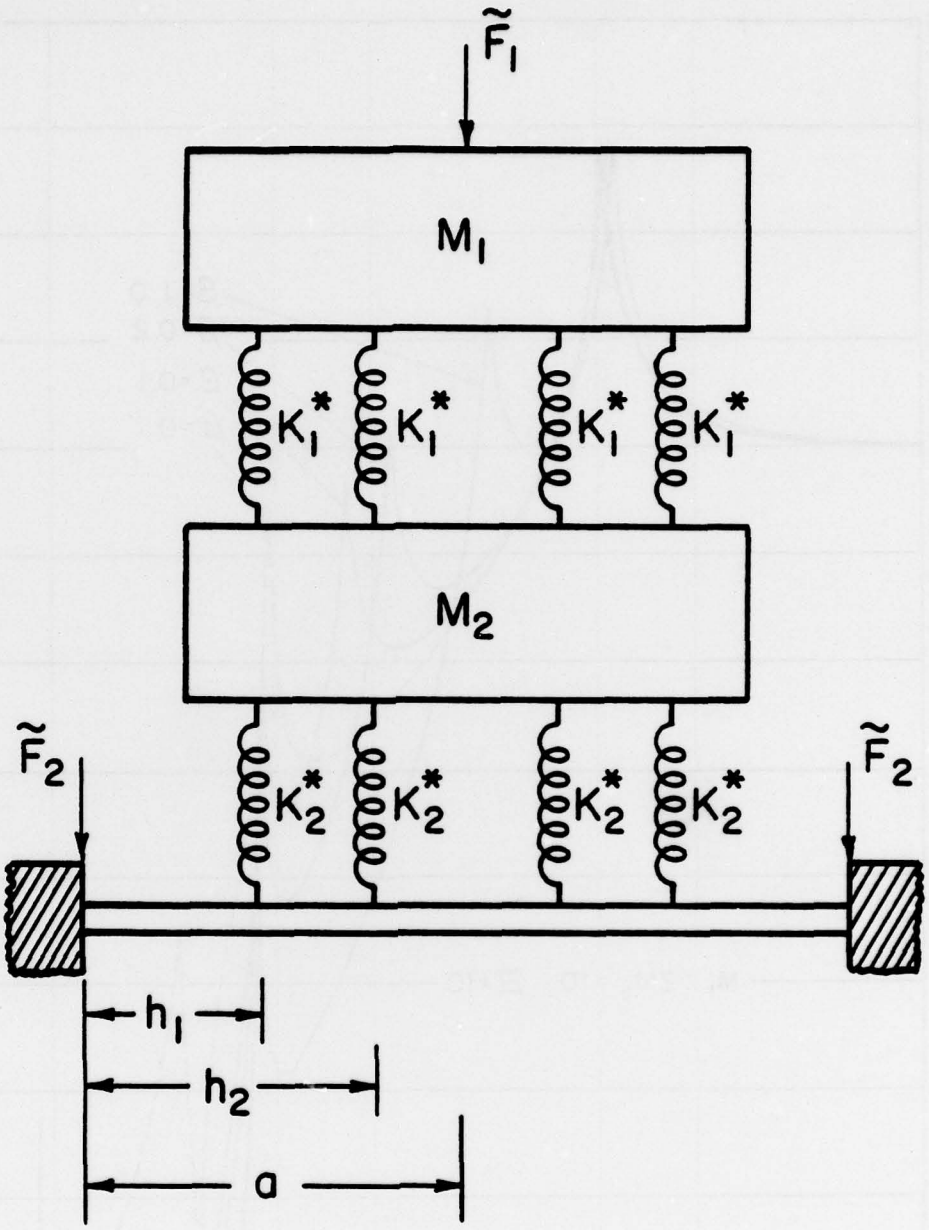

FIG. 19

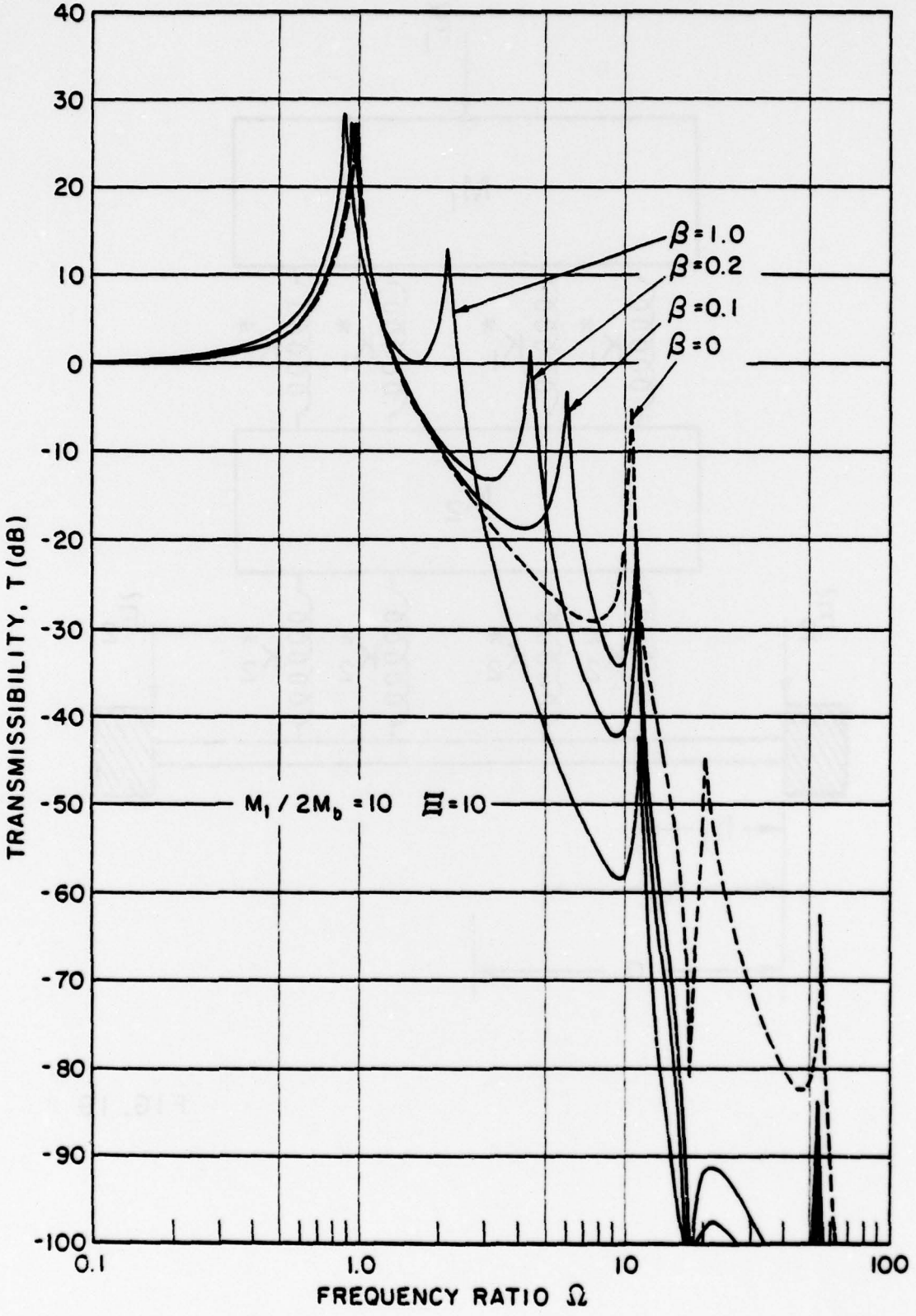
40
30
20
10
0
-10
-20
-30
-40
-50
-60
-70
-80
-90
-100
TRANSMISSIBILITY, T (dB)
β = 1.0
β = 0.2
β = 0.1
β = 0
M1 / 2Mb = 10 Ξ = 10
0.1
1.0
10
100
FREQUENCY RATIO Ω

FIG. 20

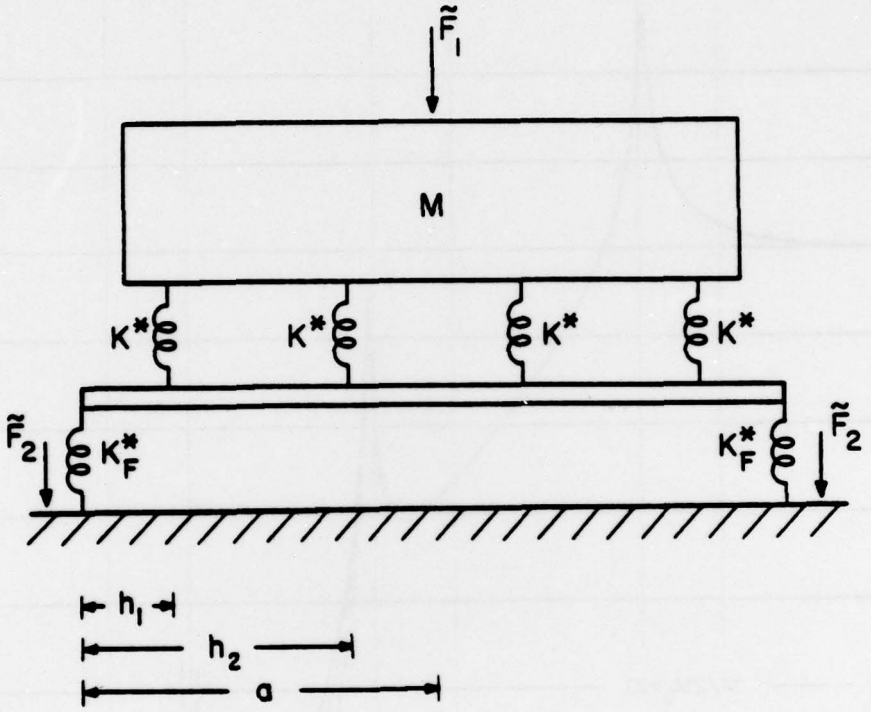

FIG. 21

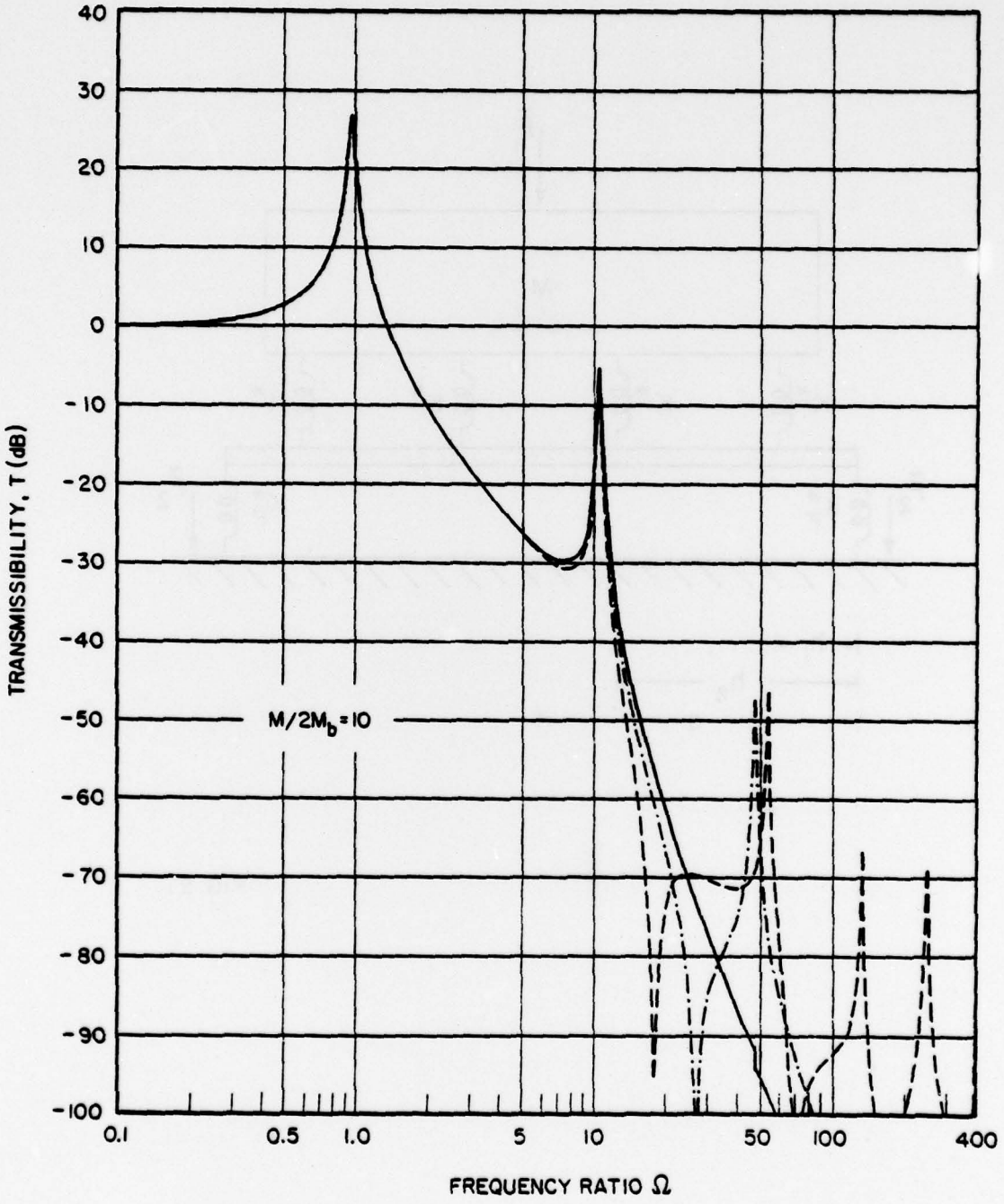
40
30
20
10
0
-10
-20
-30
-40
-50
-60
-70
-80
-90
-100
TRANSMISSIBILITY, T (dB)
M/2M_b=10
0.1
0.5
1.0
5
10
50
100
400
FREQUENCY RATIO Ω

FIG. 22

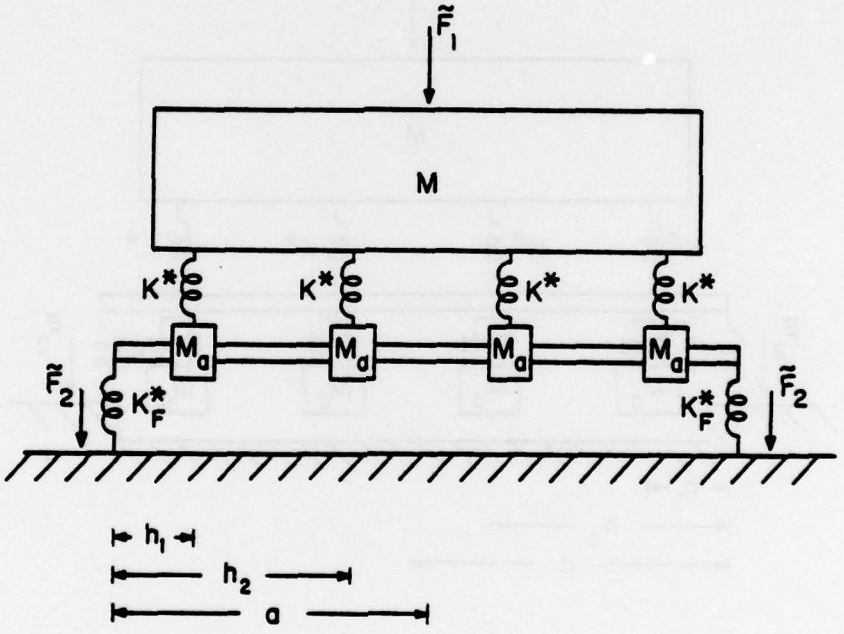

FIG. 23

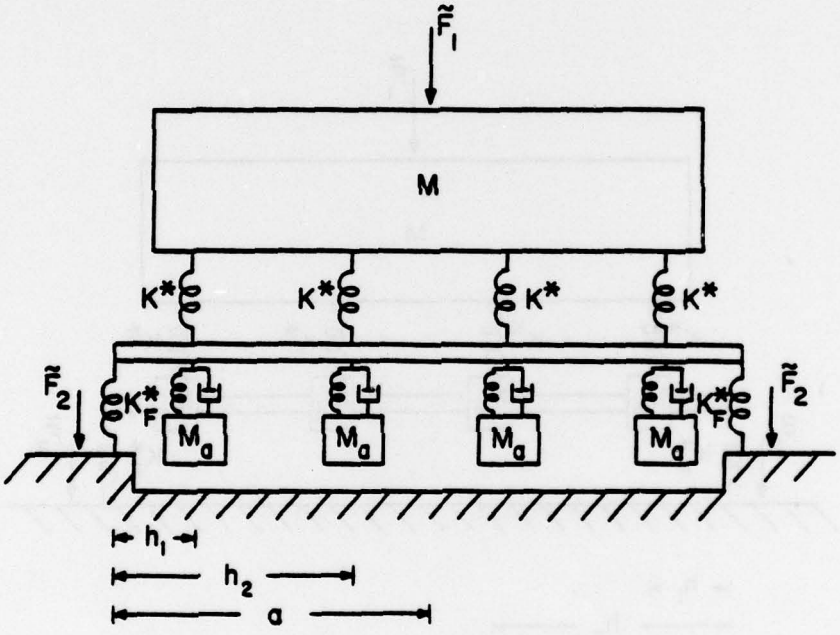

FIG. 24

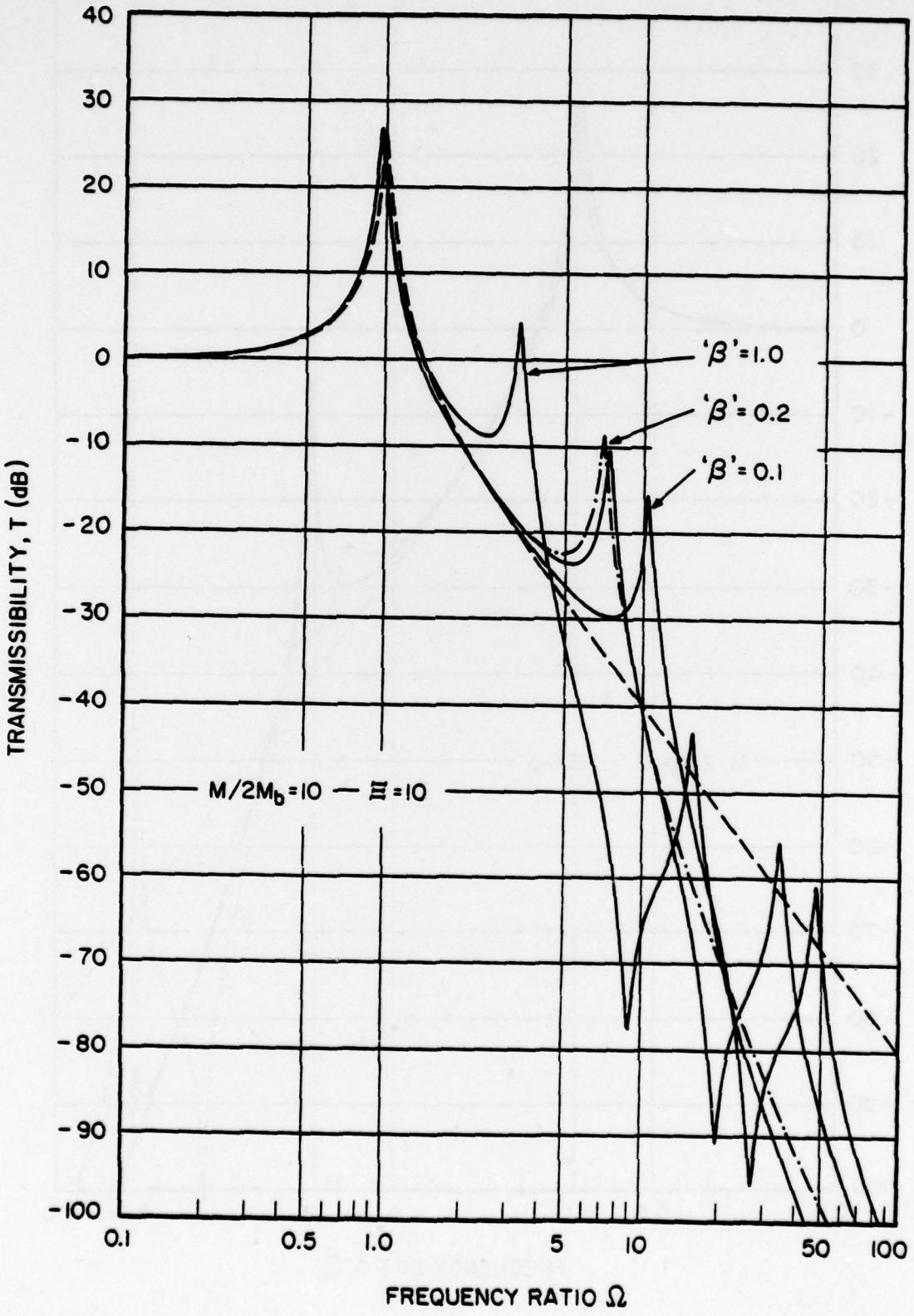
40
30
20
10
0
-10
-20
-30
-40
-50
-60
-70
-80
-90
-100
TRANSMISSIBILITY, T (dB)
0.1
0.5
1.0
5
10
50
100
FREQUENCY RATIO Ω
'β' = 1.0
'β' = 0.2
'β' = 0.1
M/2M_b = 10 — Ξ = 10

FIG.25

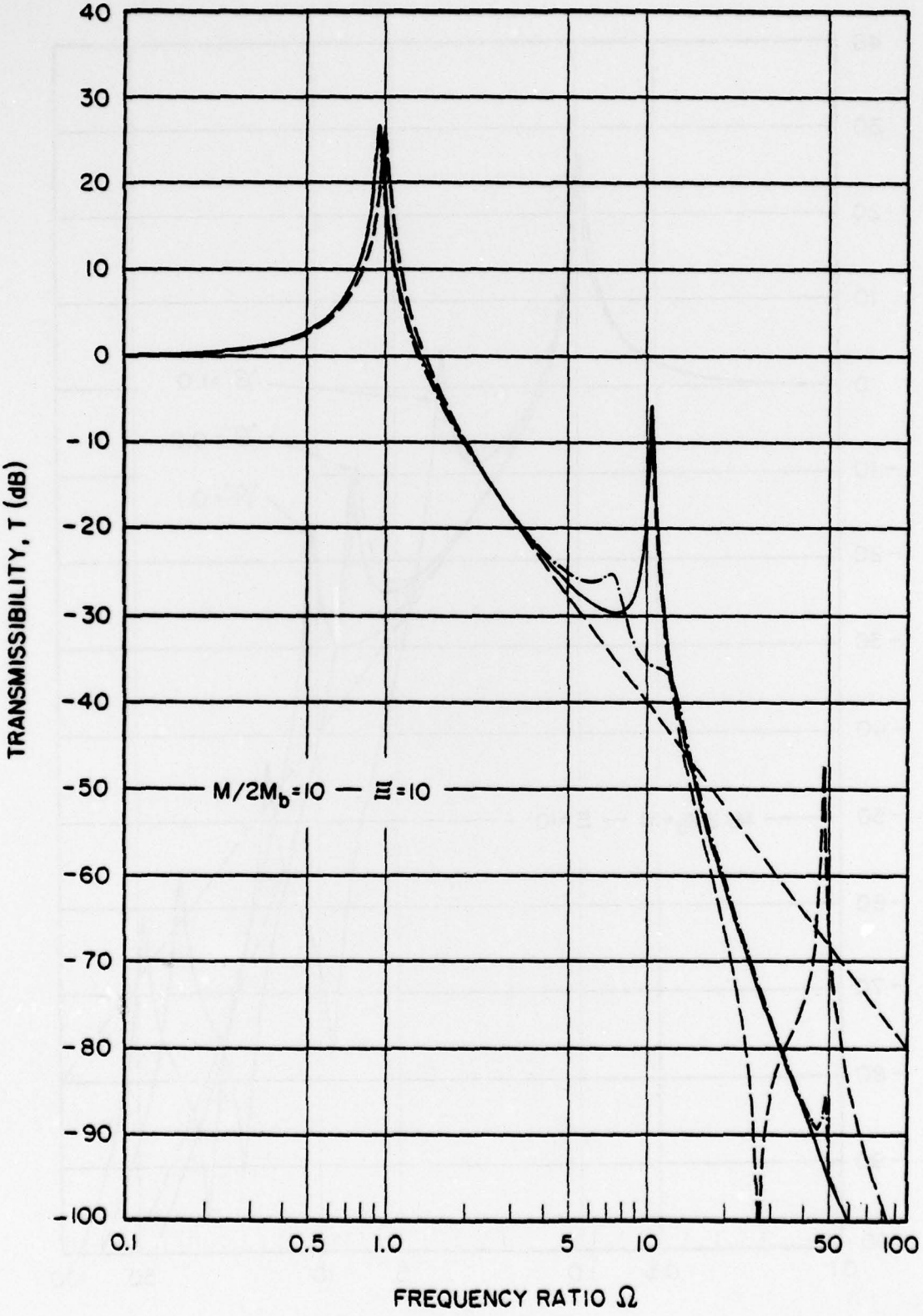
40
30
20
10
0
-10
-20
-30
-40
-50
-60
-70
-80
-90
-100
TRANSMISSIBILITY, T (dB)
M/2M_b=10 — Ξ=10
0.1
0.5
1.0
5
10
50
100
FREQUENCY RATIO Ω

FIG.26

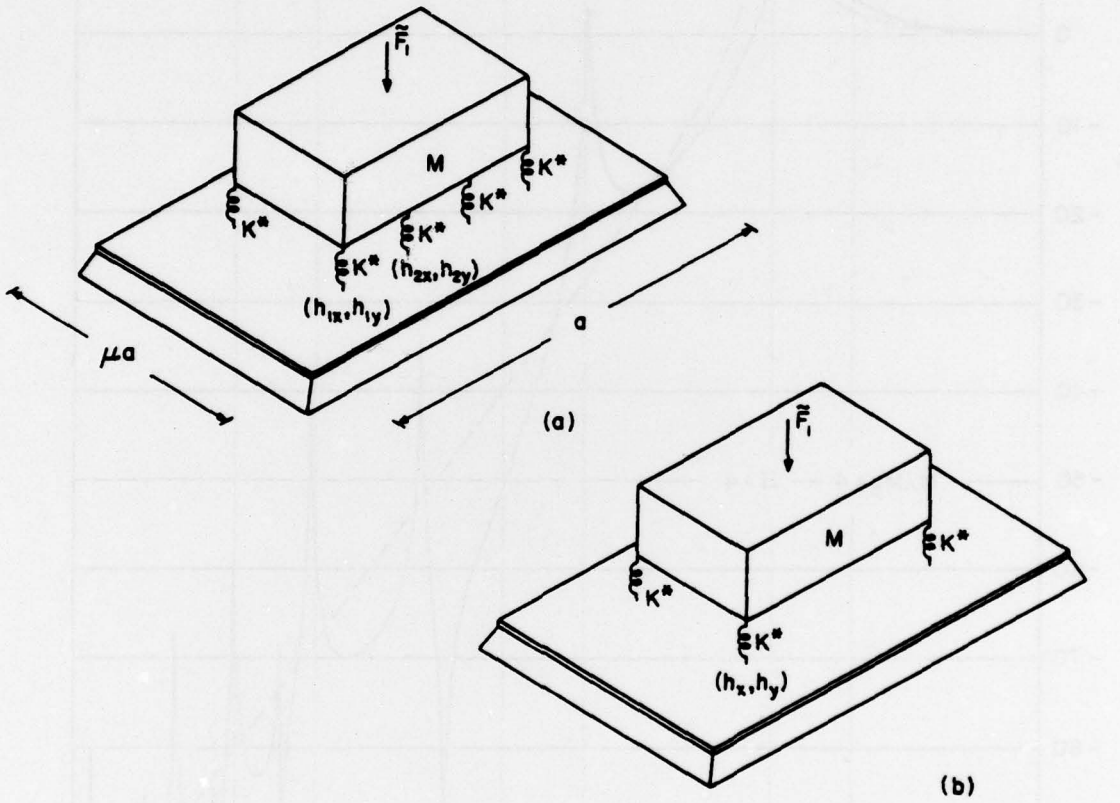

FIG. 27

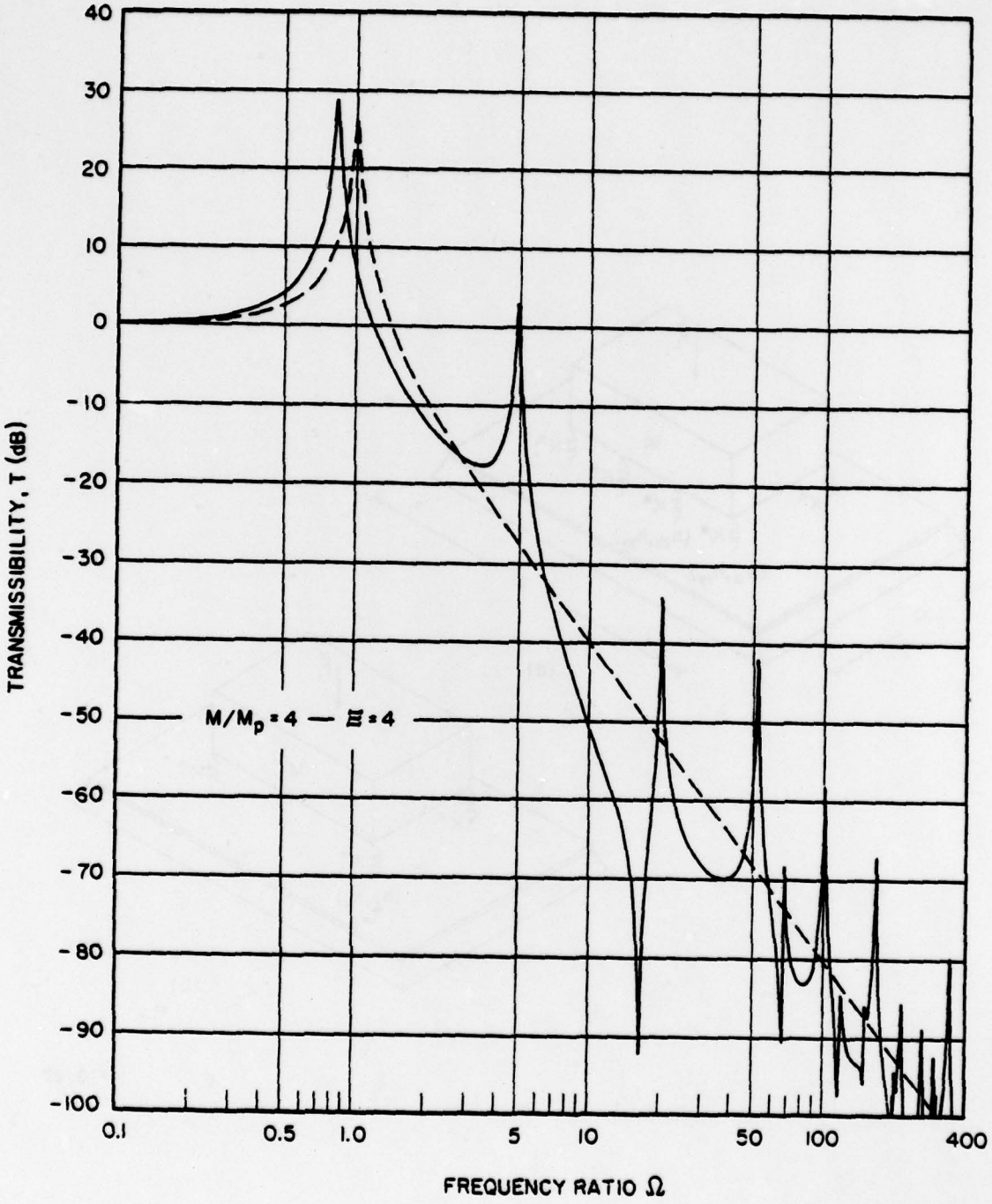
40
30
20
10
0
-10
-20
-30
-40
-50
-60
-70
-80
-90
-100
TRANSMISSIBILITY, T (dB)
M/Mp = 4 — Ξ = 4
0.1
0.5
1.0
5
10
50
100
400
FREQUENCY RATIO Ω

FIG. 28

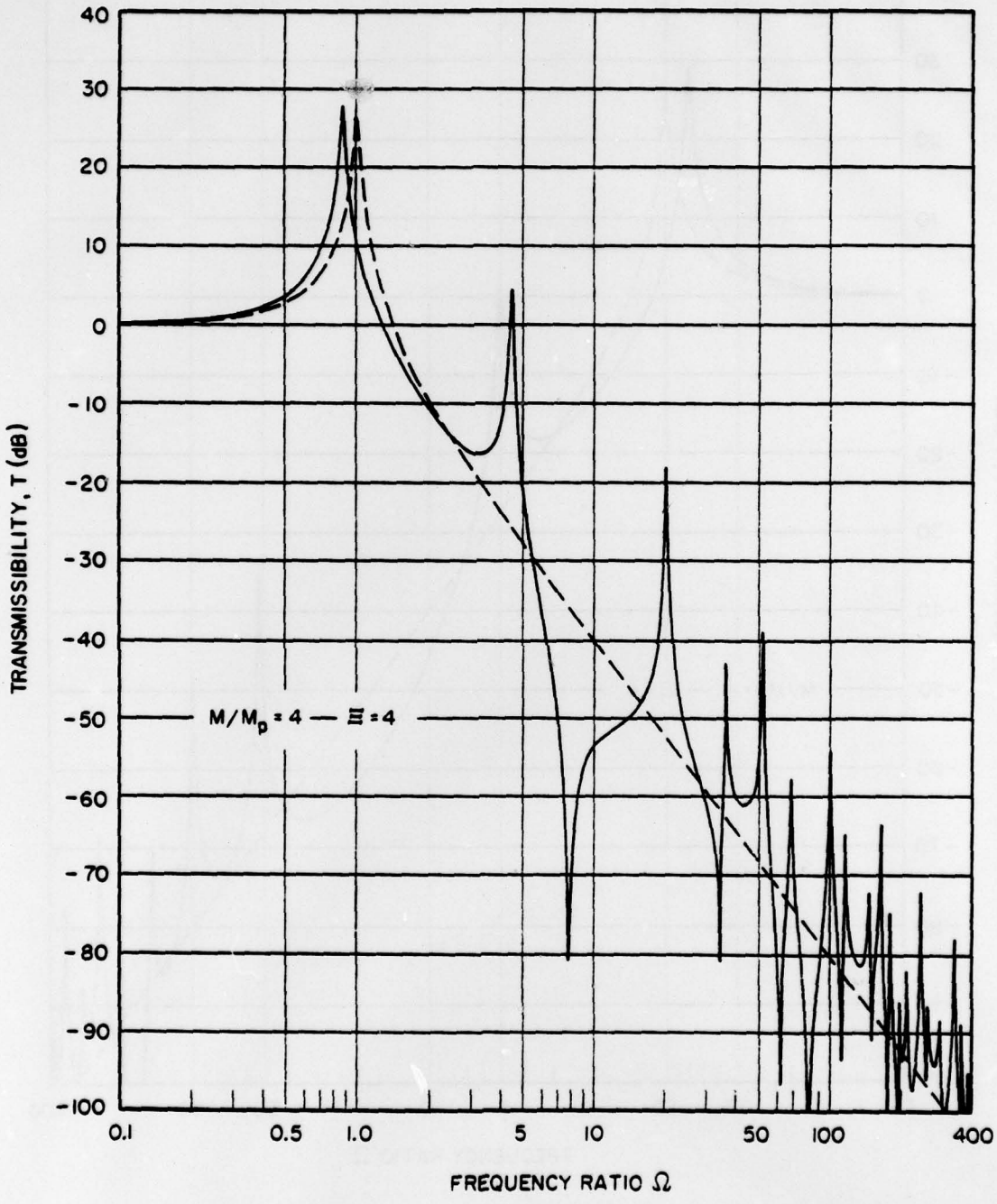
40
30
20
10
0
-10
-20
-30
-40
-50
-60
-70
-80
-90
-100
TRANSMISSIBILITY, T (dB)
M/Mp = 4 — Ξ = 4
0.1
0.5
1.0
5
10
50
100
400
FREQUENCY RATIO Ω

FIG. 29

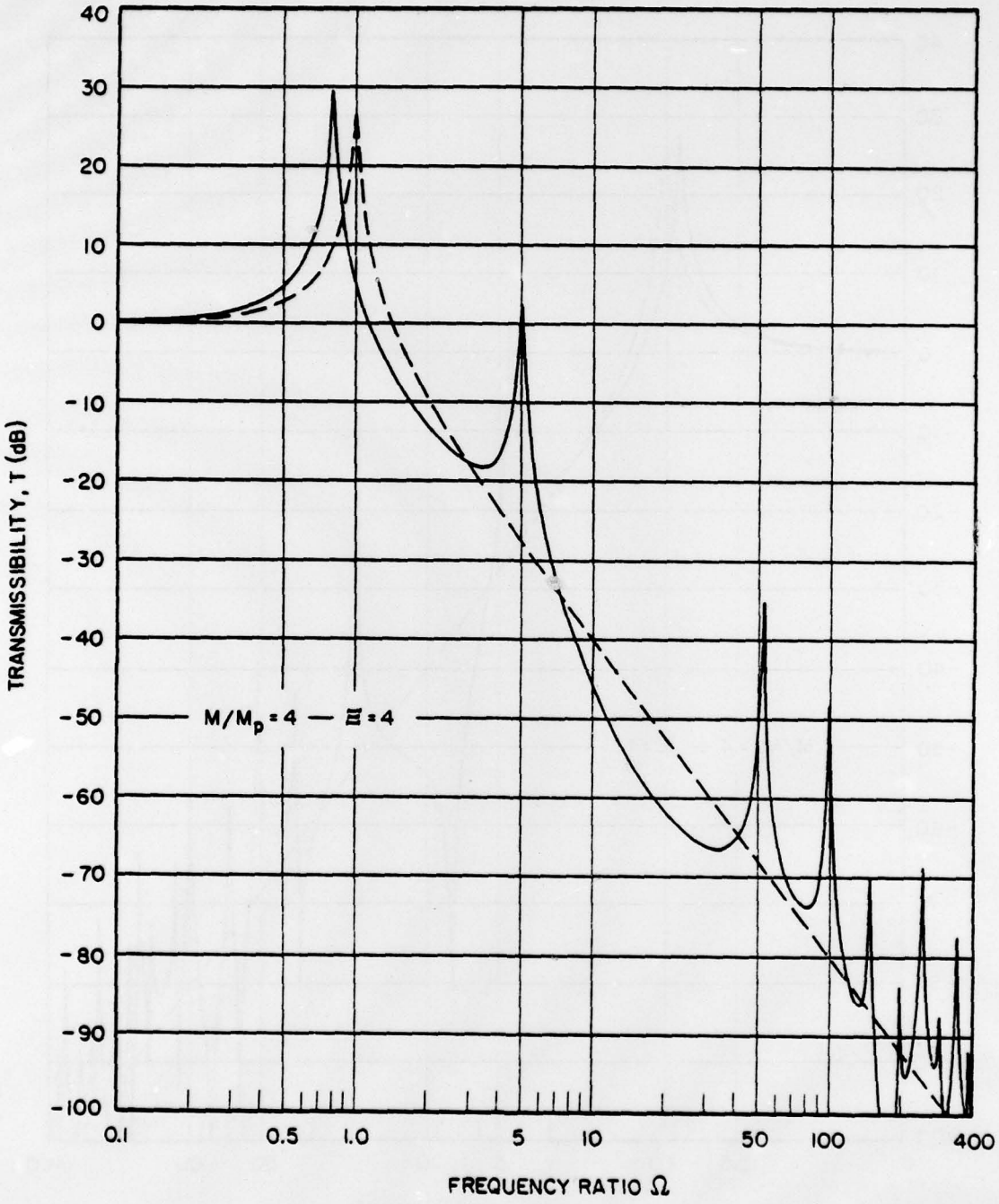
40
30
20
10
0
-10
-20
-30
-40
-50
-60
-70
-80
-90
-100
TRANSMISSIBILITY, T (dB)
M/Mp = 4 — Ξ = 4
0.1
0.5
1.0
5
10
50
100
400
FREQUENCY RATIO Ω

FIG. 30

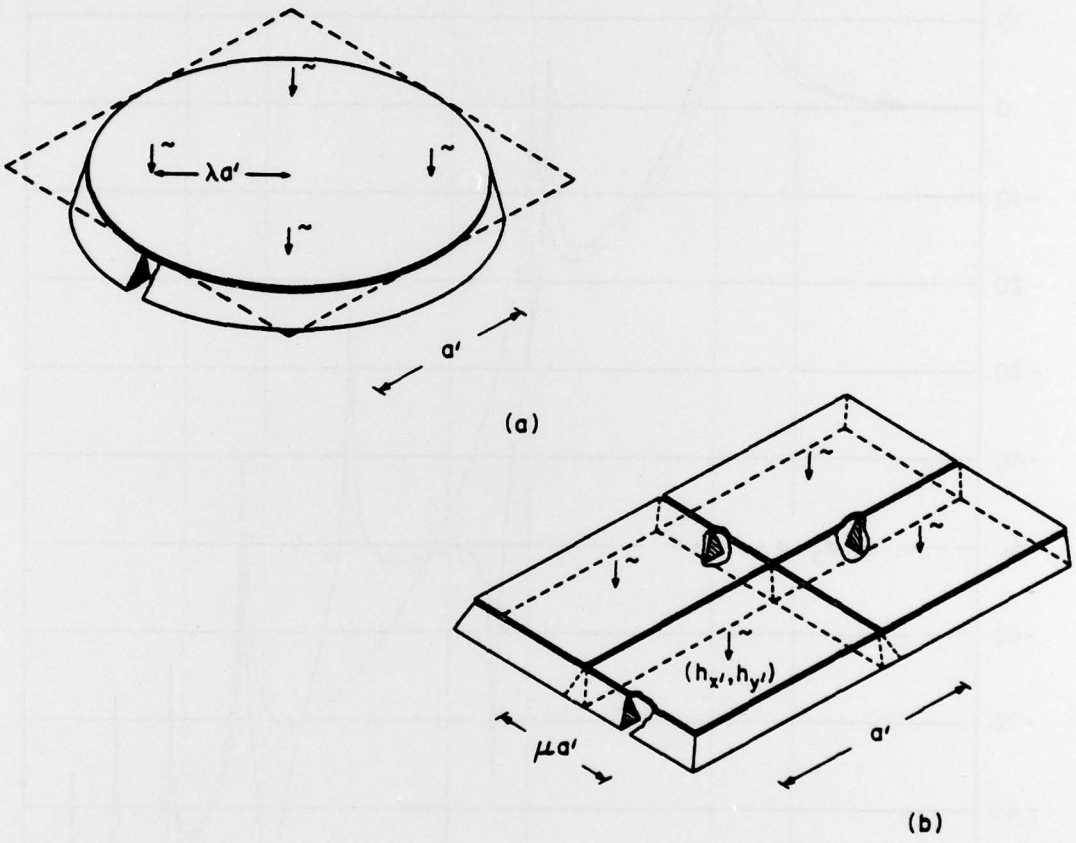

FIG. 31

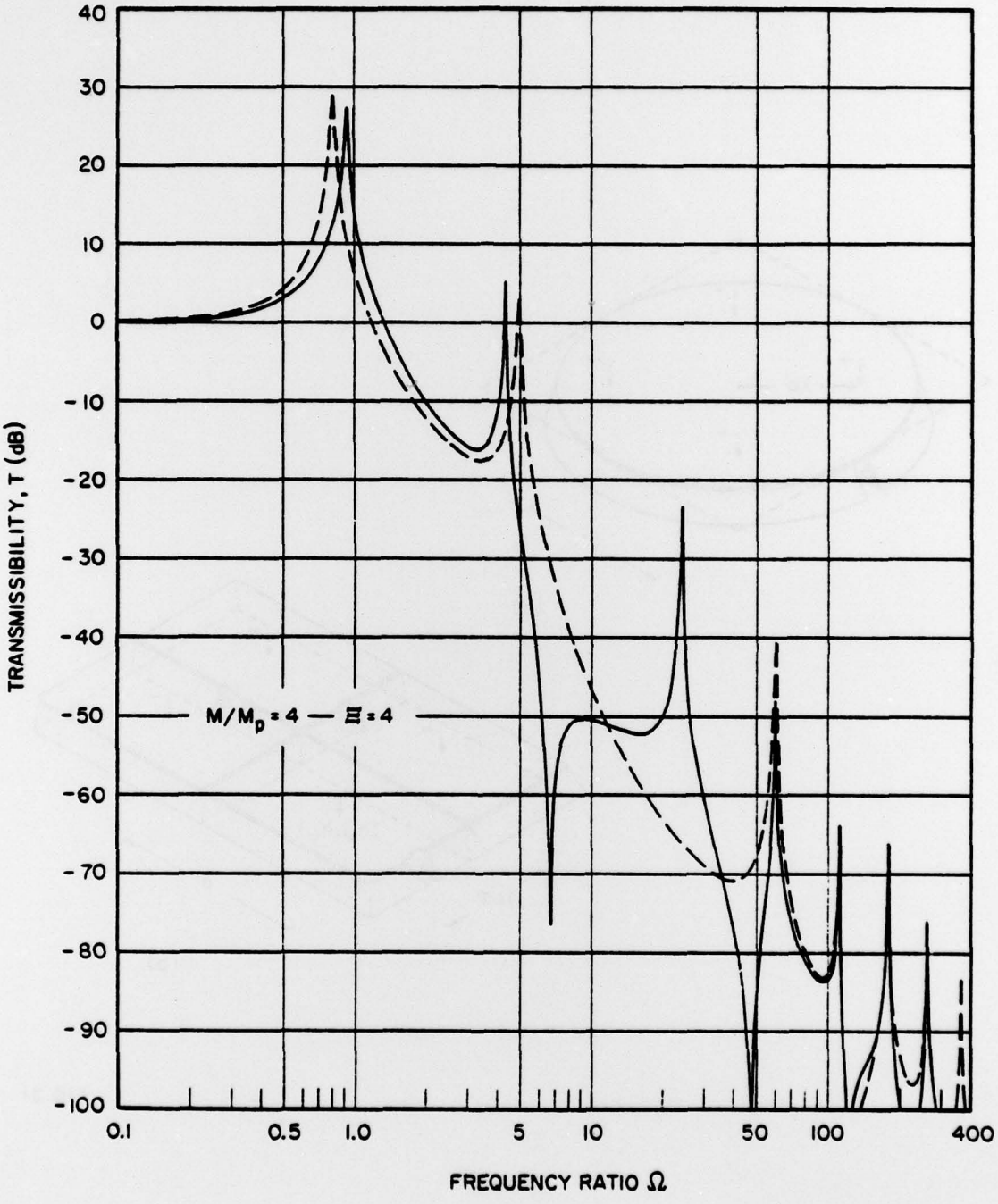
40
30
20
10
0
-10
-20
-30
-40
-50
-60
-70
-80
-90
-100
TRANSMISSIBILITY, T (dB)
M/Mp = 4 — Ξ = 4
0.1
0.5
1.0
5
10
50
100
400
FREQUENCY RATIO Ω

FIG. 32

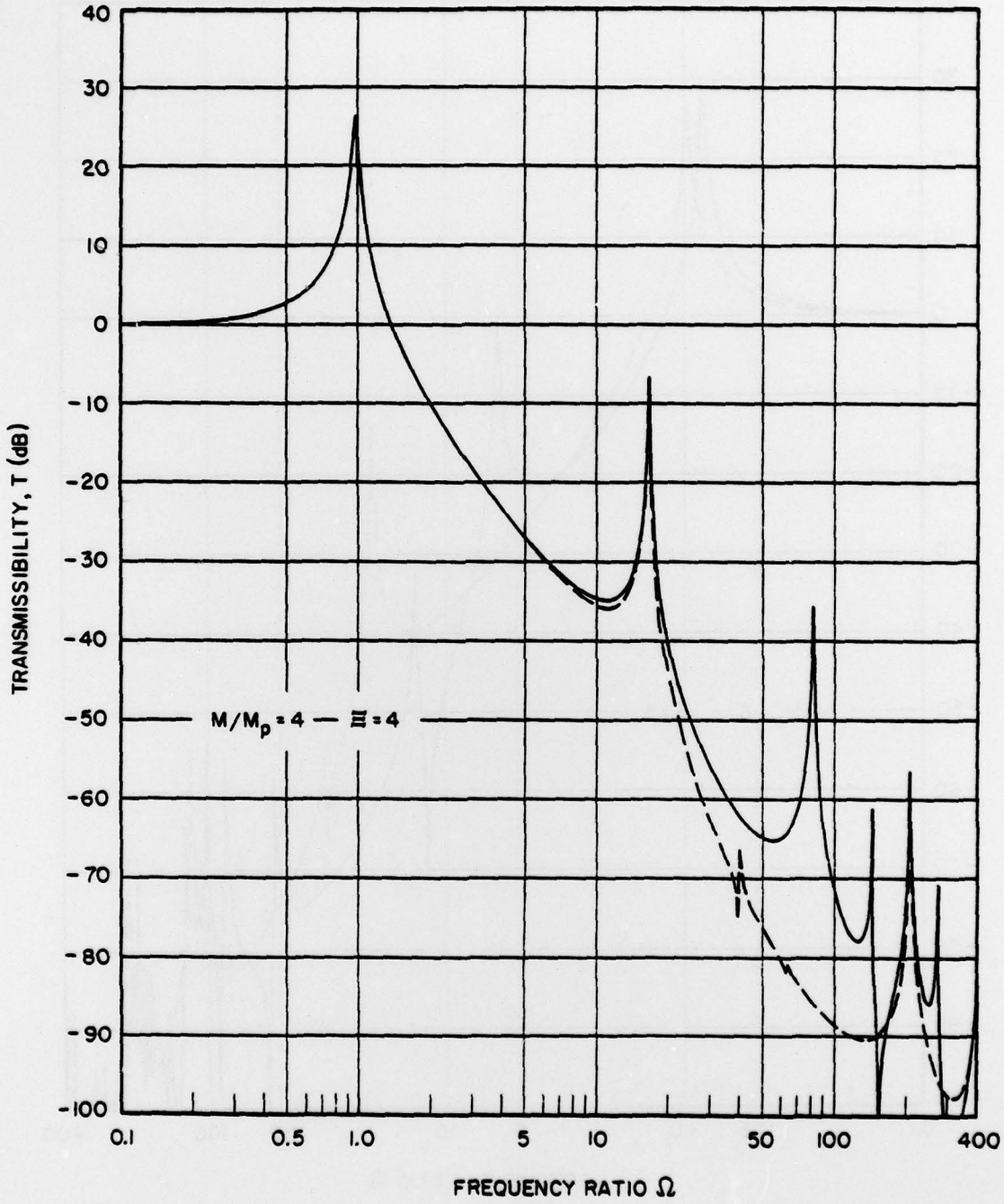
40
30
20
10
0
-10
-20
-30
-40
-50
-60
-70
-80
-90
-100
TRANSMISSIBILITY, T (dB)
M/Mp = 4 — Ξ = 4
0.1
0.5
1.0
5
10
50
100
400
FREQUENCY RATIO Ω

FIG. 33

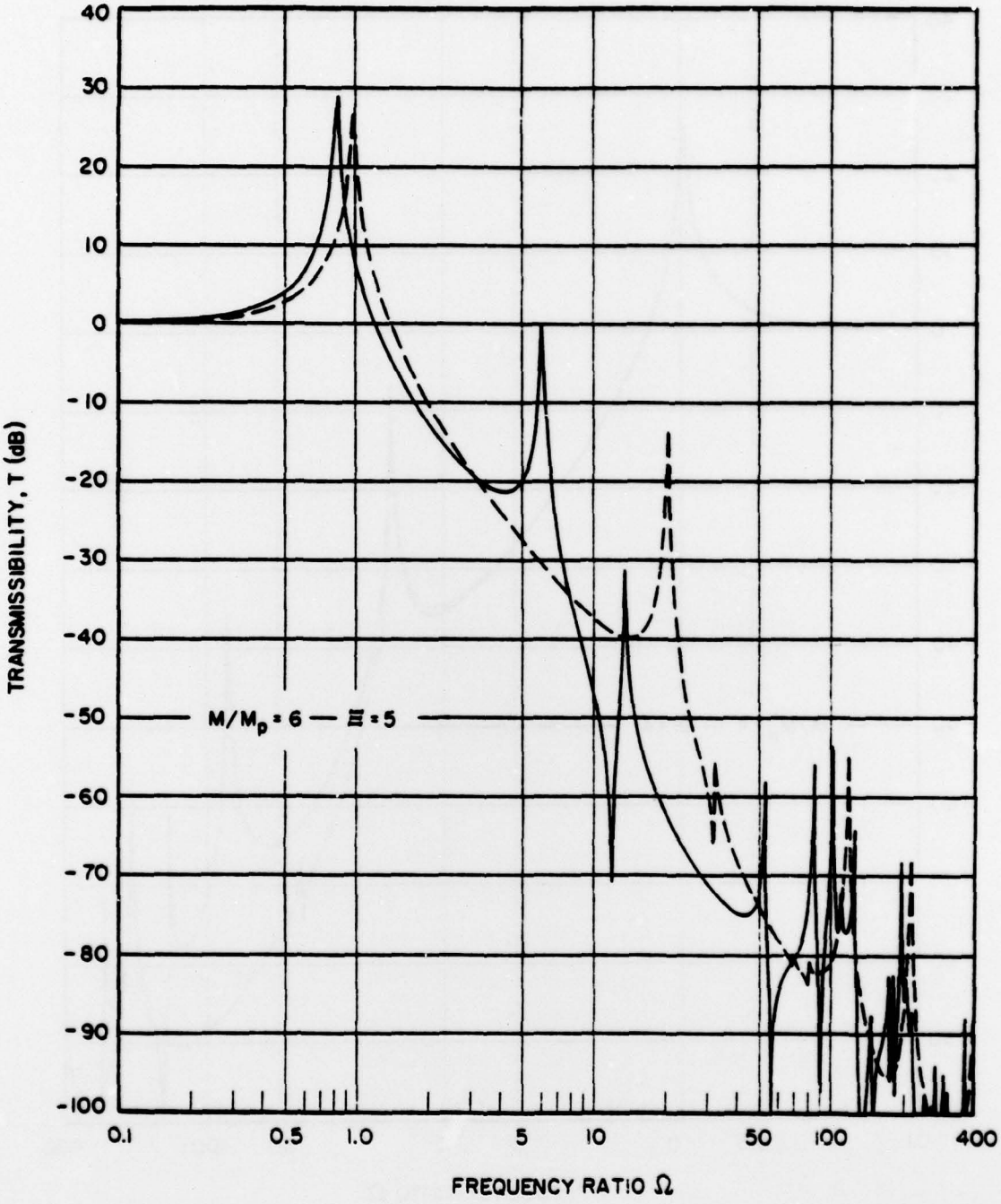
40
30
20
10
0
-10
-20
-30
-40
-50
-60
-70
-80
-90
-100
TRANSMISSIBILITY, T (dB)
M/Mp = 6 — Ξ = 5
0.1
0.5
1.0
5
10
50
100
400
FREQUENCY RATIO Ω

FIG. 34

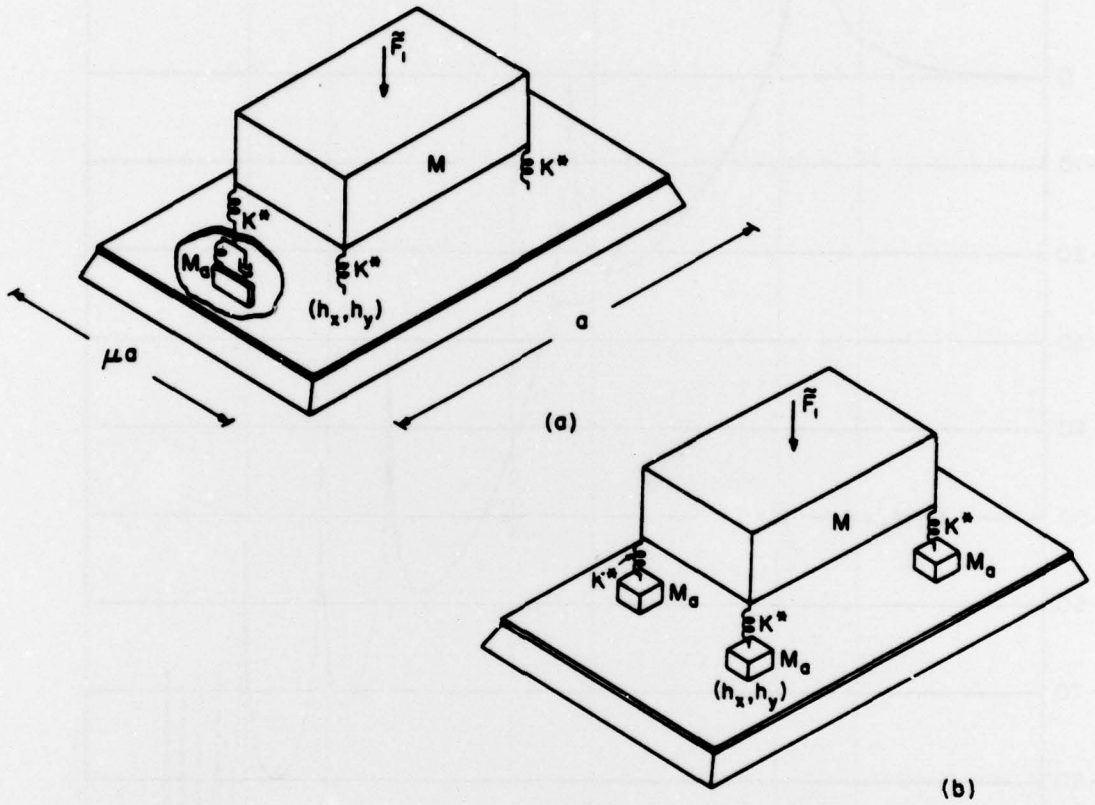

FIG. 35

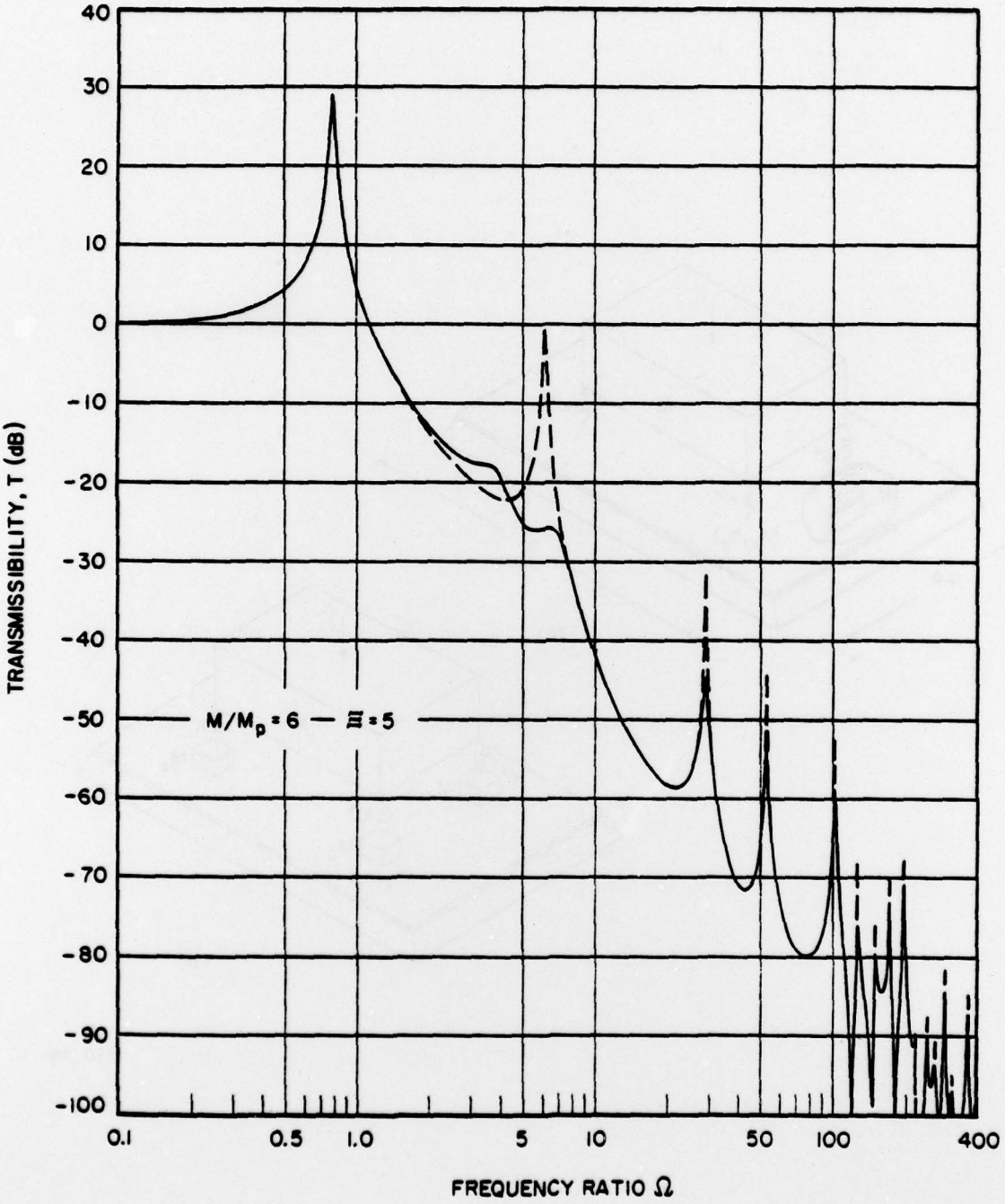
40
30
20
10
0
-10
-20
-30
-40
-50
-60
-70
-80
-90
-100
TRANSMISSIBILITY, T (dB)
M/Mp = 6 — Ξ = 5
0.1
0.5
1.0
5
10
50
100
400
FREQUENCY RATIO Ω

FIG. 36

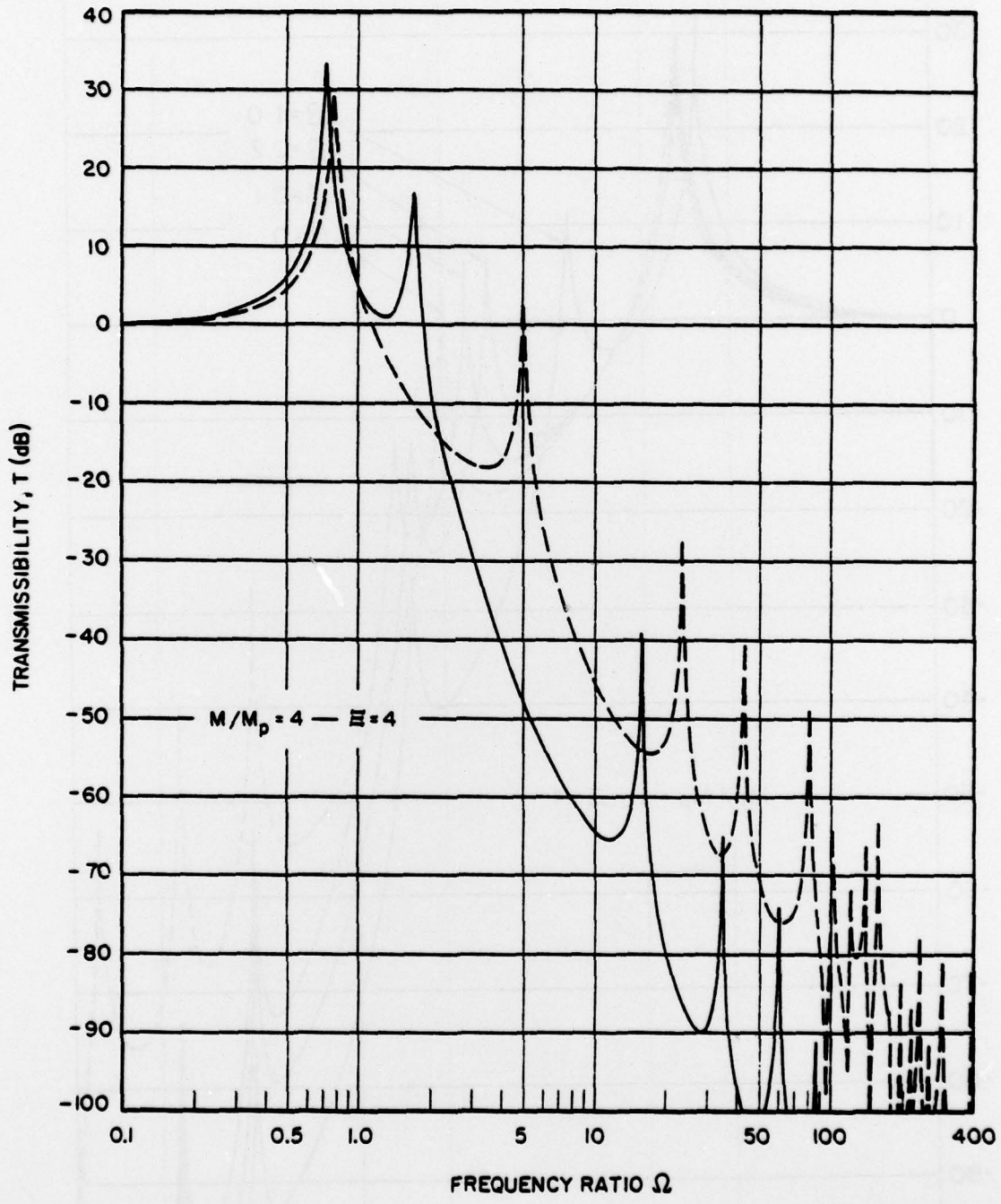
40
30
20
10
0
-10
-20
-30
-40
-50
-60
-70
-80
-90
-100
TRANSMISSIBILITY, T (dB)
M/Mp = 4 — Ξ = 4
0.1
0.5
1.0
5
10
50
100
400
FREQUENCY RATIO Ω

FIG. 37

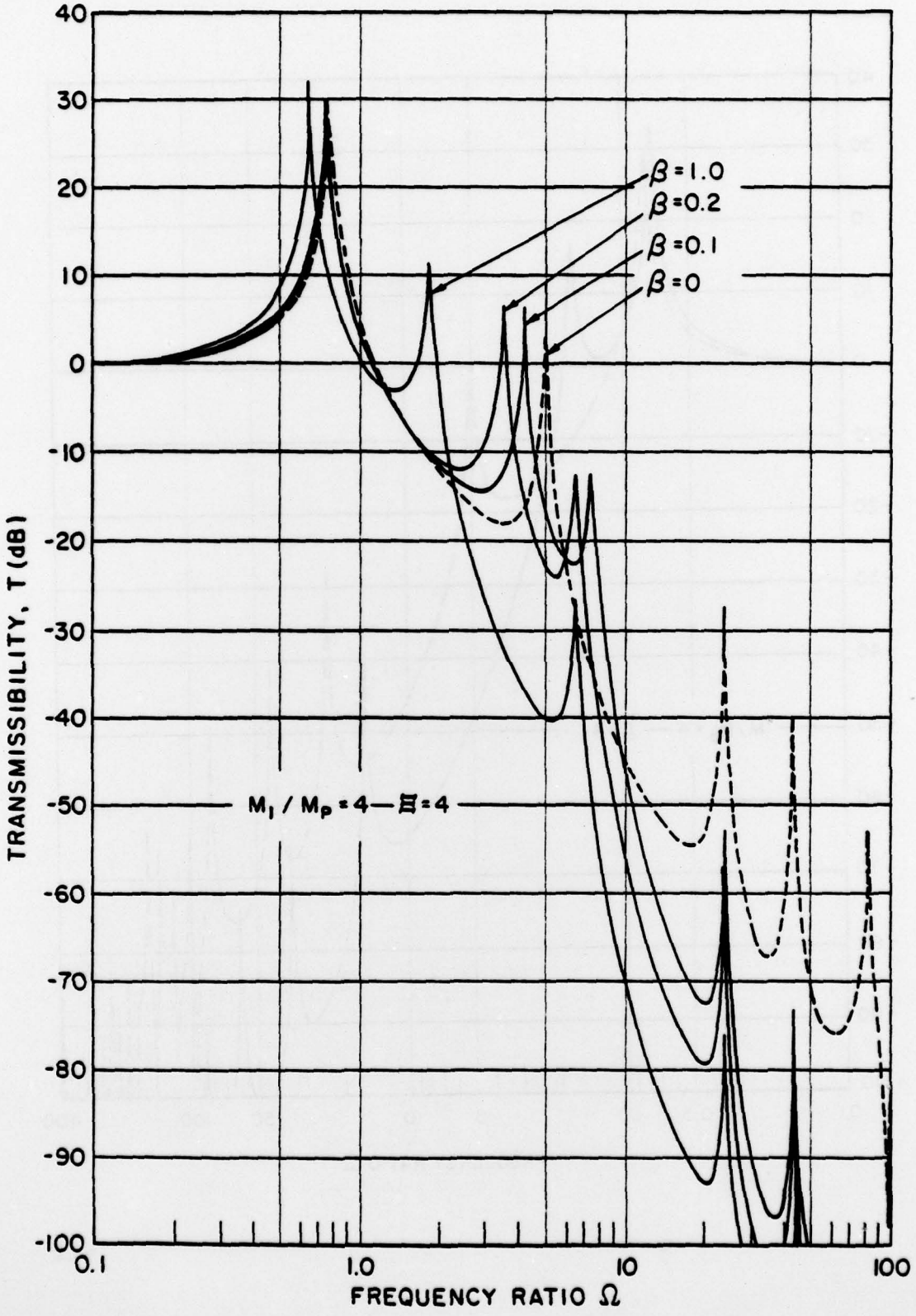
40
30
20
10
0
-10
-20
-30
-40
-50
-60
-70
-80
-90
-100
0.1
1.0
10
100
TRANSMISSIBILITY, T (dB)
FREQUENCY RATIO Ω
β = 1.0
β = 0.2
β = 0.1
β = 0
M1 / Mp = 4 — Ξ = 4

FIG. 38

DISTRIBUTION LIST FOR UNCLASSIFIED TM 79-137

Commander
Naval Sea Systems Command
Department of the Navy
Washington, DC 20362
Attn: SEA 924N
(Copy No. 1)

Commander
Naval Sea Systems Command
Department of the Navy
Washington, DC 20362
Attn: PMS-393
(Copy No. 2)

Commander
Naval Sea Systems Command
Department of the Navy
Washington, DC 20362
Attn: PMS-395
(Copy No. 3)

Commander
Naval Sea Systems Command
Department of the Navy
Washington, DC 20362
Attn: PMS-396
(Copy No. 4)

Commander
Naval Sea Systems Command
Department of the Navy
Washington, DC 20362
Attn: Mr. Stephen M. Blazek
SEA 05H
(Copy Nos. 5, 6, 7, 8)

Commander
Naval Sea Systems Command
Department of the Navy
Washington, DC 20362
Attn: Mr. Stephen G. Wieczorek
SEA 05H
(Copy Nos. 9 and 10)

Commander
Naval Sea Systems Command
Department of the Navy
Washington, DC 20362
Attn: Mr. C. C. Taylor
SEA 05H
(Copy Nos. 11 and 12)

Commander
Naval Ship Engineering Center
Center Building
Prince George's Center
Hyattsville, MD 20782
Attn: NAVSEC 6103E
(Copy Nos. 13 and 14)

Commander
Naval Ship Engineering Center
Center Building
Prince George's Center
Hyattsville, MD 20782
Attn: NAVSEC 6105C
(Copy Nos. 15 and 16)

Commander
Naval Ship Engineering Center
Center Building
Prince George's Center
Hyattsville, MD 20782
Attn: Mr. Kenneth G. Hartman
NAVSEC 6105N
(Copy Nos. 17, 18, 19, 20, 21, 22)

Commander
Naval Ship Engineering Center
Center Building
Prince George's Center
Hyattsville, MD 20782
Attn: NAVSEC 6111B
(Copy Nos. 23 and 24)

Commander
Naval Ship Engineering Center
Center Building
Prince George's Center
Hyattsville, MD 20782
Attn: NAVSEC 6111D
(Copy Nos. 25 and 26)

Commander
Naval Ship Engineering Center
Center Building
Prince George's Center
Hyattsville, MD 20782
Attn: NAVSEC 6113C
(Copy Nos. 27 and 28)

Commander
Naval Ship Engineering Center
Center Building
Prince George's Center
Hyattsville, MD 20782
Attn: NAVSEC 6113D
(Copy Nos. 29 and 30)

Commander
Naval Ship Engineering Center
Center Building
Prince George's Center
Hyattsville, MD 20782
Attn: NAVSEC 6120
(Copy Nos. 31 and 32)

Commander
Naval Ship Engineering Center
Center Building
Prince George's Center
Hyattsville, MD 20782
Attn: NAVSEC 6129
(Copy Nos. 33 and 34)

Naval Ship Research and Development Center
Annapolis Division
Annapolis, MD 21402
Attn: Mr. J. Smith
(Copy No. 35)

Naval Ship Research and Development Center
Annapolis Division
Annapolis, MD 21402
Attn: Mr. L. J. Argiro
(Copy Nos. 36, 37, 38, 39, 40, 41)

Naval Ship Research and Development Center
Bethesda, MD 20084
Attn: Dr. M. Sevik
Code 19
(Copy Nos. 42 and 43)

Naval Ship Research and Development Center
Bethesda, MD 20084
Attn: Dr. W. W. Murray
Code 17
(Copy Nos. 44 and 45)

Naval Ship Research and Development Center
Bethesda, MD 20084
Attn: Dr. M. Strasberg
Code 1901
(Copy No. 46)

Naval Ship Research and Development Center
Bethesda, MD 20084
Attn: Dr. G. Maidanik
Code 1902
(Copy No. 47)

Naval Ship Research and Development Center
Bethesda, MD 20084
Attn: Dr. G. Chertock
Code 1903
(Copy No. 48)

Naval Ship Research and Development Center
Bethesda, MD 20084
Attn: Dr. D. Feit
Code 196
(Copy Nos. 49, 50, 51, 52, 53, 54)

Naval Ship Research and Development Center
Bethesda, MD 20084
Attn: Dr. J. T. Shen
Code 1942
(Copy No. 55)

Director
Defense Documentation Center
Cameron Station
Alexandria, VA 22314
(Copy Nos. 56, 57, 58, 59, 60, 61,
62, 63, 64, 65, 66, 67)

Director
Naval Research Laboratory
Washington, DC 20390
Attn: Code 8440
(Copy Nos. 68 and 69)

Ocean Structures Branch
U. S. Naval Research Laboratory
Washington, DC 20390
Attn: Mr. G. J. O'Hara
(Copy No. 70)

Office of Naval Research
Department of the Navy
Arlington, VA 22217
Attn: Dr. G. Boyer
Code 222
(Copy Nos. 71, 72, 73)

Office of Naval Research
Department of the Navy
Arlington, VA 22217
Attn: Dr. A. O. Sykes
Code 222
(Copy Nos. 74, 75, 76)

Office of Naval Research
Department of the Navy
Arlington, VA 22217
Attn: Mr. Keith M. Ellingsworth
Code 473
(Copy No. 77)

Office of Naval Research
Department of the Navy
Arlington, VA 22217
Attn: Dr. N. Perrone
Code 474
(Copy No. 78)

Commander
Mare Island Naval Shipyard
Vallejo, CA 94592
(Design Division)
(Copy No. 79)

Commander
Portsmouth Naval Shipyard
Portsmouth, NH 03801
(Copy No. 80)

Supervisor of Shipbuilding,
Conversion and Repair
General Dynamics Corporation
Electric Boat Division
Groton, CT 06340
Attn: Mr. John Wilder
Dept. 440
(Copy Nos. 81 and 82)

Supervisor of Shipbuilding,
Conversion and Repair
Ingalls Shipbuilding Corporation
Pascagoula, MS 39567
(Copy No. 83)

Supervisor of Shipbuilding,
Conversion and Repair
Newport News Shipbuilding and Drydock Company
Newport News, VA 23607
(Copy No. 84)

Naval Ship Research and
Development Center
Underwater Explosion Research
Division
Code 780
Portsmouth, VA 23709
(Copy No. 85)

Naval Underwater Systems Center
New London Laboratory
New London, CT 06320
Attn: Mr. G. F. Carey
(Copy No. 86)

Naval Underwater Systems Center
New London Laboratory
New London, CT 06320
Attn: Dr. R. S. Woollett
(Copy No. 87)

Naval Undersea Warfare Center
San Diego, CA 92152
Attn: Mr. G. Coleman
(Copy No. 88)

Dr. J. Barger
Bolt Beranek and Newman, Inc.
50 Moulton Street
Cambridge, MA 02138
(Copy No. 89)

Dr. D. I. G. Jones
Air Force Materials Laboratory
Wright-Patterson Air Force Base
Ohio 45433
(Copy No. 90)

Dr. M. C. Junger, President
Cambridge Acoustical Associates, Inc
1033 Massachusetts Avenue
Cambridge, MA 02138
(Copy No. 91)

Acquisitions Supervisor
Technical Information Service
American Institute of Aeronautics
and Astronautics, Inc.
750 Third Avenue
New York, NY 10017
(Copy No. 92)

Dr. R. S. Ayre
Department of Civil Engineering
University of Colorado
Boulder, CO 80302
(Copy No. 93)

Dr. D. Frederick
Chairman, Engineering Science and Mechanics Department
Virginia Polytechnic Institute and State University
Blacksburg, VA 24061
(Copy No. 94)

Dr. D. E. Hudson
Department of Mechanics
California Institute of Technology
Pasadena, CA 91109
(Copy No. 95)

Dr. G. Herrmann, Chairman
Department of Applied Mechanics
Stanford University
Stanford, CA 94305
(Copy No. 96)

Dr. A. Kalnins
Department of Mechanical Engineering and Mechanics
Leheigh University
Bethlehem, PA 18015
(Copy No. 97)

Dr. D. D. Kana
Southwest Research Institute
8500 Culebra Road
San Antonio, TX 78206
(Copy No. 98)

Dr. Y. -H. Pao, Chairman
Department of Theoretical and Applied Mechanics
Cornell University
Ithaca
New York, NY 14850
(Copy No. 99)

Dr. J. R. Rice
School of Engineering
Brown University
Providence, RI 02912
(Copy No. 100)

Dr. P. S. Symonds
School of Engineering
Brown University
Providence, RI 02912
(Copy No. 101)

Dr. W. J. Worley
Department of Theoretical and Applied Mechanics
University of Illinois
Urbana, IL 61801
(Copy No. 102)

Dr. Dana Young
Southwest Research Institute
8500 Culebra Road
San Antonio, TX 78206
(Copy No. 103)

Commander
Naval Sea Systems Command
Department of the Navy
Washington, DC 20362
Attn: SEA-09G32-Library
(Copy Nos. 104 and 105)

Dr. R. M. Gorman
Bolt Beranek and Newman, Inc.
Union Station
New London, CT 06340
(Copy No. 106)